Electrical Energy Storage Factual Status Document

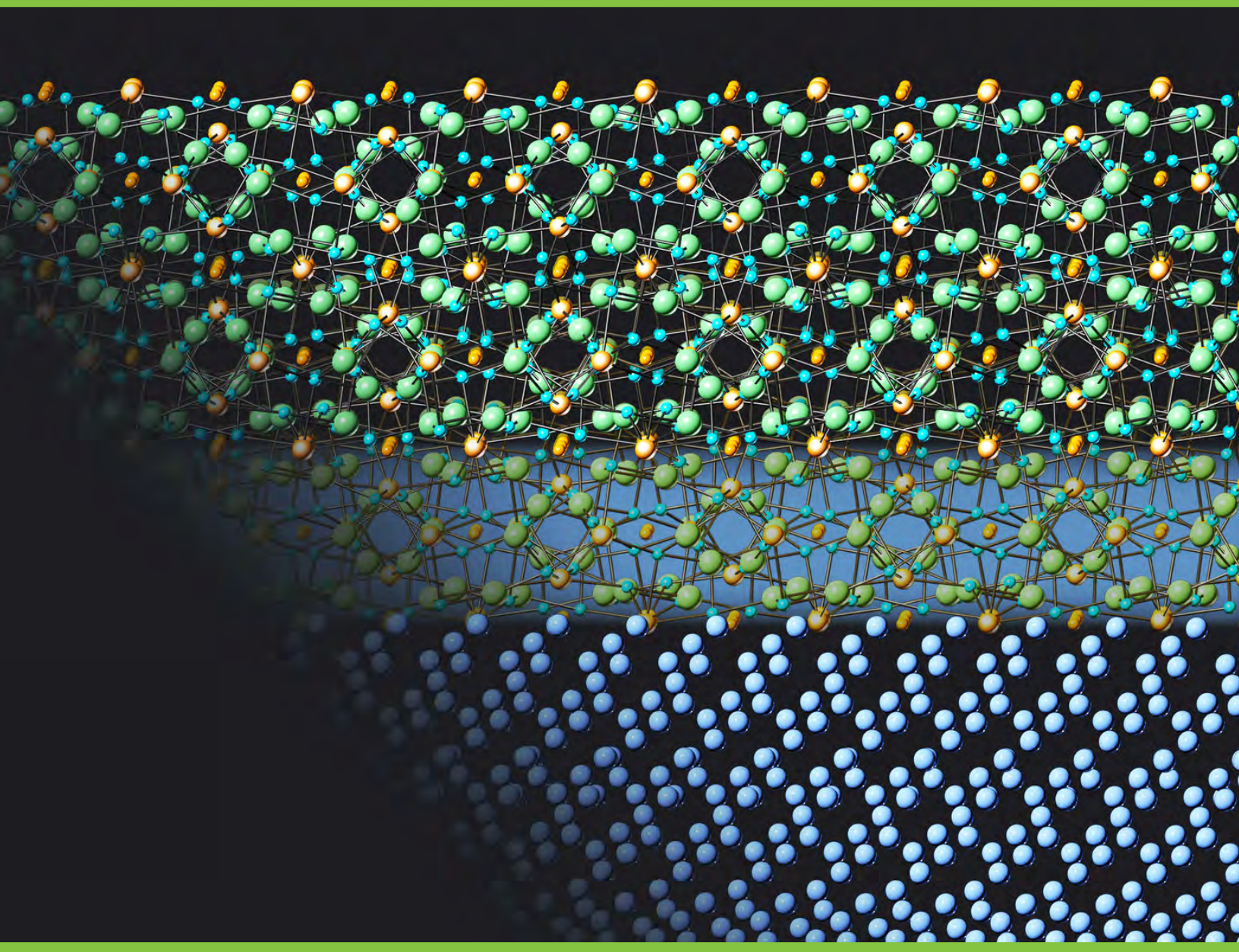

Resource Document for the Workshop on Basic Research Needs for

Next Generation Electrical Energy Storage

March 2017

The cover image is a schematic representation of a lithium metal anode (bottom) and solid electrolyte (top) at the atomic scale. Scanning transmission electron microscopy revealed both the structure and chemistry of the interface region ($Li_{7-3x}Al_xLa_3Zr_2O_{12}$) between the anode and electrolyte—a key discovery if this promising next generation battery is ever to become a commercial reality. Image courtesy of Oak Ridge National Laboratory (Ma et al., *Nano Letters* 16: 7030–7036, 2016. DOI: 10.1021/acs.nanolett.6b03223).

APPENDIX

ELECTRICAL ENERGY STORAGE FACTUAL STATUS DOCUMENT

Resource Document for the Workshop on Basic Research Needs for Next Generation Electrical Energy Storage

March 2017

Contributors

Dan Buttry, ASU

Gerd Ceder, UC Berkeley

Babu Chalamala, SNL

Rob Darling, UTRC

Nancy Dudney, ORNL

Bruce Dunn, UCLA

Brian Ingram, ANL

Jun Liu, PNNL

Amy Marschilok, Stony Brook U.

Bryan McCloskey, UC Berkeley

Kristin Persson, UC Berkeley

Amy Prieto, Colorado State

Vincent Sprenkle, PNNL

Venkat Srinivasan, ANL

Eric Stach, BNL

Mike Toney, SLAC

Feng Wang, BNL

Yiying Wu, Ohio State

Kevin Zavadil, SNL

CONTENTS

1 INTRODUCTION

Electrical energy storage is of growing importance to energy – with increasing use in transportation and on the electrical grid. Batteries are used in all types of vehicles, but have increased in importance with the growth of hybrid and all-electric powered vehicles. For the electrical grid, batteries have a wide diversity of applications from grid stability to storage of electricity generated when the load is low so it is available when there is more demand. Distributed generation of electricity by solar panels and wind generation are also drivers for enhanced energy storage. In both industries, a key enabler will be low-cost batteries with long life, excellent safety, and superior performance. In addition to these two big markets, consumer electronics powered by rechargeable batteries continues to grow into new areas with the advent of wearable technology, internet-of-things, and virtual reality. Today's energy storage technologies fall far short of the requirements for many of these growing applications. Because of these technology gaps, advances in energy storage are expected to play a critical role for a secure energy future.

The requirements for batteries for these different applications vary, sometimes widely. Consumer batteries for laptops and cell phones require high volumetric energy density, while the cycle and calendar life are not as critical, considering the typical 2-year lifespan of these devices. Although better batteries are needed that can meet the increasing demands of consumer electronics, the lower life requirements and the ability to handle higher costs mean that this application serves as the first market for many new technologies before they can mature to other more stringent applications such as vehicles and the grid. Wearable technology adds additional layers of constraint because of the miniature nature of these devices; in such systems, the packaging imposes a large volume and weight penalty, and some require the storage to be integrated into curved structures.

Fully electrified vehicles share the requirement for high energy requirements of consumer batteries; however, the need for long cycle and calendar life, the stringent safety constraint, and the newly emerging fast charge requirement adds additional constraints. More important, as devices become bigger, the need for lower cost increases dramatically. Moving toward hybrid systems, such as plug-in hybrids, non-plug-in hybrids, and start-stop hybrids, changes the primary requirement from high energy capacity to increased power capability. This spectrum of vehicle applications means that many kinds of storage devices start to come into play: from higher energy Li-ion batteries, to high power Li-ion systems, to electrochemical capacitors and hybrid capacitors.

The need for a spectrum of storage concepts is even more pronounced on the grid, where the requirements range from short time storage for frequency regulation, to few hours of storage for time shifting, all the way to many weeks of storage for seasonal adjustments. This means that many systems, ranging from capacitors, to container batteries, to flow batteries start to come into focus. The need for very high cycle and calendar life becomes an even more critical need for stationary storage devices considering the large and expensive nature of these installations.

This document was produced in preparation for a Department of Energy (DOE) Office of Basic Energy Sciences Workshop titled "Basic Research Needs for Next Generation Electrical Energy Storage." This workshop will identify key basic research directions that could provide revolutionary breakthroughs needed for meeting future requirements for electrical energy storage. This document was intended to provide a high-level assessment of current technologies used for electrical storage—focusing specifically on batteries and electrochemical capacitors—and to define requirements that are foreseen for the future application of these technologies in transportation vehicles, stationary storage applications, and consumer electronics. Thus, it provides a common background for the workshop participants and sets the technological basis for the workshop.

2 ELECTRICAL ENERGY STORAGE APPLICATIONS

2.1 Electrical Power for Transportation - Introduction to Challenges for Vehicle Technology

The development of energy storage for vehicles is being pursued by the DOE Energy Efficiency and Renewable Energy, Vehicle Technology Office, and the automotive industry with several overarching goals in mind:

- increasing vehicle energy efficiency,
- reducing the cost and improving the performance of energy storage for electric vehicles (EVs), plug-in hybrid electric vehicles (PHEVs), and hybrid electric vehicles (HEVs), including 12-V start/stop systems, and
- decreasing vehicle emissions with harmful environmental impacts.

Electrical energy storage technology is an important component of all major approaches for advanced vehicle technology (see Table 2-1).

TABLE 2-1: The functional role of electricity storage in vehicles

Vehicle Type	Functional Role of Energy Storage	Top Level Requirements
12-V Start/Stop Vehicle	Power for ancillary services during vehicle stops, frequent engine starts	Lower cost, high cycle life, cold starts
Strong HEV	Stop-and-go power plus propulsion assist	Lower cost, high cycle life
Plug-in HEV	Propulsion over 40- to 60-mile all-electric range	Lower cost, high energy density, high deep discharge cycle life
All-electric vehicle	Vehicle propulsion	Lower cost, high energy density, fast charge, improved low temperature performance

As shown in Table 2-1, electrochemical energy storage technologies can enhance the efficiency of vehicles in various vehicle architectures; from 12-V start stop systems through long range (300 mile) EVs. Over the past several years, all of these advanced technologies have become much more widespread, with 12-V start/stop systems becoming very common in Europe. Many car manufacturers predict that this technology will be ubiquitous by 2020.

At the same time, the cost of high-energy Li-ion batteries for propulsion applications (EVs and PHEVs) has dropped by approximately five times in the past seven years. This, along with government incentives and consumer demand, has led many automakers to introduce PHEVs (20-40 mile electric range) like the Chevy Volt, Ford Fusion, and Toyota Prius Prime, or pure EVs like the Nissan Leaf, Chevy Bolt, and Tesla Model S.

Although the cost of Li-ion batteries has decreased faster than almost anyone predicted five years ago, the technology is still more expensive than a standard gasoline internal combustion engine (ICE) vehicle, which is limiting market adoption of EVs and PHEVs to under 1% to date. Thus, the main thrust of current R&D efforts is to discover and develop technologies that will result in reduced cost for energy storage.

2.1.1 VEHICLE TECHNOLOGY USING ELECTRIC OR HYBRID PROPULSION

2.1.1.1 Hybrids

Hybrid electric vehicles are based upon combining an ICE, an electric motor, and an electrical storage system in a flexible architecture: the drive train operates either with electrical power from the battery or with power from the ICE. HEVs achieve higher fuel efficiency by

- use of battery power to allow the ICE to avoid operating conditions and transients in which the ICE operation is inefficient (idling, acceleration, deceleration), and
- recuperation of braking energy to replenish the energy storage system.

The ICE sustains the charge level of the battery. During periods when combustion engine operation is inherently inefficient and the vehicle operates on battery power, the engine is turned off. The key HEV systems include efficient electric motors and energy storage systems capable of long cycle life in a charge-sustaining mode—a mode in which the state-of-charge does not undergo large swings because the ICE is used to recharge it.

Historically, nickel metal hydride (Ni-MH) battery technology has been used in the majority of HEVs due to its relatively low cost and excellent shallow-cycling cycle life. However, recently, most major automakers have begun to introduce Li-ion batteries into their HEV lineups due to their reduced weight. Research into high-power Li-ion batteries has subsided over the past five-seven years because the relative maturity of the technology has advanced and because the consensus in the battery industry was that the next major cost reductions would occur through manufacturing scaleup, as opposed to new chemistries.

Start-stop systems permit the ICE to be turned off each time the vehicle comes to a stop, which improves mileage approximately 5-10%, especially in city driving; but start/stop systems do not provide traction assist. Start/stop batteries perform two main functions: 1 – power the auxiliary systems in a vehicle when the engine is off, such as radio, lights, and air conditioning or heating; and 2 – frequently re-start the engine, estimated to be 450,000 times over the vehicle's life. Thus, a recent focus has been on Li-ion chemistries for 12-V start/stop systems that can compete with traditional lead-acid batteries on cost, but significantly outperform them on life (both calendar and cycle life). Toward that end, new couples that offer significantly enhanced power, and reduced cost, are of interest. Recent developments in this area include the lithium titanate (LTO) anode and the 5-V nickel manganese spinel cathode. A continued challenge with this application is the requirement for engine start at -30°C.

2.1.1.2 Plug-in Hybrids (PHEVs)

PHEVs function in a manner similar to EVs except that the ICE acts as range extender for the battery. High power is demanded from the energy storage system during acceleration, passing maneuvers, and braking. High energy is demanded from the energy storage system to maximize the all-electric range of the vehicle. In addition, it is anticipated that the PHEV battery will undergo more charge/discharge cycles than an EV as the battery can and will often be at least partially recharged by the ICE. Thus, a cycle-life requirement of 5,000 cycles is imposed on PHEV batteries.

Expansion of the usable state-of-charge window for electricity storage operation, along with long electricity storage system life over many deep discharge cycles, is a critical requirement for reducing the costs of PHEVs. The desire to run in “all electric” mode, and the relatively small size of the PHEV battery (compared to the EV battery, which provides an all-electric range of 200-300 miles vs. 20-40 miles for a PHEV) results in much higher power/energy (P/E) ratios for the PHEV battery. This much higher P/E ratio results in an incrementally higher cost battery (on a $/kWh basis).

2.1.1.3 All-Electric Vehicles (EVs)

Development of EVs started in the early 1970s, and initially lead–acid batteries were used for energy storage. Storage levels for EVs were nominally 30 kWh because of weight considerations and cost. A range of 60 miles to over 100 miles, depending on driving conditions and ancillary loading, was typical for EVs.

Recently, cost has come down significantly, approximately five times over the past five to seven years, and as a result, range has increased. The General Motors Bolt provides over 230 miles of range and is offered in the mid- $30,000 price range. Nissan recently announced that the next generation Leaf will provide over 200 miles of range, and the Tesla Model 3 promises a similar range.

Although these gains at the battery and vehicle level are impressive, it is still important to recognize that a vehicle comparable to the Bolt, but with an ICE, would likely cost in the mid-$20,000 range or less, although direct comparisons are difficult. In addition, consumers have come to expect flexibility from their vehicles, enabling them to pick up children from school and to drive 500 miles for a family vacation. To enable similar functionality from an EV, fast charge (on the order of 5-10 minutes) would be necessary. All automakers are working on this capability, in addition to the continued drive to reduce cost.

2.1.2 COMPARISON OF BATTERY REQUIREMENTS FOR VEHICLE ENERGY STORAGE

Energy storage technologies and their respective applications are summarized in Figure 2-1. The vertical axis corresponds to the energy discharged in a cycle. HEVs are shallow discharge systems and thus lie beneath PHEVs and EVs on the chart. The horizontal axis corresponds to power needed from the battery. The U.S. Advanced Battery Consortium (USABC) has published requirements for energy storage systems for a large number of vehicle types. Sample requirements for 12-V start-stop batteries are shown in Table 2-2, sample requirements for PHEV batteries are shown in Table 2-3, and those for EV batteries and cells are shown in Table 2-4.

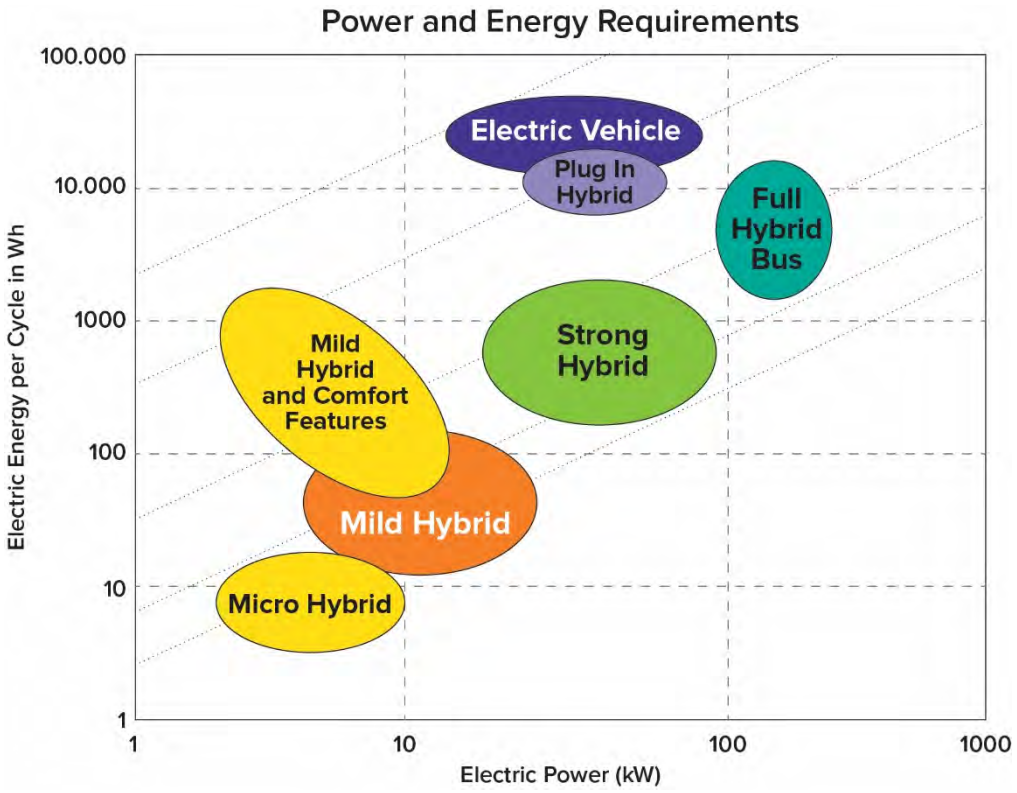

Figure 2-1. The total power and discharge power requirements for HEVs, including PHEVs and EVs. The deep discharge cycles required for PHEVs and EVs, combined with the requirements for long battery life, are now attainable with current Li-ion batteries, but high cost, relative to ICE, remains an issue. From J.B. Goodenough et al., *Basic Research Needs for Electrical Energy Storage* (2007).

TABLE 2-2: Sample storage requirements, as published by the USABC for 12-V start/stop (http://www.uscar.org/guest/article_view.php?articles_id=85)

End of Life Characteristics	Units	Target	
		Under Hood	Not Under Hood
Discharge Pulse, 1 s	kW	6	
Cold Cranking Power at -30 °C	kW	6 kW for 0.5 s followed by 4 kW for 4s	
Min. Voltage under Cold Crank	V (dc)	8.0	
Available Energy (750-W accessory load power)	Wh	360	
Peak (sustained) Recharge Rate, 10 s	W	2200 (750)	
Cycle Life	Engine starts/miles	450k/150k	
Calendar Life	Years	15 at 45°C	15 at 30°C
Peak Operating Voltage, 10 s	V (DC)	15.0	
Maximum System Weight	kg	10	
Maximum System Volume	L	7	
Maximum System Cost (@250k units/year)	$	220	180

TABLE 2-3: Sample electricity storage requirements, as published by the USABC for PHEV40 (http://www.uscar.org/guest/article_view.php?articles_id=85)

End of Life Characteristics		Target
Electric Range	miles	40
Peak Pulse Discharge Power (2 sec/10 sec)	kW	46/38
Peak Regen Pulse Power (10 sec)	kW	25
Available Energy	kWh	11.6
Cold Cranking Power at -30°C	kW	7
Deep Discharge Cycle Life	Cycles	5,000
Calendar Life, 35°C	year	15
Maximum System Weight	kg	120
Maximum System Volume	Liter	80
Production Price @ 100k units/yr	$	$3,400

TABLE 2-4: Sample electricity storage requirements, as published by the USABC for EVs (http://www.uscar.org/guest/article_view.php?articles_id=85)[3]

End of Life Characteristics	Units	System Level	Cell Level
Peak Discharge Power Density	W/L	1000	1500
Peak Specific Discharge Power	W/kg	470	700
Peak Specific Regen Power	Wh/L	200	300
Usable Energy Density (C/3)	Wh/L	500	750
Calendar Life	Year	15	15
Dynamic Stress Test Cycle Life	Cycles	1000	1000
Cost	$/kWh	125	100

2.1.3 MAJOR UNMET REQUIREMENTS

As mentioned above, Li-ion chemistries have advanced significantly over the past several years; energy densities and life have gone up, and costs have come done. It is notable that there are both 200 and 300 mile EVs on the market today. Thus, it is not immediately obvious that significantly higher energy densities are needed. However, it is generally accepted that higher energy cells will result in reduced number of cells in the full pack, with reduced interconnects, voltage and current sensors, etc., thus reducing the full pack cost.

Partially as a result of that, and the realization that further major improvements may be realized through the use of other chemistries, the battery R&D community has intensified efforts to solve major issues with both next-generation Li-ion chemistries – like silicon anodes and very high voltage cathodes – and beyond Li ion (BLI) chemistries that use Li metal anodes and non-intercalation cathodes, including sulfur and air. Table 2-5 presents the major remaining unmet requirements in three categories.

TABLE 2-5: Sample unmet performance requirements for three storage technologies (http://www.mass.gov/eea/docs/doer/state-of-charge-report.pdf).

Unmet Requirement	Li Ion	Next Gen Li Ion	BLI
Energy and power densities	Reasonable	Relatively slow kinetics of silicon anodes could limit power. High voltage operation leads to increased cell impedance over time, thus limiting power.	Poor power of solid state cells. Reduced energy density of Li/S cells due to the use of excess electrolyte.
Cycle and calendar life	Reasonable	Cycle life 2x-3x too low, calendar life 3x-10x too low. Poor silicon solid-electrolyte interface (SEI) stability, reduced electrolyte stability at high voltage, cathode surface instability at high voltage.	Cycle life 10x too low. Lithium metal SEI instability; sulfur self-discharge limits calendar life; severe impedance increase limits solid state cells' cycle life.
Extreme fast charge (XFC)	Li ion can support XFC, but not without major cost increase introduced through use of thin electrodes. Lithium plating remains a major concern.	Relative slow kinetics of silicon anodes could be an issue.	Unknown. Poor conductivity of solid state electrolytes could be a major impediment to fast charging.
Low temperature operation	Severe reduction in EV range, lack of cold start in 12-V system.	Severe reduction in EV range.	Unknown.
High temperature life	Poor high temperature life, perhaps related to the use of $LiPF_6$ salt. High temperature excursions can also lead to thermal runaway.	Poor high temperature life is an issue with most next gen Li-ion cells. High temperature excursions can also lead to thermal runaway.	Unknown. High temperature performance could be better than room temperature performance in solid state cells
Abuse tolerance	Flammability of carbonate electrolytes continues to be an issue with Li-ion cells. Internal short circuits are the least understood abuse issue. Extreme fast charge may increase likelihood of Li plating and internal short circuits.	Flammability of carbonate electrolytes will likely be an issue with next gen Li-ion cells, Extreme fast charge may increase likelihood of Li plating and internal short circuits.	Lithium dendrites remain a major abuse tolerance concern for Li metal batteries. Solid state cells should have better abuse tolerance than Li-ion and next gen Li-ion cells.

Unmet Requirement	Li Ion	Next Gen Li Ion	BLI
Cost	Manufacturing cost of active materials, electrodes, and cells. Raw material costs of Co and Ni are concerning.	Manufacturing cost of Si is currently high. It is unknown whether this will come down with increasing volumes. Raw material costs of many transition metal cathodes are concerning.	Current solid state electrolytes are unacceptably expensive.

2.2 Electrical Power for Grid

2.2.1 BACKGROUND ON GRID SCALE STORAGE

The electricity grid is central to the nation's infrastructure and security. Energy storage is emerging as an integral component to a resilient and efficient grid through a diverse range of potential applications across the grid infrastructure. The modernization of the grid will result in a greater need for services best provided by energy storage, including energy management, backup power, load leveling, frequency regulation, voltage support, and grid stabilization. Energy storage is also becoming increasing necessary to accommodate large-scale integration of distributed generation into the grid. The increase in demand for specialized services will further drive energy storage research to produce systems with greater efficiency at a lower cost.

Advanced energy storage solutions have become increasingly critical with growing demands for a more resilient and reliable grid with improved power quality and the ability to accommodate an increasingly diverse portfolio of electric generation technologies. The growth in the numbers of hybrid, fuel cell, and electric vehicles, and an aging grid infrastructure with serious bottlenecks in transmission and distribution infrastructure can also be accommodated with grid energy storage. Energy storage provides an intelligent buffer between generation and demand that provides grid operators an essential tool for a reliable, resilient, and flexible power grid. Thus, energy storage becomes an enabling technology that can supply energy when it is needed and provides enhanced flexibility under the increasingly dynamic generation and demand needs to ensure the resiliency of the grid infrastructure when severe disruptions occur.

Worldwide, the electric grid with an installed generation capacity is about 7 TW with a generation mix largely consisting of coal, natural gas, nuclear, and hydro. In 2014, worldwide electricity generation was 24 trillion kilowatt-hours with an operating storage reserve of less than 170 GWh.[1] More than 95% of the existing energy storage capacity is in the pumped hydro plants that were built as part of the expansion of the nuclear power plants in the 1970s and early 1980s. Figure 2-2 captures historical growth of energy storage around the world. Over the last few years, deployment of battery-based energy storage has begun to get traction in the marketplace. Recent data from the DOE Global Energy Storage Database, shown in Figure 2-3, indicate that the pace of battery energy storage deployments is accelerating. In fact, 2016 is the first year when the annual deployment of battery-based storage crossed the 1 GWh mark.

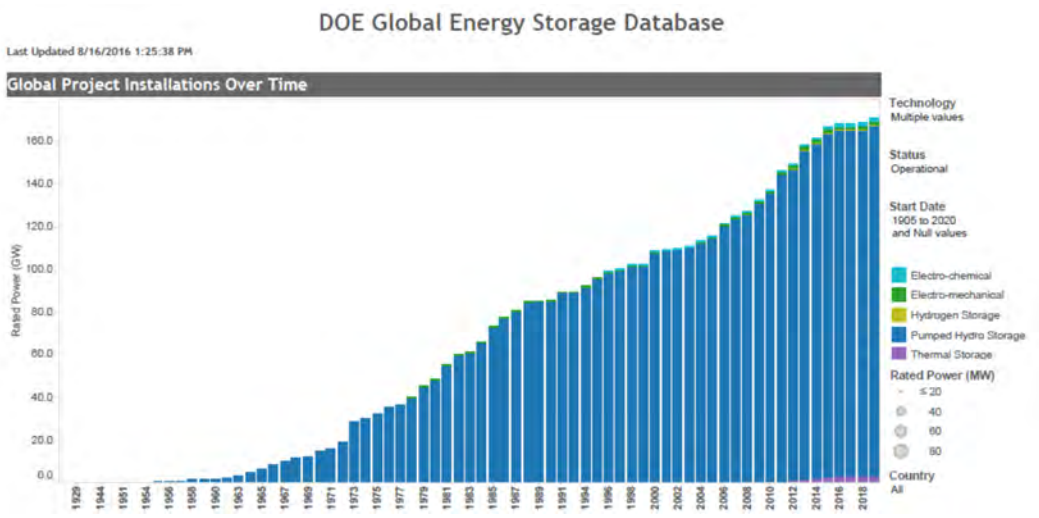

Figure 2-2. Worldwide energy storage installations: 171 GW installed in 1267 projects[2]

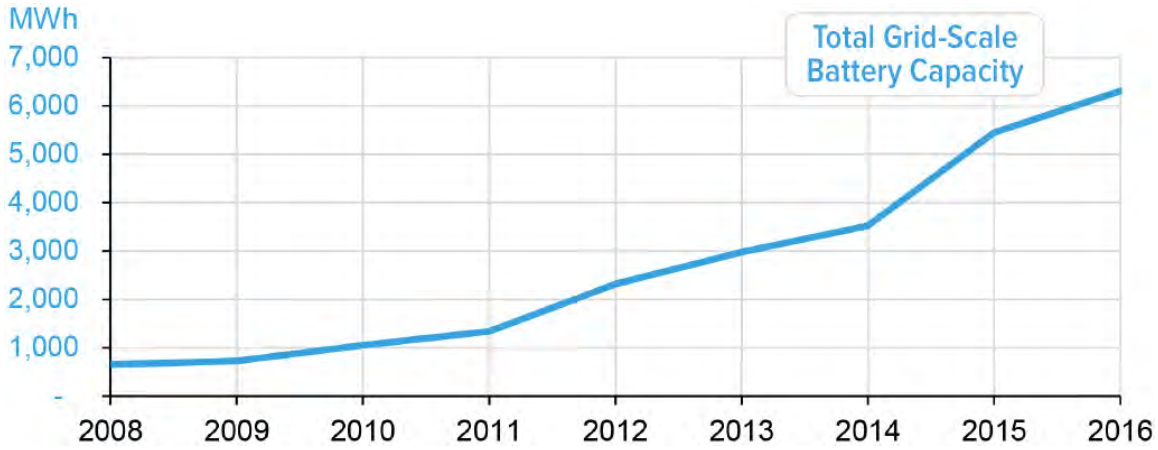

Figure 2-3. Grid-scale battery-based energy storage deployments across the world (MWh)[2]

Electrochemical energy storage via battery storage systems offers the greatest flexibility in power and power capacity across the vast majority of application markets; from the kWh class behind the meter applications, to 50-100 MWh peaker replacements, to large projects to support transmission and distribution infrastructure deferrals. The U.S. and global market for energy storage technologies is set to expand quickly, with most market studies pointing to rapidly increasing deployments across all market segments.[3] According to BNEF, the world-wide grid storage market is expected to increase over tenfold by 2025, with nearly 80% of the growth outside of the U.S. Further reductions in cost and improved understanding of economic benefits can dramatically accelerate this adoption.

2.2.2 CHALLENGES FOR STATIONARY ENERGY STORAGE TECHNOLOGY

The use of energy storage within the U.S. electrical system has long been championed by DOE as a critical and enabling element of a smarter, more flexible, and resilient future grid. In 2013, DOE outlined the current status of grid energy storage[4] and identified four primary challenges:

- **Cost-Competitive Energy Storage—**Develop material and system enhancements to resolve key cost and performance challenges with respect to novel flow, lithium, sodium, magnesium, and thermo-

electrochemical batteries and associated electrodes, dielectrics, membranes, electrolytes, interconnects, and supporting power electronics.

- **Validated Reliability and Safety—**For energy storage systems to be ubiquitously accepted, the technology must be demonstrated to be safe and reliable. This activity's goal is to develop a scientifically derived knowledge base that will improve understanding and predictability, engineer safer and more reliable systems, and ultimately lead to the development of new protocols, codes, and standards for safety and reliability.

- **Regulatory Environment—**Value propositions for grid storage depend on reducing institutional and regulatory hurdles to levels comparable with those of other grid resources. To accomplish this objective, the DOE Office of Electrical Delivery and Energy Reliability's Energy Storage program has partnered with Federal, state, and municipal entities to analyze the use, benefits, and costs of energy storage systems and to develop tools for utility customers and regulatory agencies for planning and implementing the effective deployment energy storage. This accelerates the community's ability to overcome regulatory hurdles and provides an environment where energy storage deployment and service opportunities are recognized, appropriately valued, and implemented.

- **Industry Acceptance—**Demonstrating the value, performance, and reliability of energy storage systems in both controlled and fielded deployments is critical to achieving industry acceptance. DOE support of these effort enables confident development, deployment, and operation of grid energy storage through controlled testing of prototype commercial storage and installation, commissioning, monitoring, and reporting of results from field demonstrations of grid storage systems. The development of tools for utility customers and regulatory agencies for planning, deployment, and use of energy storage also plays a critical role in enabling industrial acceptance of energy storage technology.

Ultimately, the value proposition for grid-scale energy storage comes down to the fundamental tradeoff between storage costs and the economic benefits. The costs for energy storage systems have been steadily declining over the past 5 years, primarily driven by the availability of lower cost Li-ion technologies developed for automotive EV applications. The capital cost of the battery system, however, is only part of the overall cost equation. Along with the storage device, there are costs associated with the battery management system, power conditioning, integration, and installation soft costs. In general, the battery pack accounts for > 40% of the overall systems cost, as shown in the Figure 2-4 cost distribution for a typical 1 MW/L, MWh Li-ion installation.

Levelized costs for all battery technologies have decreased over the past several years, making the capital cost of battery-based storage comparable with pumped hydro storage for large utility class applications.[5] However, in addition to the capital costs, the entire lifecycle cost must also be considered for projects to be economically viable.

A number of recent market studies have made an effort to develop a uniform framework to evaluate energy storage across large market segments. For example, Lazard has developed levelized cost of storage as a metric that effectively captures capital costs and overall performance of the system based on delivered energy.[6] The Lazard analysis shows that the levelized costs for energy storage systems are still too expensive for most applications and further cost reductions of 2-3X are still required for storage to replace, for example, gas peaker facilities.

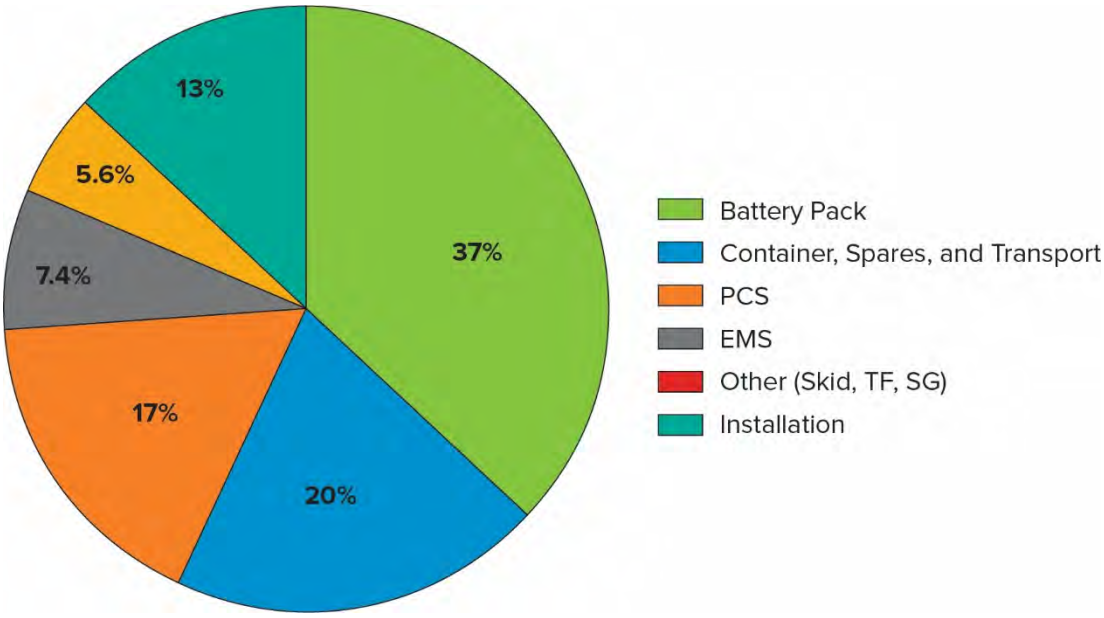

Figure 2-4. Projected cost line items for a 1 MW/L MWh Li-ion energy storage system ($600/kWh and above depending on the system configuration)

There is the opportunity for storage to have a greater role in the grid infrastructure; however, the current cost structure does not allow for implementation of storage at the scale needed. Most large-scale deployments have been limited to select markets, where the essential services that energy storage can provide have been adequately monetized. For example, storage has found application for regulation services where market mechanisms exist that pay for faster response storage assets. Since 2011 when storage was allowed to compete in the PJM Regulation Market, over 300 MW of new energy storage systems has been deployed, resulting in a fourfold decrease in the cost of regulation services.[7] In numerous other applications, energy storage can provide faster or better than conventional resources; however, markets mechanisms are not in place. Unlike frequency regulation, bulk applications in other markets such as infrastructure deferrals, generation optimization, and resiliency are not economically viable with the relatively high cost of current technology. For example, energy storage can effectively be used to defer a portion of the nearly $100B in annual upgrades to the transmission and distribution infrastructure required. The same can be said about applications in outage mitigation where energy storage can be utilized to reduce the $50-100B in annual economic losses for commercial and industrial customers from power outages while providing backup power and islanding capability during natural disasters.

Further advances are needed to move lower-cost technologies toward large-scale manufacturing, improve the overall system safety and reliability, and develop the engineering and market solutions to make large-scale deployments attractive for utilities in the U.S. and around the world.

2.2.3 FUTURE OUTLOOK

Over last five years, there has been tremendous across-the-board price reduction in the cost of energy storage. So far, most of the cost reductions have come through improvements in battery technologies. Further cost reductions will yield additional value realization through advances in power electronics and power conversion systems, sensors, and software and control systems. In addition, there is greater opportunity to reduce soft costs through improved plant layouts, system level standardization, streamlined permitting processes, and lower construction and startup costs. Greater deployment and operational experience will help to make continued improvements in the safety, reliability, and operational performance of energy storage systems. This

will lead to predictable maintenance schedules and improved operational performance, further enabling greater adoption of energy storage by utilities and grid operators.

Energy storage technology is at a stage where further research is needed to ensure that the technology becomes cost-effective and reaches the technical maturity needed to become viable across all application markets. Unlike other technologies, energy storage is a complex system that requires advancements from materials science and manufacturing, to applications that are beyond the scope of many in industry.

References

1 *IEA Key World Energy Statistics*, 2016.

2 *DOE Global Energy Storage Database*, www.energystorageexchange.org, 2016

3 *Global Energy Storage Forecast, 2016-24*, Bloomberg New Energy Finance (BNEF), 2016.

4 *USDOE Grid Energy Storage*, http://energy.gov/sites/prod/files/2013/12/f5/Grid Energy Storage December 2013.pdf, December 2013.

5 CES Ltd and IESA, *State of Charge: Massachusetts Energy Storage Initiative*, Mass DOER, p. 8, 2016.

6 *Lazard's Levelized Cost of Storage*, Version 2.0, December 2016.

7 Karen H. Queen, "PJM leverages federal rule changes to lead country in energy storage," Southeastern Energy News, http://southeastenergynews.com, November 28, 2016.

2.3 Consumer Electronics

2.3.1 INTRODUCTION

Over the last two decades, consumer electronics (laptops and cell phones) have been the main market for Li-ion batteries. Indeed, the tremendous progress in Li-ion energy densities, the cost reductions, and the engineering advances have all been driven by the growing requirements in the consumer market. This access to this early market, with much less stringent requirements compared to the vehicle and grid markets described above, provides a testing ground for new technologies. In addition, new markets that will require newer batteries, including wearables, virtual and augmented reality headsets, and internet of things (IOT), are emerging. This section briefly describes the battery requirements for these applications and the challenges ahead.

2.3.2 TECHNOLOGY AND CHALLENGES

In all consumer applications, the run time (i.e., energy density and specific energy) remains the most important metric. While run time is maximized, the battery has to meet a number of second tier requirements, including:

- Enough power achieving peak computing needs
- High temperature range of operation
- Fast charge
- Intrinsically safe
- Long cycle life

In addition, smaller devices such as wearables and IOT require batteries that are not curved and can be integrated into the rest of the device (e.g., watch bands). In addition, as the devices become smaller, the weight and volume of the packaging become a bigger fraction of the total weight and volume of the cell, dramatically decreasing energy density. Figure 2-5 plots the energy density of the battery with increasing height of the cell. While the energy density limit is 750 Wh/L for today's Li-ion cells, the energy density can be an order of magnitude lower for smaller devices, if the same architecture is used. This suggests that newer ways to improved battery architecture are needed to decrease the penalty of the packaging in small dimension devices.

2.3.3 BATTERY REQUIREMENTS AND PRESENT STATUS

Table 2-6 describes the technology needs for various consumer electronics applications and the present status of battery technology. All the consumer devices described below use Li-ion batteries with a graphite anode, $LiCoO_2$ cathode, and a liquid organic electrolyte in a pouch cell configuration.

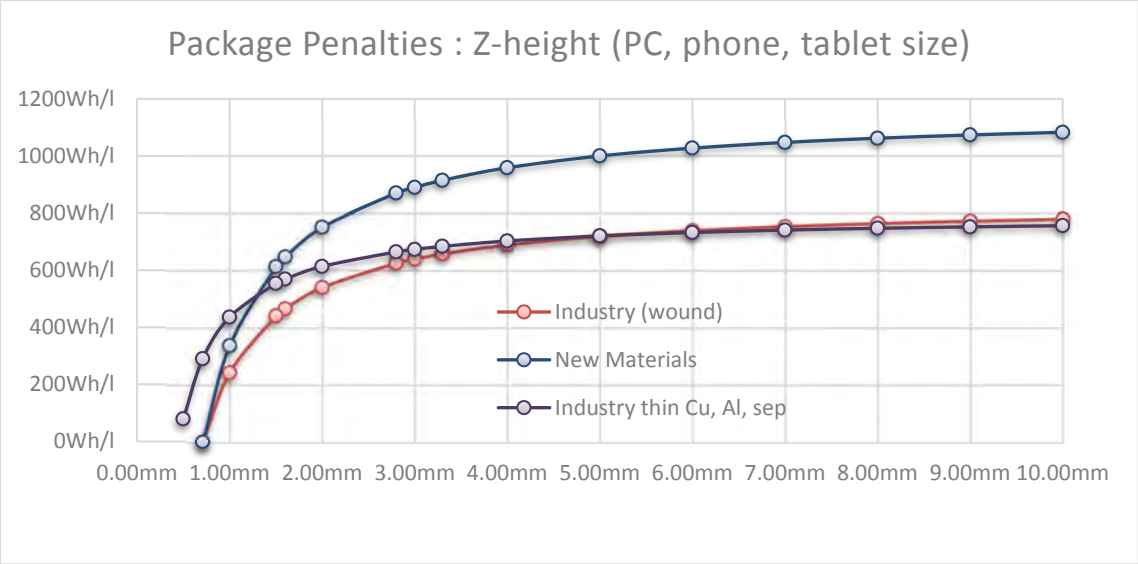

Figure 2-5. Energy density of Li-ion batteries and the penalty of decreasing height of the cell while maintaining the packaging the same. The plot demonstrates the importance of new architectures to minimize the penalty of packaging in small dimension devices. Courtesy: Andy Keates, Intel Corp.

TABLE 2-6: Battery status and targets for various consumer electronic applications. Courtesy: Jerry Hallmark, Enovix Corp. and formerly from Motorola Corp.

	Energy Density (Wh/l)		Energy Density (Wh/kg)		Power Density (W/kg)		Charge Rate		Discharge Rate		Cycle Life	
Market	Status 2017	Target	Status 2017	Target	Status 2017	Target	Status 2017	Target	Status 2017	Target	Status 2017	Target
IoT	200-300	500	100	200	200	400	1C	2C	2C	4C	500	1000
Wearables	450-500	600-700	150	300	200	400	1C	2C	2C	4C	400-500	500-700
Cell Phones	700-720	800-1000	150	300	200	400	1.5C	3C	2C	3C	500	800-1000
Tablet/Laptop	710-730	800-1000	150	300	200	400	1.5C	3C	2C	3C	800	1000

3 ELECTRIC ENERGY STORAGE SYSTEMS: PRESENT AND NEXT GENERATION

3.1 Overview of Rechargeable Electrochemical Energy Storage

Electrochemical energy storage devices store energy either in an electrical double layer or in the form of chemical energy which is converted to electrical energy, on demand. While the former mode of charge storage is referred to variously as an “electrochemical capacitor,” “supercapacitor,” or “double layer capacitor,” the latter is referred to as a “battery.” Rechargeable batteries reversibly convert from electrical to chemical energy, with the voltage of each half cell dictated by the thermodynamics of the respective electrochemical reaction. The more positive half-cell is referred to as the positive electrode (or cathode), and the more negative potential as the negative electrode (or anode), with the cell voltage being the difference between the positive and negative half-cell reactions.

During charge, external energy is provided to allow reactions to proceed at each electrode, with the positive electrode undergoing oxidation and the negative electrode, reduction; and the chemicals are now in an unstable state. Upon discharge, the process is reversed, the chemicals are moved back to the ground state, and energy is provided to the external circuit for useful work. As the electrons are moved away from the reactant sites to the external circuit, ions move across the electrolyte to complete the circuit. While the thermodynamics provides the potential of the battery under an infinitely small load, the actual cell potential and the level of utilization of the chemicals in the reaction are dictated by the ion and electron transport and conductivity in the various phases, as well as the rate of charge transfer at the electrode/electrolyte interface.

There are four basic mechanisms to store energy in electrochemical systems:

- In the electrochemical double layer, as described above, wherein no electrochemical reaction occurs. Ions need only to move small distances (i.e., the Debye length), allowing fast charge/discharge. No structural changes occur, allowing long cycle life; however, relegating charge storage to the surface results in low energy density.

- By reacting at the interface and storing the products in the bulk of the electrode material, *via* intercalation or alloying. Examples include Li-ion intercalation systems and the Ni-MH battery. The bulk charge storage allows high specific energy compared to capacitors. Intercalation systems, especially, allow the possibility of little structural change and long life. However, storing a large amount of charge can result in degradation of the materials due to volume expansion and/or structural changes. In addition, storing products in the bulk requires diffusion in solid phases, which can limit power capability as the diffusion length increases.

- By reacting at the interface and converting from one form of matter to another, such as conversion, electroplating, or dissolution/precipitation. Examples include the lead-acid battery, the cadmium and zinc electrode, sulfur and oxygen cathodes, metal-anode batteries, and Li-ion conversion cathodes. Such systems allow very high capacities because of the possibility of continuous conversion without increasing the diffusion length. However, this mechanism relies on changes in the physical morphology, which can be a detriment to achieving long cycle life.

- By storing the reactants and the products in the electrolyte in the form of a redox molecule. The amount of storage capacity is dictated by the solubility of the redox molecule in the electrolyte, which can be significantly smaller than what is possible in the solid state. This constraint can be circumvented by storing the reactants outside the electrochemical cell, and is used in a flow battery configuration. Examples include vanadium, iron, and chromium. Reactants are also stored in the gaseous phase, such as the hydrogen electrode.

The choice of material dictates the mechanism of charge storage. The design of the electrode and of the cell is influenced by the mechanism of storage and the thermodynamic, kinetic, and mass transport characteristics of the electrode and electrolyte materials. The following sections explore different materials choices that are presently being pursued, the status of the chemistry, and the challenges that remain to be solved. Also explored is the assembly of materials into electrodes and cells with some of the recent developments in the last decade.

3.2 Pre Li-Ion Electrochemistries

The remainder of this chapter is a review and assessment of present and future electrical energy storage systems.

3.2.1 LEAD-ACID BATTERIES

Introduction

Lead–acid batteries (~2 V per cell) are based on the reversible electrochemical conversion of lead to lead sulfate (anode) and quadrivalent lead oxide to lead sulfate (cathode) in a concentrated sulfuric acid electrolyte. The electrodes are generally formed by a detailed process to give a thick coating (~1 mm) of lead compounds and additives on current collectors (grids) of lead, alloys, or carbons. For good cycling, the active electrode materials must remain connected electrically to the current collectors and wetted by the electrolyte. The many morphologies that can form upon cycling complicate the reactions at the electrodes. Most common lead–acid batteries are formed as stacked electrode plates, whereas some advanced designs are spiral-wound. The half-cell reactions for the cell discharge, the open circuit potential for a charged cell, and the theoretical energy density based on the cell reactions and mass of active material are shown in the following formulas. The reactions are reversed upon charge of the cell.

Anode: $Pb + SO_4^{2-} \longrightarrow PbSO_4 + 2\,e^-$

Cathode: $PbO_2 + 4\,H^+ + SO_4^{2-} + 2\,e^- \longrightarrow PbSO_4 + 2\,H_2O$ 2.1 V; 252 Wh/kg

State of the Art

Lead–acid batteries have complete acceptance for automobile starting, lighting, and ignition (SLI), tasks for which low cost has been the most compelling factor. Batteries for SLI applications in ICE vehicles operate from a state-of-charge (SOC) of about 90% and are required to provide power for engine cranking of up to 10 kW. This translates to a specific power of up to 600 W kg^{-1}, normally sustained for less than 1 second.[1] SLI batteries can provide a cumulative energy throughput of about 100 times the nominal capacity, and an end-of-life condition is reached after 5,000 to 10,000 cranking events (4–6 years in temperate climates). Lead–acid batteries reliably meet the requirements for SLI applications. The end-of-life failure is due to either corrosion of the grid or shedding of the active material from the positive plate. This limited lifetime is tolerated because of the low cost of the replacement batteries. The poor specific energy of the lead–acid battery is not sufficient to offset the cost advantage for the SLI applications.

Electric and Hybrid Vehicles

Batteries for EVs must be capable of being discharged to a rather low state of charge and then being fully recharged. For lead–acid batteries, cycling over a wide SOC range maximizes the volume change of the active material and exacerbates the tendency for active material to be shed from the plates. Full cycle duty can also lead to corrosion of the positive grid.

Such failure mechanisms can be held at bay in valve-regulated lead–acid (VRLA) batteries by the use of high levels of compression to the plate stack and by the use of corrosion-resistant alloys in the manufacture of the grids. Deep cycle lives of up to 1000 cranking events have been achieved by using these methods. The specific energy of lead–acid batteries is limited to around 35 Wh kg^{-1}; however, if the weight of batteries is to be held within reasonable bounds, it is unlikely that the range of an EV with lead–acid batteries could exceed 100 miles. This was the maximum range achieved by the lower-cost version of the GM EV1.

Neither conventional 12-V SLI batteries nor present-generation deep-cycle batteries can provide the performance required by the new high-power HEV systems for an acceptable life. Batteries for these high-power systems will operate from a partial-SOC baseline and will be discharged, and particularly recharged, at extraordinarily high rates (albeit within a small SOC range). Under such conditions, the life-limiting mechanism appears to involve the progressive accumulation of lead sulfate on the negative plate. This failure mode appears as a result of the very high rates of recharge and persists because the battery is not routinely returned to a full state of charge in the required duty cycle.

To offer an acceptable life in such applications, conventional designs of VRLA batteries must be revised. The battery must be able to sustain the negative plate charge reaction at very high rates, overcoming diffusion limitations (leading to reduced lead sulfate solubility, etc.) that would otherwise lead to the onset of secondary reactions, such as hydrogen evolution, and charge inefficiency.

Two straightforward design modifications offer the potential to redeem this situation and to allow the lead–acid battery to perform successfully in the high-rate partial (HRP) SOC routine demanded in HEVs. Providing an appropriate grid design allows the plates in the battery to accept the high charge rates required, and incorporating elevated concentrations of carbon (a few wt % instead of the traditional 0.2 wt %) alleviates the tendency for sulfate to accumulate and appears to offer the route to a long operating life in the HRP-SOC regime.

Batteries assembled with these relatively straightforward design elements are generally able to match the DOE FreedomCAR peak power goals for minimum power assist (625 W kg^{-1}) and, in some cases, to approach the peak power goals for maximum power assist (1000 W kg^{-1}). Such batteries are also able to perform 300,000 simulated HEV cycles without failing, thus achieving the FreedomCAR lifetime goal.[2]

Batteries rated at 144 V of all three types shown in Table 3-1 have been running successfully in Honda Insight HEVs from which the original Ni-MH batteries have been removed.[3] In the medium hybrid application (offering regenerative braking and power assist but little or no all-electric range), the specific energy of the battery is less important than its ability to provide adequate power for an acceptable life.

TABLE 3-1: Batteries specifically designed for high-rate partial-state-of-charge operation—as in power-assist HEVs

Battery type, manufacturer	Design elements
"RHOLAB" (8 Ah), Enersys	Twin-tab to boost power, spiral wound
Bipolar (7 Ah), Effpower	Bipolar plate of porous ceramic impregnated with lead
Ultra (7 Ah), Furukawa/CSIRO	Additional carbon capacitive element in common with negative plate

A frequent mistake is to point to the SLI battery as evidence that lead–acid batteries are unable to satisfy the performance requirements of other, quite different, applications. In fact, when designed specifically for that purpose, batteries that make use of the lead–acid chemistry are capable of providing useful service in deep discharge and, particularly, in HRP-SOC regimens.

Technical and Cost Barriers

Although a list of critical technological barriers will differ for different applications, the following are the main issues limiting development and expanded use of lead–acid batteries.

Technical barriers and needs	Component(s)
• Low specific capacity and energy	• Active materials and grids
• Progressive buildup of a resistive lead sulfate layer with cycling	• Negative electrode
• Corrosion of current collector with cycling	• Positive electrode
• Loss of active material due to shedding as the result of volume changes for the active materials	• Active materials
• Need for lightweight grids that can operate at extremely high rates	• Grids
• Need for a way in which elevated levels of carbon (graphite) in the negative plate can dramatically improve the performance of VRLA batteries in the high-rate partial-state- of-charge duty required by HEVs	• Negative electrode

3.2.2 NICKEL BATTERIES

Introduction

Nickel batteries of approximately 1 V all share the same cathode, which is nickel oxyhydroxide in the charged state. In an aqueous KOH electrolyte, the cathode discharges to form nickel hydroxide. The anodes are either metals that oxidize to form a hydroxide, or metal hydrides that lose hydrogen when discharged. In the following general half-cell reactions, *M* indicates the metal or alloy at the anode. The theoretical specific energy is also listed.

Cathode: $2\ NiOOH + 2\ H_2O + e^- \longrightarrow 2\ Ni(OH)_2 + 2\ OH^-$

Anode 1: $M + 2\ OH^- \longrightarrow M(OH)_2 + 2\ e^-$ 1.35–1.7 V, 244–372 Wh/kg

Anode 2: $2\ MH + 2\ OH^- \longrightarrow 2\ M + 2\ H_2O + 2\ e^-$ 1.35 V, 240 Wh/kg

where M = Cd or Zn

The open-circuit voltage and other specifications for this family of batteries are listed in Table 3-2. A complication with this cell chemistry arises from the formation of oxygen gas at the cathode upon recharge of the cell. After ~80% charge, oxygen is generated via this formula (Figure 3-1):

$$2\ OH^- \longrightarrow H_2O + \tfrac{1}{2}\ O_2 + 2\ e^-$$

TABLE 3-2: Overview of the performance characteristics of nickel battery systems

System	Ni-Cd (pocket)	Ni-Cd (sealed)	Ni-MH	Ni-Zn	Ni-Fe (pocket)	Ni-H_2
Open-circuit volt.	1.2	1.2	1.2	1.6	1.4	1.2
Wh/L	40	100	75	60	55	105
Wh/kg	20	35	240	120	30	64
Power	Low	High	High	High	Low	Med
Discharge	Flat	Flat	Flat	Flat	Flat	Flat
Cycle life	2000	700	600	500	4000	6000

In a sealed cell, with a minimum amount of electrolyte, this oxygen can diffuse back to the anode, where it reacts to generate water and prevent any buildup of gas pressure. In a vented cell, also known as a pocket cell, the cell is flooded with excess electrolyte and includes a gas barrier to prevent this occurrence. This arrangement is described in more detail in the following section. The capacities of the anode versus cathode are adjusted to control reactions. All systems in Table 3-2 have a flat discharge voltage characteristic and must use electronic controls for SOC determination.

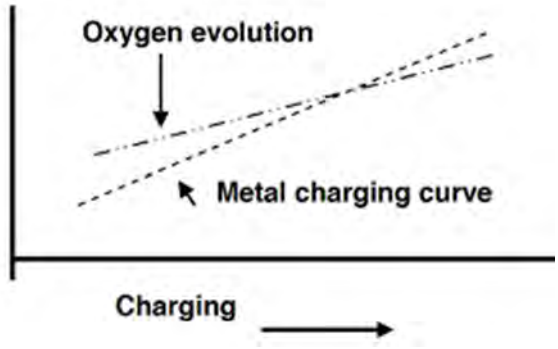

Figure 3-1. Oxygen forms at the cathode after 80% cell recharge

State of the Art

Nickel-Cadmium (Ni-Cd)

$$Cd + 2\ NiOOH + 2\ H_2O = Cd(OH)_2 + 2\ Ni(OH)_2$$

Ni-Cd batteries have two incarnations. One is the Edison construction with nickel or nickel-plated-steel pocket plates to hold the active mass, or reactants, with conductive KOH media. This was the basis for the original Edison cell that has excellent low-rate performance with extremely long cycle life and a calendar life of 30 or more years. It is used today mainly in railroad cars in Europe and was incorporated in a recent utility energy storage demonstration in Alaska. The initial cost is significantly more than for lead–acid batteries, but the overall cost is lower when increased reliability, maintenance, and length of service are considered.

The second incarnation was a sealed cell developed for jet planes in Germany during WWII. The active mass was vacuum-impregnated into original sintered carbonyl-powdered nickel to form the electrode structure. Cells are flat plate or spiral wrap construction. Today, high-performance electrodes use an open nickel fiber or nickel

foam structure impregnated with high-density spherical $Ni(OH)_2$. For portable power applications, Ni-Cd was the original mobile phone and notebook battery but lost out to Li-ion with its lighter weight and higher energy storage capability. It is characterized by an excellent high-rate and low-temperature capability, as well as resistance to abuse and overcharge. For full charge, the nickel electrode operates above the oxygen potential; and for full charge, oxygen is liberated. Oxygen then diffuses through the porous separator structure and recombines on the cadmium electrode. The high-surface-area nickel provides a good reaction surface to recombine oxygen formed during charge and on overcharge. It can be overdischarged without damage. Ni-Cd batteries are used universally for starting and emergency power on jet aircraft because of their reliability and wide temperature operating range.

The depiction of the overcharge mechanism is shown in Figure 3-2. For sealed Ni-Cd, a simple charger can be used, and charge can be terminated by temperature or voltage measurement. Cadmium is toxic and, because of environmental issues, is banned in several countries in Europe. Recycling processes are in place but do not recover the materials for reuse in the Ni-Cd cell assembly.

Nickel-Metal Hydride (Ni-MH)

$$(M)H + 2\ NiOOH = M + Ni(OH)_2$$

The Ni-MH cell was first proposed at COMSAT and Bell Laboratories as a substitute for Ni-Cd in satellite applications. It does not have the same environmental restrictions as Ni-Cd. Ni-MH is used in all HEVs on the market today. Basically, Ni-MH has the Ni-Cd cell construction and replaces the cadmium electrode with an AB_5 hydride storage electrode composition, where A is Ni and B is lanthanum (or another rare earth element). The AB_2 alloy with a different structure has found acceptance for its higher hydrogen storage capability. Most commercial systems use the AB_5 alloy, as it has better high rate and longer cycle life. Recently, a new alloy, A_2B_7, based on a combination of structures, has been developed that has greater performance. The change also allows a rebalancing of the capacities of the anode and cathode to deliver a higher-performing system. The composition of the hydride electrode is a complex mixture, with additives to prolong cell life, reduce self-discharge, etc. The composition has been referred to as a "kitchen sink" alloy because of its many components.

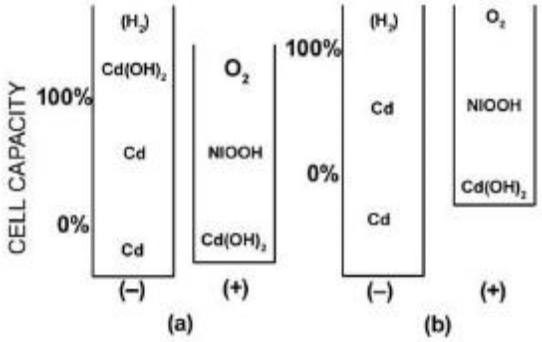

Figure 3-2. Cell balance for (a) sealed and (b) vented Ni-Cd cells. In sealed cells it is essential to prevent H_2 evolution on charge and essential that only O_2 be evolved. The oxygen evolved from the nickel electrode diffused to the Cd electrode, where it reacts to form cadmium metal. From J.B. Goodenough et al., *Basic Research Needs for Electrical Energy Storage* (2007).

The flat discharge characteristic, excellent high rate, long cycle life, and abuse tolerance has made Ni-MH the first choice for use in HEVs. The flat discharge makes determination of the state of charge more difficult. Performance falls off quickly below 0ºC and becomes rate sensitive because of the hydride electrode. The Ni-MH system has a self-discharge rate of about 15–30% per month, depending on the hydride alloy composition. The Ni-MH has the same ability to withstand overcharge and overdischarge as does the Ni-Cd system, along with a significant increase in energy storage capability. As a result, the Ni-MH is a high-performance system that is very robust and can tolerate abuse without damage. The charge process for Ni-MH is depicted in Figure 3-3. Significant research activity on alloy compositions and new higher-performance spherical nickel hydroxides have improved performance considerably.

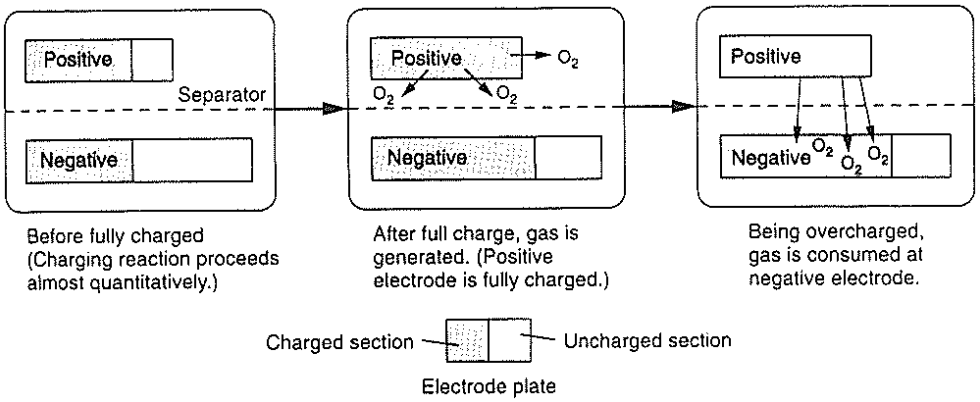

Figure 3-3. Charge and overcharge processes for a sealed Ni-MH cell. The different cell balance for Ni-MH results in a higher capacity for Ni-MH over Ni-Cd for the same size cell. From J.B. Goodenough et al., *Basic Research Needs for Electrical Energy Storage* (2007).

Nickel-Zinc (Ni-Zn)

$$Zn + 2\ NiOOH + 2\ H_2O = Zn(OH)_2 + 2\ Ni(OH)_2$$

The Ni-Zn battery has a spiral wrap construction similar to that of the sealed Ni-Cd, but the cadmium electrode is replaced by a zinc electrode. The result is a higher-voltage unit cell than in either the Ni-Cd or Ni-MH, coupled with the excellent high-rate capability of the zinc electrode. Zinc has faster kinetics than cadmium for better high-rate performance. Past issues with Ni-Zn center around the tendency of zinc electrodes to undergo shape change (densification), passivation, and dendrite formation. At one time, GM had a sizable Ni-Zn battery development effort aimed at use in EV and SLI applications. Recently, PowerGenix has addressed these issues and has developed new electrolyte compositions that prolong the integrity of the zinc electrode to increase cycle life and minimize passivation, dendrite formation, and shape change. The high-rate capability of the zinc electrode leads to excellent power capability for Ni-Zn. There are no resource limitations on zinc, and it can be lower in cost than the Ni-Cd or NiMH.

Nickel-Iron (Ni-Fe)

$$Fe + 2\ H_2O + 2\ NiOOH = Fe(OH)_2 + 2\ Ni(OH)_2$$

$$3\ Fe(OH)_2 + 2\ NiOOH = 2\ Ni(OH)_2 + Fe_3O_4 + 2\ H_2O$$

The Ni-Fe battery has a two-plateau discharge characteristic. This system is not in general use except in the former Soviet Union. The batteries use the pocket plate construction, which has an extremely long service life and is virtually indestructible. Their main use has been for lighting on railroad cars. The cells must be vented, as hydrogen is evolved on recharge as a result of the low hydrogen overvoltage on the negative electrode. Since the iron electrode operates near the hydrogen potential, it also releases hydrogen on storage, creating potentially hazardous conditions. Although the Ni-Fe battery was initially viewed as a less expensive substitute for Ni-Cd, the hydrogen gassing problems limited its use. The cost lies between those of lead–acid and Ni-Cd batteries.

Nickel-Hydrogen ($Ni-H_2$)

$$H_2 + NiOOH = Ni(OH)_2$$

The $Ni-H_2$ system was developed for space power. It couples a hydrogen fuel cell anode with an NiOOH cathode. It has good high-rate capability, extremely long cycle life, and resistance to abuse but is an expensive construction with a titanium pressure vessel containment. For long life, the nickel positive electrode is fabricated by using an electrochemical impregnation process. The hydrogen negative electrode uses a platinum catalyst on a nickel substrate hydrogen electrode construction. The cells have extremely long life but are expensive. The H_2 pressure provides an accurate state of charge determination. The cell can tolerate overcharge and overdischarge without damage.

Technical and Cost Barriers

In general, nickel battery technology would benefit from a better understanding of the mechanisms associated with the operation of the porous electrode. This should be feasible, as electrochemical modeling of the electrode operation is now becoming fairly sophisticated. The most urgent issue requiring attention is the low-temperature performance of the hydride anode. Here, a better understanding of hydrogen in the alloys, including the diffusion and bonding, might identify new alloy compositions. For zinc electrodes, the technical concern is the tendency to form dendritic and mossy deposits and also undergo passivation in certain electrolyte compositions. Identifying new electrolytes or additives might provide a way to avoid this process during cycling. Finally, the energy efficiency and stability of nickel cathodes should be improved. Nanostructured materials or additives may improve the rate capability, while electrolyte additives may be used to raise the oxygen overvoltage.

Technical barriers and needs	Component(s)
• Poor rate performance at temperatures below 0°C; new alloys needed for −30°C operation with good efficiency (no. 1 need)	• Hydride anode
• Need for higher storage capacity	• Hydride anode
• Need for increased stability and corrosion resistance	• Hydride anode
• Tendency to form dendritic, mossy, and passivating deposits at zinc surface	• Zinc anode, electrolyte
• Energy efficiency of nickel oxide cathodes needs to be improved, particularly against oxygen generation during the last 20% of the charge	• Ni oxide cathode, electrolyte
• Need to improve stability of crystalline structure	• Ni oxide cathode
• Need to improve high rate capability	• Ni oxide cathode

Additional Reading:

D. Linden and T. Reddy, *Handbook of Batteries*, 3rd ed., McGraw Hill, New York, 2002; R. Brodd, *Batteries for Cordless Appliances*, Research Studies Press, Lechworth, 1987; J. Dunlop, W. Earl, and G. Van Ommering, U.S. Patent 3.850,694, November 26, 1974; D. Feder and D. Mauer, U.S. Patent 3,980,501, September 14, 1976; www.powergenix.com (web site for PowerGenix, maker of nickel-zinc rechargeable battery); M. Fetcenko, presentation at the 23rd International Battery Seminar, Ft. Lauderdale, FL, March 15, 2006.

3.2.3 HIGH-TEMPERATURE SODIUM BETA BATTERIES

Introduction

Beta batteries employing Na/S or Na/$NiCl_2$ (ZEBRA) unit cells are rechargeable energy storage systems utilizing sodium-ion conducting, polycrystalline β″-Al_2O_3 solid electrolytes (BASE) stabilized with either Li_2O or MgO.[4] These batteries operate at moderate temperatures (i.e., ~270–350°C) using liquid sodium as anodes. Cathodes are either molten S/Na_2S_x in porous graphite felts or, in the case of ZEBRA cells, molten $NaAlCl_4$ impregnated in porous Ni/$NiCl_2$ structures. Impervious BASE membranes separate molten electrodes and provide a transport medium for Na^+ ions. During discharge, sodium ions migrate through BASE ceramic membranes from anodes to cathodes, where they react with sulfur to form sodium polysulfide (see cathode 1), or alternatively, reduce $NiCl_2$ to Ni via migration of sodium ions in $NaAlCl_4$ (see cathode 2).

Anode:	$2\ Na \longrightarrow 2\ Na^+ + 2\ e^-$	
Cathode 1:	$2\ Na^+ + 2\ e^- + x\ S \longrightarrow Na_2Sx$	2.08–1.78 V; 755 Wh/kg
Cathode 2:	$2\ Na^+ + 2\ e^- + NiCl_2 \longrightarrow Ni + 2\ NaCl$	2.58 V; 787 Wh/kg

State of the Art

Tubular Design

BASE membranes are manufactured in cost-effective processing operations from spray-dried powders formed into tubular shapes by automatic isostatic pressing and sintered/annealed in gas-fired furnaces. Fully dense with diametral strengths of ~320 MPa and sodium-ion resistivities of ≈3 Ω•cm @ 300°C, BASE ceramics exhibit long-term durability in operating cells and batteries. Structural components in tubular Na/S cells with central-sodium configurations include (1) cylindrical thin-walled BASE tubes, closed at one end, encapsulating liquid sodium; (2) dense α-Al_2O_3 ceramic headers glass-sealed to open ends of BASE tubes, providing electrical insulation between anode and cathode compartments; and (3) tubular cathode containers fabricated from corrosion-protected metals or alloys, closed at one end, serving as current collectors for sulfur electrodes. Because sulfur and sodium polysulfide are electronic insulators, molten cathodes are encapsulated in porous graphite felts serving as electronic shunts.

Unit cells in ZEBRA batteries are similar to Na/S cells in that they include liquid sodium anodes, central impervious BASE tubes, and electrically-insulating ceramic seal headers. However, the porous, central Ni/$NiCl_2$ cores impregnated with molten $NaAlCl_4$ auxiliary electrolytes are placed inside BASE tubular membranes. Liquid sodium metal anodes are located outside tubular BASE ceramics (not inside, as in Na/S cells) with clover-leaf cross sections (required to improve power densities in unit cells) in mild steel containers with rectangular or square cross sections. Inverted tubular-cell designs effectively eliminate corrosion of cathode containers by molten cathode reactants, a significant problem that gradually degrades performance and limits effective lifetimes of Na/S cells. In ZEBRA cells, auxiliary liquid electrolytes, sodium tetrachloroaluminate ($NaAlCl_4$) melting at 154°C, are required. They permit sodium ions passing through BASE membranes to reach various reaction sites in porous nickel chloride structures. Formation of metallic nickel during discharge of ZEBRA cells provides effective electronic shunts between central metallic cores and BASE ceramic membranes.

Significant numbers of batteries have been manufactured and tested successfully in EVs and load-leveling (LL) energy storage systems. Several million thin-walled (1–3 mm) BASE tubular membranes of various sizes—i.e., diameters of between 25 mm (for EV cells) and 60 mm (for LL cells) and lengths of up to ~ 500 mm—have

been fabricated in pilot-scale operations in North America, Europe, and Asia. A variety of large-scale Na/S LL battery systems varying in size between 400 kWh (50 kW) and 64 MWh (8 MW) with cumulative energy-storage capacity of several hundred MWh have been manufactured and placed into operation in Japan by NGK Insulators. Manufacturing operations capable of fabricating ~ 400,000 632-Ah LL Na/S cells and ~400,000 30-Ah EV ZEBRA cells per year have been installed by NGK Insulators in Japan and MES-DEA in Switzerland, respectively.

Electric Vehicle Batteries

Since they can store significant quantities of energy and generate relatively high peak power per unit of battery weight and volume, beta batteries are attractive energy storage systems for power sources in EVs**.** State-of-the-art EV batteries up to 130 kWh in size with required endurance characteristics have been successfully demonstrated in ~1000 road tests with EVs in North America and Europe. Calendar lifetimes of ~11 years have been demonstrated in ZEBRA batteries. Cycle lives equivalent to ~3500 complete discharge/charge cycles have been achieved in EV battery modules, and more than 1450 cycles have been achieved in full-scale EV batteries. Vehicle performance parameters—i.e., acceleration capabilities and driving ranges between charging cycles, which are characteristic of EVs propelled by beta batteries—are substandard compared with motor vehicles powered by conventional ICEs. However, state-of-the-art performance characteristics of unit cells and batteries summarized in Table 3-3, which meet mid-term requirements of the USABC, should be acceptable for many urban applications. For beta batteries in EVs to be fully competitive, substantially improved cell designs are required. They will involve planar or multi-tube unit cells with significantly higher ratios of the active electrochemical area to cell volume (A/V) and, consequently, a lower area-specific resistance (ASR). Redesigned unit cells are projected to have stored energy ratios of over 300 Wh/L and 200 Wh/kg and peak power ratios over 600 W/L and 400 W/kg.

TABLE 3-3: Optimum performance of beta cells and batteries with tubular cell designs. From J.B. Goodenough et al., ***Basic Research Needs for Electrical Energy Storage*** **(2007).**

	EV cells (30–40 Ah)		**EV batteries (25–40 kWh) ~ 360 cells per EV battery**	
Stored energy ratios				
	Wh/L	**Wh/kg**	**Wh/L**	**Wh/kg**
Na/S[a]	360	180	151	105
$Na/NiCl_2$ [b]	340	145	183	118
Peak power ratios				
	W/L	**W/kg**	**W/L**	**W/kg**
Na/S	727	390, 0% DOD	234	210, 0% DOD
		337, 80% DOD		181, 80% DOD
ZEBRA	613	271, 0% DOD	276	185, 0% DOD
$Na/NiCl_2$		146, 80% DOD		170, 80% DOD

[a] ASEA-BBC (Germany).

[b] MES-DEA (Switzerland).

Batteries for Load Leveling

Beta batteries, because of their high volumetric energy density and small footprints, can also be used effectively in stationary LL energy storage systems in electric utilities and at industrial facilities in urban/suburban locations. A variety of LL systems up to 64 MWh in size (i.e., 8 MW delivered over 8-hour discharge cycles) have been demonstrated successfully with acceptable degradation in performance in field tests lasting several years. LL Na/S modules and batteries have been produced that satisfy all performance, lifetime, endurance, and safety requirements. These batteries have been constructed from self-contained battery modules 400 kWh (50 kW) in size. These 400-kWh modules have specific energies of ~120 Wh/kg, energy densities of ~160 Wh/L (~370 Wh/L at the unit cell level), and very small footprints, ≈100 kWh/m^2. Energy efficiencies are ~87% initially, declining to ~81% after ~2500 cycles. Very large LL battery systems have been operated continuously for periods of more than 8 years, compiling more than 1800 discharge and charging cycles. Individual LL unit cells have demonstrated lifetimes of >4500 cycles with ~10% reduction in capacity. Since LL Na/S batteries can be discharged rapidly at five times base-load rates for short periods of up to 10 seconds, they can also be employed in power quality applications.

Advanced Cell Designs in R&D

High-performance, durable unit cells with planar/bipolar designs are projected to have (1) relatively high open-circuit voltages (≥2 V); (2) lower ASRs; (3) failure modes with low electrical resistance; (4) increased depths of discharge compared with Na/S cells; (5) liquid-phase cathodes, which are mixed ionic and electronic conductors and chemically compatible with iron-based metal alloys; and (6) operating temperatures consistent with metallic components employed in cell interconnections and flexible seals, all self-contained in stainless steel enclosures.[5]

A vapor-phase process has been developed for fabricating strong (~900 MPa), fine-grained (several microns), thin-walled (150–300 microns), and flat plates of BASE membranes suitable for planar/bipolar beta cells with high power and energy densities.[6] Electrolytes are formed by reaction of Na_2O vapor with impervious, cast sheets of α-Al_2O_3/zirconia composite precursors. Reasonably rapid and direct conversion to conductive β″-Al_2O_3 phases at 1450°C occurs without loss of Na_2O. BASE membranes formed by this potentially economical process are very resistant to attack by moisture. Another advantage of vapor-phase processing is formation of substantial crystallographic texture, wherein conduction-planes in β″-Al_2O_3 align themselves perpendicular to walls of flat BASE membranes. Planar BASE electrolytes—which have been produced previously by tape casting followed by sintering and annealing in conventional processing operations—are relatively weak mechanically and possess undesirable conduction anisotropy.

Technical and Cost Barriers

Commercial state-of-the-art beta batteries have a variety of limitations, which are summarized in the list below. In view of problems related to containment of cathode reactants, corrosion of metallic containers, brittle glass seals, and failure of cells in modes with high electrical resistance, development of Na/S batteries with planar/bipolar and other advanced cell designs will be very challenging. Evolving designs for beta cells with higher A/V ratios, lower ASRs, and higher-capacity cathodes will eventually replace unit cells with tubular designs. Advanced cathodes will be improved alternatives to sulfur, and $NiCl_2$ and will be more compatible chemically with iron-based metals used in cell construction. Advanced vapor-phase processing will produce flat BASE membranes, which are strong, fine-grained, and tolerant to water exposure and have high sodium-ion conductivities in preferred directions.

Technical barriers and needs	Component(s)
• Relatively high ASR and low A/V of tubular unit cell, which severely limits EV battery performance	• Unit cell
• Restricted energy storage capacity and limited energy densities	• Na/S unit cells
• Long-term corrosion of metallic cathode containers	• Na_2S_x containers
• Failure of Na/S cells with high electrical resistance in relatively small EV batteries (ZEBRA cells do not have this problem)	• Unit cells in EV batteries
• Need for cost-effective techniques are needed for manufacturing thin (150–300 µm), flat BASE membranes with optimum mechanical and electrical properties	• Planar BASE membranes
• Expensive carbon felts in cathode structures of Na/S cells	• Cathode structure
• Expensive encapsulation devices to prevent loss of Na_2O during sintering of BASE membranes at 1585°C	• BASE fabrication
• Water sensitivity of polycrystalline BASE membranes fabricated by conventional liquid-phase sintering	• BASE storage
• Brittle glass seals	• Seals
• Corrosion in ZEBRA cells between $NiCl_2$ and mild steel cell components (avoided in tubular cells with central cathode designs)	• Mild steel cell components

References

1 D. A. J. Rand, P. T. Moseley, J. Garche, and C. D. Parker, eds., *Valve-regulated Lead–Acid Batteries*, Elsevier, Amsterdam, 2004.

2 U.S. Department of Energy, *FreedomCAR Energy Storage System Performance Goals for Power-assisted Hybrid Electric Vehicles*, November 2002.

3 Internal reports, *Advanced Lead–Acid Battery Consortium*.

4 J. L. Sudworth and A.R. Tilley, *The Sodium Sulfur Battery*, Chapman and Hall, London, 1985; J. L. Sudworth, "High Temperature Cells," pp. 243–274 in *Modern Batteries: An Introduction to Electrochemical Power Sources*, eds., Colin A. Vincent and Bruno Scrosati, Chapter 8, Arnold (Hodder Headline Group), London, and John Wiley and Sons, New York, 1997; C.-H. Dustmann, Advances in ZEBRA batteries, *J. Power Sources*, 127 (2004) 85; R. S. Gordon, W. Fischer, and A. V. Virkar, *Century of Progress in Electrochemical Ceramics Technology: Energy Storage, Power Generation, Chemical Processing and Sensing*, unpublished.

5 R. S. Gordon, W. Fischer, and A. V. Virkar, *Century of Progress in Electrochemical Ceramics Technology: Energy Storage, Power Generation, Chemical Processing and Sensing*, unpublished.

6 A. V. Virkar, T. J. Armstrong, N. Weber, K-Z. Fung, and J-F Jue, “Role of Coupled Transport in the Fabrication of sodium β″-Alumina-Containing Ceramics by a Vapor Phase Process,” p. 200 in *Proceeding—High Temperature Materials: A Symposium in Honor of the 65th Birthday of Professor Wayne L. Worrell*, ed., S.C. Singhal, Electrochemical Proceedings, Vol. 2002–2005, Pennington, NJ , 2002.

3.3 Li-Ion Systems

3.3.1 CURRENT GENERATION

Introduction

Lithium-ion batteries (LIBs) are preferred power sources for portable electronic devices and are increasingly being adopted for electric vehicles (EVs) and other large-scale applications due to higher energy density and longer life span than most other batteries.[1, 2] The LIB is first of all an electrochemical system with high complexity; while at a fundamental level, it can be simply depicted as three layers, the anode, electrolyte, and cathode. LIBs operate *via* a “rocking-chair” mechanism, with Li ions moving back and forth between anode and cathode (through the electrolyte) during charge/discharge cycles. A distinguishing feature of Li ion cells is that at assembly, the Li ions are stored in the cathode, i.e., at the discharged state. The cells are activated *via* charging, wherein Li ions move from the cathode to the anode and so Li ions will be stored in the anode by this step. During discharge of a cell, Li ions move from the anode to the cathode through the electrolyte, and electrons generated from the anode migrate through the external circuit to supply electricity. Most rechargeable LIBs on the market today are based on intercalation reactions, that is, insertion and extraction of Li ions in and out of the crystalline lattices of solids without causing significant change to lattice structure.

An important parameter of performance for LIBs is their specific or volumetric energy density, which is determined by two factors: 1) the specific capacity of the anode and cathode, namely, the amount of Li that can be stored per unit weight or volume and 2) the difference of the electrochemical potentials between the anode and cathode. The practical energy density of today’s LIBs is typically below 150 Wh/kg. For LIBs to be widely adopted for EV applications, an energy density of 300 Wh/kg or above is desired in order to meet the requirements for cost and driving range. Low capacity of electrodes is currently the limiting factor, and so extensive efforts have been devoted to searching for new materials with higher Li storage capacity. In addition, further effort is needed for better understanding of the basic science associated with the gap between the usable output of batteries and their theoretical energy contents.[3]

State of the Art

Conventional LIBs were initially based on hard carbon and lithium cobalt oxide ($LiCoO_2$; LCO) as anode and cathode, respectively, in the first cells commercialized by Sony Corporation in 1991. Graphite was soon introduced to replace hard carbon, for its flat working potential, high theoretical capacity (372 mAh/g), and high stability in the non-aqueous electrolyte *via* forming an interfacial layer, the so-called solid-electrolyte interphase (SEI). Over the decades, graphite/LCO based cells have been dominant in the market even until today. Due to the low capacity (156 to 165 mAh/g), high cost and thermal instability, among other issues that limit its use in EVs and other large-scale applications, LCO is now phasing out and being gradually replaced by different types of cathodes for greater energy density. On the anode side, graphite is still dominant, but $Li_4Ti_5O_{12}$ and Si have now been preferentially used for some applications with specific requirements; see Figure 3-4 for the anodes and cathodes on the roadmap of development for the start-of-the-art and next-generation LIBs.

Ni-rich NMC

Following the commercialization of LCO, transition metal (TM) layered oxides have been extensively studied over the past two decades. $LiNiO_2$ attracted immediate attention in the initial search for alternatives to LCO because of its isostructural characteristics, low cost and even higher practical capacity (~200 mAh/g). However,

stoichiometric $LiNiO_2$ is hard to synthesize, and its thermal instability at high SOC is a safety concern. Therefore, strategies were developed to mitigate these issues, such as adding a second and even third cation into the transition metal layers to construct solid solutions of $LiNi_{1-x}M_xO_2$ (M=Co, Mn, Al, …), which has been widely taken an effective way of stabilizing the layered structure and further tailoring their electrochemical properties. For example, in the second generation of LIBs, $LiNi_{0.8}Co_{0.15}Al_{0.05}O_2$ (NCA) and $LiNi_{1/3}Mn_{1/3}Co_{1/3}O_2$ (NMC) were developed, with substitution of Co to improve the structural ordering, and Al or Mn to strengthen the thermal stability. NCA and NMC are now starting to find applications in EVs and other large-scale applications; however, their capacity is still low, ~160-180 mAh/g.

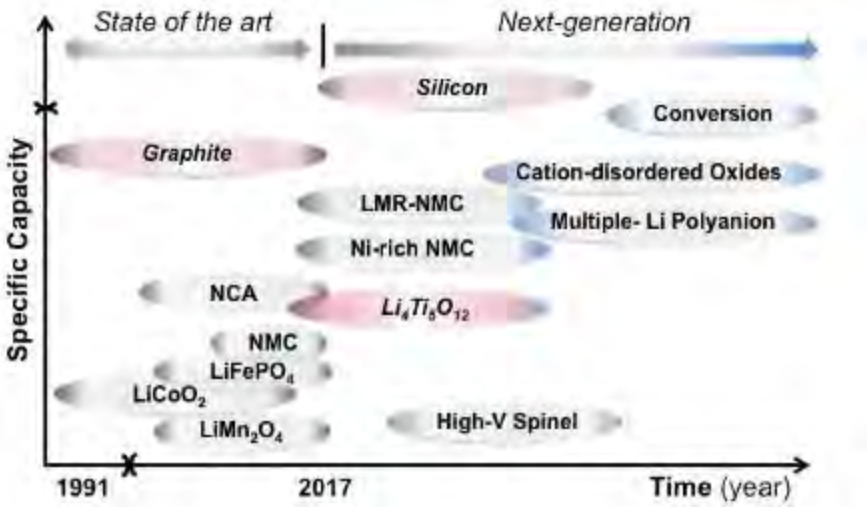

Figure 3-4. Anodes (*red-shadowed*) and cathodes on the roadmap of developing lithium-ion batteries. From J.B. Goodenough et al., *Basic Research Needs for Electrical Energy Storage* (2007).

Research efforts are now increasingly focused on developing Ni-rich NMC ($1\text{-}x \geq 0.5$), aiming for even higher capacity (>200 mAh/g); however, cycling stability and safety are compromised as a result of high Ni reactivity and structural reconstruction on the particle surface.[4] Some of these issues may be solved or mitigated by surface protection via coatings, or the synthesis of particles with core-shell structure or concentration gradient (at either primary or secondary particle levels).[5,6,7] In a recent development, high capacity (up to 215 mAh/g) and long cycling stability (> 1000 cycles) have been demonstrated in full-concentration-gradient Ni-rich NMC cathodes composed of micron-sized secondary particles with Ni (Mn) concentration continuously decreasing (increasing) from the center towards the outer surface. However, due to the complexity of synthesis and processing, implementation of those strategies in large-scale production is difficult, especially under the requirement of high structural ordering in particles with such high compositional heterogeneity.

Li/Mn-rich (LMR)-NMC ($xLi_2MnO_3 \cdot (1\text{-}x)LiMO_2$; M=Mn, Ni, Co)

LMR-NMC oxides are generally modeled as composite materials with monoclinic Li_2MnO_3 integrated with hexagonal $LiMO_2$ to form *layered-layered* structures.[8,9] LMR-NMC is attractive for its high capacity (up to 300 mAh/g), low cost, and high thermal stability. Recent experimental and *first principles* studies demonstrated that excess capacity may come from oxygen redox reaction induced by local configurations associated with partial Li substitution in the TM layers.[10,11] This is an exciting finding in that it may open new opportunities for battery research aimed at increasing capacity through both cationic and anionic redox processes. However, there are some critical issues of this type of cathode, including voltage fade and the correlated voltage hysteresis, first-cycle efficiencies, and rate capabilities, which prevent their use in practical applications. These phenomena are a result, in part, of phase transitions into spinel-like configurations, or more precisely, migration of cations ions into Li layers, triggered by oxygen involvement during the first-cycle “activation” process. In addition, surface

oxygen loss and electrolyte interactions further hinder high-rate performance. Among many proposed solutions, incorporating a lithiated spinel component has been shown most promising for addressing these issues. There are potential advantages such as inherent stability against TM migration, improved rate capability, and offset of first-cycle irreversible capacity losses.[12] However, the drawbacks of this approach can be related to precise control over structural and elemental compositions when using general solid-state reaction methods, which may prove difficult from a thermodynamic point of view. In addition, voltage fade may not be sufficiently mitigated by using this approach, especially when excess Li and Mn concentrations are high (e.g., >~0.3).

There are two other large categories of cathodes in the second generation of LIBs, spinel ($LiMn_2O_4$) and olivine ($LiFePO_4$), both being featured by low cost and high safety. A number of cathodes have now been made commercially available (Figure 3-4, left), providing flexibility of choices for different applications. However, when paired with a graphite anode, neither of them have met the target miles of all-electric-range within the weight and volume constraints as defined by DOE in the *EV Everywhere Blueprint*.[13]

New cathodes with even higher energy density are needed before LIBs can be widely commercialized for EV and other large-scale applications. One active area in battery research is to develop high capacity anodes and cathodes that can accommodate more than one Li /redox center; some of the promising cathodes under this category are given in Figure 3-4 (right), including high-voltage cathodes, cation-disordered oxides, multiple-Li polyanionic compounds, and conversion-type cathodes. Recent progress in this research area is summarized below, along with perspectives on the challenges and opportunities.

3.3.2 NEXT GENERATION

Anodes

Graphite is an excellent anode, with capacity two times of most commercial cathodes, and thus not easily replaceable by other materials.[14] One alternative that is being explored is in the use of alloying materials, predominantly silicon, which is capable of delivering up to 10 times higher capacity since Si can bind as many as 4 Li (forming Li_4Si), in contrast to LiC_6, which binds 1 Li with 6 C. The use of Si is also advantageous due to its abundance and cost. However, the Si anode suffers from large volume change during lithiation and delithiation, leading to deformation of the electrode, and an unstable SEI layer. In recent years, extensive investigations have been made into increasing the life-time through fabricating nano or porous materials and composites with carbon or other materials; however, irreversible loss in capacity due to the repeated reformation of SEI layer during cycling remains a major problem, and so its application has been limited to LIBs for potable electronics.[15] Much progress has been made recently in identifying the phase transformation/reactions at electrode/electrolyte interfaces; nevertheless, the mechanisms of electrode/electrolyte interaction leading to forming stable SEI layer are far from being understood, limiting efforts in the rational design of new electrolytes and electrodes that are required for assuring the viability of Si anodes in commercial LIBs.

Lithium titanate ($Li_4Ti_5O_{12}$), with advantages of long-term stability, extraordinary high-rate capability, and inherent safety, has become an appealing alternative for large-scale applications, grid storage, in particular. However, one main limit in using $Li_4Ti_5O_{12}$ as the anode in full cells is the high redox potential, which may be compensated by pairing with a high-voltage cathode for achieving relatively high energy density.

Cathodes

High-Voltage Cathodes

Layered NMC cathodes can be charged to high voltages, thereby providing even higher energy density. But issues related to cycling and thermal stability arise as a result of phase transformations and oxygen release. An alternative option is spinel $LiNi_{0.5}Mn_{1.5}O_4$ (LNMO), which can be taken as Ni-substituted $LiMn_2O_4$, with operating voltages of 4.7 V or above. Although the practical capacity is moderate (only 130 mAh/g), LNMO has attracted great attention and may deserve further investigation due to the inexpensive and environmentally benign constituents, good safety properties, and excellent rate capability. The commercial use of LNMO for LIBs is primarily hindered by the oxidative instability of the electrolyte, Mn dissolution, leading to severe capacity fade with cycling, especially at elevated temperatures (> 60^{o}C).

Cation-Disordered Oxides

The cation-disordered oxide (Li-M-O_2; M= Mn, Nb, Mo, Ti, Fe, etc.) is a recent addition to high-capacity cathodes, with demonstrated capacity up to 300 mAh/g. The materials have a rock-salt like structure, with partial or complete cation disordering.[16] In contrast to restrictive requirements of high cationic ordering for high Li diffusivity in traditional layered oxides, a percolation network of “0-TM” channels for Li diffusion can be created by ~10% Li-excess in the cation-disordered oxides. This new discovery is exciting as it points to a new way of designing high-capacity cathodes with *non-typical* metal elements (Mn, Nb, Mo, Ti, Fe, etc.), which is advantageous from resource and cost perspectives.[17,18] In addition, cation-disordered electrodes are dimensionally stable with low volume expansion, a desired feature for achieving long life and safe battery operation. Since it is still in the early stage of development, more studies of material optimization (i.e., composition, structure) are needed in order to further improve the energy density, lifetime, and kinetics. Strategies developed for NMC cathodes, such as surface treatment and/or coating, may also be applicable to this cation-disordered cathode.

Multiple-Li Polyanionic Compounds (LixMPO4: M=V, Mo…)

The polyanionic compounds are of great interest for use as cathodes due to the high voltages induced by phosphate groups, and the possibility of accessing multiple redox states of the metals. These two factors represent potential routes to accessing phases with very high energy density. One representative is monoclinic ε-Li_xVOPO_4, with theoretical capacity of ~310 mAh/g (almost double that of $LiFePO_4$) through V redox at 3.9 V for V^{5+}/V^{4+} and ~ 2.5 V for V^{4+}/V^{3+}. It has the same safety feature as olivines (no release of O_2 on charge). More than one Li intercalation/extraction in ε-Li_xVOPO_4 has recently been demonstrated.[19] However, one issue is the long cycling stability in the electrolyte due to the side reactions: ε-$VOPO_4$ → orthorhombic $HVOPO_4$ → tetragonal H_2VOPO_4. Surface coatings could be helpful to further improve cycling stability.

Conversion-Type Cathodes

In contrast to intercalation electrodes, wherein guest ions (i.e., Li^+) move through the relatively open lattice of the host without significant modification of lattice structure, in conversion electrodes the guest ions react directly with the host material to form new chemical compounds of completely different structures. The conversion cathodes, specifically the fluoride-based materials, are particularly interesting for their intrinsically high redox potentials and extremely high specific capacity (~ 3 times greater than commercial cathodes), enabled by more than one electron transfer per transition metal: $M^{n+}X_y + nLi^+ + ne^- = yLi_{n/y}X + M^0$ ($n \geq 2$).[20, 21] Although there are long-known issues related to low reversibility, poor cycle life, and energy efficiency in conversion electrodes, significant progress has been made in fundamental understanding of the conversion mechanisms over the past several years. In particular, recent work revealed formation of a percolating network of metallic nanoparticles for electron transport, which is crucial to enabling the high cycling reversibility in FeF_2.[22] However, due to the insulating nature of FeF_2, the electronic transport is a main limit to the kinetics of conversion process, with slow propagation of the reaction front, “layer-by-layer”, into the bulk, during which the Fe percolating network is gradually built up to provide the pathway for electronic transport.[23] In addition,

substitution of O for F to form iso-structural FeOF increases deliverable energy, with raised working voltage and improved cycling stability by introducing covalent M–O bonds into the ionic fluoride structure.[24, 25]

Compared to FeF_2, CuF_2 is more attractive for use as cathodes because of its high theoretical potential (~3.55V) and specific capacity (528 mAh/g), offering an exceptionally high energy density (1,874 Wh/kg). However, the electrochemical activity of CuF_2 is low, and utilization of its full capacity was only recently achieved by embedding CuF_2 into a conductive matrix.[26] Unfortunately, CuF_2 only found application in primary batteries due to the irreversibility of the $Cu^{2+/0}$ redox reactions. The conversion reactions in CuF_2 involve highly mobile Cu^{2+} ions, which lead to coarsening and growth of large, isolated Cu particles during lithiation, making reconversion difficult. In addition, Cu dissolution during charge results in considerable loss of capacity.[27] By incorporation of Cu into the FeF_2 crystal lattice to form solid solution $Cu_yFe_{1-y}F_2$, the redox reactions of Cu^{2+}/Cu^0 were enabled.[28] Although the reversible capacity of Cu conversion fades rapidly due to Cu dissolution, the low hysteresis and high energy density suggest that a Cu-based fluoride cathode remains an intriguing candidate for rechargeable LIBs.

Electrolyte and Interface/Interphases

In the past decade, extensive research efforts were devoted to the characterization of SEI on graphite anodes, leading to significant improvement in our fundamental understanding of the SEI formation and associated interfacial reaction processes in LIBs. On the other hand, the never-ending development of cathode materials with increasing capacity, higher operating voltages, and distinct surface chemistry/morphology and nanostructure continues to present new challenges to our understanding of, and approaches to, stabilizing the cathode-electrolyte interface, and hence the viability of new cathodes. [29] *Non-aqueous* electrolytes with the skeleton composition of $LiPF_6$ salt and organic carbonate solvents remain dominant in today's LIBs since the graphite anode and most cathodes can operate within their stable voltage window. But this may have to change as high voltage (>4.5 V) cathode materials are now being considered for commercial application. In addition, organic electrolyte is flammable, which has always been a safety concern.

Due to their tunable physical properties and generally low flammability, ionic liquids (ILs) are becoming an appealing alternative to hazardous organic electrolytes in LIBs and other battery systems.[30, 31] In addition, ILs can work over a wide voltage window and help to form a favorable electrode–electrolyte interface. For example, by using IL electrolyte, high capacity retention (>90% over more than 750 cycles) even at the 1C rate has been demonstrated in Si/LMR-NMC full cells.[32] The use of LIBs with IL electrolyte in the extreme environment of space has also been demonstrated recently.[33] ILs incorporating lone-pair-donating ether functionalities are especially studied because such groups increase the solubility and mobility of lithium ions.

References

1 M.S. Whittingham, History, evolution, and future status of energy storage, *Proceedings of the IEEE*, 100 (2012) 1518-1534.

2 B. Dunn, H. Kamath, and J.M. Tarascon, Electrical energy storage for the grid: A battery of choice, *Science*, 33 (2011) 928-935.

3 D. Abraham et al., Investigating the complex chemistry of functional energy storage systems: The need for an integrative, multiscale (Molecular to Mesoscale) perspective, *ACS Central Science,* 2.6 (2016) 380-387 (2016).

4 F. Lin et al., Surface reconstruction and chemical evolution of stoichiometric layered cathode materials for lithium-ion batteries, *Nature Communications,* 5 (2014) 3529.

5 Y.K. Sun et al., Synthesis and characterization of $Li[(Ni_{0.8}Co_{0.1}Mn_{0.1})_{0.8}(Ni_{0.5}Mn_{0.5})_{0.2}]O_2$ with the microscale core−shell structure as the positive electrode material for lithium batteries, *J. Amer. Chem. Soc.,* 127.38 (2005) 13411-13418.

6 Y.K. Sun et al., Nanostructured high-energy cathode materials for advanced lithium batteries, *Nature Materials,* 11.11 (2012): 942-947.

7 F. Lin et al., Metal segregation in hierarchically structured cathode materials for high-energy lithium batteries, *Nature Energy,* 1 (2016): 15004.

8 M. M. Thackeray, S. -H. Kang, C. S. Johnson, J. T. Vaughey, R. Benedek, and S. A. Hackney, Li_2MnO_3-stabilized $LiMO_2$ (M = Mn, Ni, Co) electrodes for lithium-ion batteries, *J. Mater. Chem.,* 17 (2007) 3112-3125.

9 J.R. Croy et al., Review of the US Department of Energy's "deep dive" effort to understand voltage Fade in Li-and Mn-rich cathodes, *Acc. Chem. Res.,* 48.11 (2015) 2813-2821.

10 K. Luo et al., Charge-compensation in 3d-transition-metal-oxide intercalation cathodes through the generation of localized electron holes on oxygen, *Nature Chemistry,* 8 (2016) 684–691.

11 D.-H. Seo et al., The structural and chemical origin of the oxygen redox activity in layered and cation-disordered Li-excess cathode materials, *Nature Chemistry,* 8 (2016) 692–697.

12 B.R. Long et al., Advances in stabilizing 'layered-layered' $xLi_2MnO_3 \cdot (1-x)\ LiMO_2$ (M= Mn, Ni, Co) electrodes with a spinel component," *J. Electrochem. Soc.,* 161.14 (2014) A2160-A2167.

13 *EV Everywhere Grand Challenge Blueprint,* https://energy.gov/sites/prod/files/2014/02/f8/eveverywhere_blueprint.pdf (2013).

14 M.N. Obrovac and V. L. Chevrier, Alloy negative electrodes for Li-ion batteries, *Chemical Reviews,* 114.23 (2014) 11444-11502.

15 J. Graetz and F. Wang, Nanoscale anodes of Si and Ge for lithium batteries, Chapter 2 in *Nanomaterials for Lithium-Ion Batteries: Fundamentals and Applications*, CRC Press (2013).

16 J. Lee et al., Unlocking the potential of cation-disordered oxides for rechargeable lithium batteries, *Science,* 343.6170 (2014): 519-522.

17 J. Lee et al., A new class of high capacity cation-disordered oxides for rechargeable lithium batteries: Li–Ni–Ti–Mo oxides, *Energ. Environ. Sci.,* 8.11 (2015) 3255-3265.

18 R. Wang et al., A disordered rock-salt Li-excess cathode material with high capacity and substantial oxygen redox activity: $Li_{1.25}Nb_{0.25}Mn_{0.5}O_2$, *Electrochemistry Communications,* 60 (2015) 70-73.

19 Y.-C. Lin et al., Thermodynamics, kinetics and structural evolution of ε-$LiVOPO_4$ over multiple lithium intercalation, *Chemistry of Materials* 28.6 (2016) 1794-1805.

20 F. Badway et al., Carbon metal fluoride nanocomposites high-capacity reversible metal fluoride conversion materials as rechargeable positive electrodes for Li batteries, *J. Electrochem. Soc.* 150.10 (2003) A1318-A1327.

21 G.G. Amatucci and Nathalie Pereira, Fluoride based electrode materials for advanced energy storage devices, *J. Fluor. Chem.* 128.4 (2007) 243-262.

22 F. Wang et al., Conversion reaction mechanisms in lithium ion batteries: Study of the binary metal fluoride electrodes, *J. Electrochem. Soc.,* 133.46 (2011) 18828-18836.

23 F. Wang et al., Tracking lithium transport and electrochemical reactions in nanoparticles, *Nature Communications,* 3 (2012) 1201.

24 N. Pereira et al., Iron oxyfluorides as high capacity cathode materials for lithium batteries, *J. Electrochem. Soc.,* 156.6 (2009) A407-A416.

25 S.-Wook Kim et al., Structure stabilization by mixed anions in oxyfluoride cathodes for high-energy lithium batteries, *ACS Nano,* 9.10 (2015) 10076-10084.

26 F. Badway et al., Structure and electrochemistry of copper fluoride nanocomposites utilizing mixed conducting matrices, *Chemistry of Materials,* 19.17 (2007) 4129-4141.

27 X. Hua et al., Comprehensive study of the CuF_2 conversion reaction mechanism in a lithium ion battery, *J. Phys. Chem. C,* 118.28 (2014) 15169-15184.

28 F. Wang et al., Ternary metal fluorides as high-energy cathodes with low cycling hysteresis, *Nature Communications,* 6 (2015) 6668.

29 K. Xu, Electrolytes and interphases in Li-ion batteries and beyond, *Chemical Reviews,* 114 (2014) 11503.

30 M. Watanabe et al., Application of ionic liquids to energy storage and conversion materials and devices, *Chemical Reviews,* 117 (2017) 7190–7239.

31 M.M. Huie et al., Ionic liquid hybrid electrolytes for lithium-ion batteries: A key role of the separator–electrolyte interface in battery electrochemistry, *ACS Applied Materials & Interfaces,* 7.22 (2015) 11724-11731.

32 T. Evans et al., In situ engineering of the electrode–electrolyte interface for stabilized overlithiated cathodes, *Advanced Materials,* (2017) 1604549.

33 M. Yamagata et al., The first lithium-ion battery with ionic liquid electrolyte demonstrated in extreme environment of space, *Electrochemistry,* 83.10 (2015) 918-924.

3.4 Solid-State Li-Metal Batteries

Introduction

Use of a metallic Li anode, with 3840 mAh/g, has the potential to increase the energy density over that of Li-ion batteries. However, it has been hotly debated whether this improvement justifies the safety risk associated with replacing the graphite anode used in consumer batteries with metallic lithium. Achieving a stable Li anode will also enable development of batteries with sulfur and air cathodes, providing low cost and sustainable batteries with energy densities approaching liquid fuels. This section presents the challenge of using solid electrolytes to protect the Li metal anode.

It is well understood that Li anodes can provide enhanced energy density *only when the lithium capacity is balanced* with that of the cathode. If excess Li inventory must be included in the battery to compensate for a gradual consumption of lithium by side reactions, the higher specific energy density promised by the lithium is

essentially negated. Put to numbers, if side reactions or processes leading to physical isolation of lithium reduce the lithium inventory by just 0.1% of the cell capacity for each cycle, then to achieve 1000 cycles requires that the battery be assembled with a three-fold excess lithium. There is no gravimetric advantage to use Li in this scenario.

The use of commercial Li metal batteries is limited largely because of historical safety problems when Li rechargeable batteries were first commercialized in the 1980s. Although the prototype lithium batteries were subjected to extensive testing, consumers used the batteries in unexpected ways, resulting in formation of roughened Li, which led to catastrophic failures.[1] Current studies have identified ingenious approaches, including electrolyte additives, engineered barriers, and self-healing interface coatings and host structures, to improve control of Li plating in a liquid electrolyte,[2] but clearly a better solution is to replace flammable liquids or gels with a nonflammable solid electrolyte. As described below, synthesizing the optimum solid electrolyte and fabricating a thin robust membrane are difficult, and success is not assured.

To balance the capacity of a good high-energy Li-ion cathode, of say 6-7 mAh/cm^2, requires moving ~30 μm of Li per deep cycle over a few hours. To avoid excess Li, the thickness remaining at full discharge should be just a few μm to serve as the current collector. Further, pulse rates to strip and plate Li at 10-20 nm/s are needed for the EV application. Such aggressive cycling in a solid state cell with good control of the Li inventory is rarely demonstrated in practice. This has become a key performance metric for the Advanced Research Projects Agency-Energy (ARPA-E) IONICs program[3] seeking demonstration of an accumulated Li plating exceeding 2 Ah/cm^2 at 3 mA/cm^2, which approaches 700 h. Few room-temperature Li batteries have come close, although cycling polymer electrolyte batteries at elevated temperature is promising,[4] as is room temperature cycling of some thin film batteries with a Lipon electrolyte.[5]

Strong R&D efforts are underway at many locations to identify robust solid electrolytes that can be manufactured as thin, cost-effective membranes; have high electronic resistivity; have low bulk and interface ionic resistance; can achieve current densities of >1 mA/cm^2; and are chemically and mechanically stable for protecting the Li metal over the lifetime of the device.

State of the Art

The Solid Electrolyte

Many different classes and families of materials are being studied to meet this need, including some with Li^+ ion conductivities as high as typical liquid electrolytes (> 1 mS/cm), considered superionic paths or sublattices. Others are more traditional with ionic conduction via point defect carriers. A later section will discuss thin film solid electrolytes, one example being Lipon, which in a thin-film lithium battery provides good cycle life and stability.[6] While valuable for smaller devices, this is not cost effective for grid and vehicle application.

Lithium polymer electrolytes[7] are among the first and still most successful solid electrolytes demonstrated in rechargeable lithium batteries. For better mechanical stability, block copolymers replaced homopolymers and blends.[8] Because the ionic conductivity is low, commercial batteries with these electrolytes generally operate at 60-80°C. Gradual roughening of the lithium interface is still a concern, as are nodules formed in the lithium perhaps due to impurities that can puncture a thin polymer membrane.[9] Single-ion conducting polymer electrolytes with good mechanical properties are being sought. For most polymer electrolytes, the Li^+ transference number is just 0.2-0.5; with a much higher t_{Li+}, the requirement for very high conductivity is relaxed by about an order of magnitude.

Ceramic electrolytes with a variety of structures, including polyanionic materials, can provide extraordinarily high Li^+ lattice conductivities,[10] although grain boundaries often limit the total conductivity. Because stoichiometries vary, but also need to be precisely controlled for optimum transport, the electrolytes are simply abbreviated as LAGP, LATP, LLTO, LLZO, Li_3OX, etc., for oxides containing P, Ge, Al, Ti, La, Zr, and

halides X. Similarly, the families of ceramic sulfide and thiophosphate electrolytes are abbreviated as LPS and LMPS, where Si, Ge, As, and Sn are common substitutions. Insight from theory and simulation has examined different anion-host structures, demonstrating that lattices with interconnected tetrahedral sites provide lower activation barriers for ion motion.[11] Cation substitutions that minimize the energy barrier were also examined in this work. Anion substitutions are less examined, although substitutions of S and N for O,[12] and substitutions of halides for S,[13] are yielding better conductivities and Li and air stability. Much attention is directed to the electrochemical stability windows for these electrolytes.[14] As discussed further below, only a few prove either stable or readily passivated for Li anodes. Most of the sulfide electrolytes appear to form thick reaction layers with lithium metal. The choice of oxides versus sulfides presents other tradeoffs in membrane fabrication, elastic shear modulus, and fracture toughness, which require more attention.

Glasses and glass-ceramic electrolyte have been synthesized by melts and recently by mechanochemical mill processing.[15] Because of the quenched amorphous structure, glasses offer greater compositional flexibility for materials design. The Lipon solid electrolyte composition, for example, exists well outside of the normal glass forming region.[6] Some of the most highly conductive electrolytes are thiophosphates and thiogermanates partially substituted with oxide phosphates.[16,17]

Although there are promising oxide, sulfide, polymer, ionomer, and glassy electrolyte materials at hand, no single solid electrolyte can so far serve all the functional roles and practical manufacturing needs to enable long-lived, room-temperature, solid-state Li batteries. Pragmatically, thin membranes formed as a composite[18] or laminate[19] of multiple electrolytes are an attractive solution, yet the interfaces between different electrolytes may greatly impede the Li^+ ion conductivity and perturb the uniformity of the current distribution. There are few publications of the interface resistance between different electrolytes, and the results differ by many orders of magnitude.[20] Using single-ion polymers may eliminate some polarization at polymer/ceramic interfaces[21]; also a composite electrolyte which is self-healing was formed by penetrating the void of a porous electrolyte compact.[22] To achieve high shear modulus for a polymer-ceramic composite requires either ~60 vol % ceramic for randomly packed ceramic particles or less if the ceramic phase forms a continuous 3D network.[23] A 3D mesh of fused LLZO fibers was recently fabricated.[24]

Interface with Lithium Metal

Recent assessments of the electrochemical stability for a variety of Li electrolytes[14] provide a computational method to evaluate the interfacial phases that may form at a Li/solid electrolyte interface. For many proposed solid electrolyte materials, a thick reaction layer forms at the Li interface and/or the electrolyte is reduced leading to electronic conductivity. Only a few solid electrolytes, one being lithium lanthanum zirconate (LLZO), are expected to be stable with Li metal. Furthermore, LLZO is predicted to have a wide electrochemical window, consistent with experiments finding a 6-V band gap.[25,26] Interestingly, Lipon, on the other hand, is predicted to have a small electrochemical window yet thin film batteries cycle with exceptional stability. Presumably, the Li /Lipon interface is readily passivated such that the atomically thin reaction neither consumes significant capacity nor overwhelms the bulk resistance of the electrolyte.

Aside from this intrinsic reaction or passivation with lithium, the interface adhesion, uniformity, and possibly contamination will also effect the cycling performance. This has been carefully investigated for the Li/LLZO interface. When a polished Li sheet is simply pressed onto the solid electrolyte surface, the interface may be very resistive. Cleaning the LLZO surface and heating the Li/LLZO together under pressure decrease the interface resistance by 10- to 100-fold.[27] Furthermore, deposition of an interface reaction layer, such as Si or ZnO, also greatly reduces the Li interface resistance and provides effective wetting of molten Li to the surface.[28] The lowest area specific resistances with either a coated or optimally cleaned surface are on the order of 1-10 ohm·cm^2.

Most solid electrolyte are evaluated by cycling symmetric cells with Li metal contacts, or in some cases Li-In contacts, to evaluate current density and aging performance. For LLZO, there is a temperature-dependent

critical current density or a critical applied voltage above which a lithium short circuit forms suddenly across even a thick solid-electrolyte membrane.[27] Such a failure mode is similar to decades-old reports of the beta-alumina electrolyte failure modes. For LLZO this critical behavior appears to be related to the grain size, as well as the temperature, and post-failure study indicates that lithium plates out along the grain boundaries.[29,30] There is evidence of internal reduction of the lithium, as well as Li incursion from the anode.[31] Not all studies report cycling pushed to failure, and thus it is possible that short circuits are avoided with very thin electrolytes or for membranes with porous or 3D interfaces that provide a much higher Li contact area.

As above, the Li is most often applied to solid electrolytes by pressing and heating carefully prepared or commercial Li sheets to the electrolyte surface; however, this may trap impurities at the interface. Alternatives include: filling of a porous surface with molten Li,[28] extrusion of Li in direct contact with the solid electrolyte,[4] and vacuum deposition from an evaporation source.[32] Vapor deposition forms a dense and uniform film of Li at the surface of the solid electrolyte, and because the solid electrolyte interface is rapidly buried by the growing Li film, this surface is protected from contamination by background gases. Furthermore, the thickness of the vapor grown Li film can be easily controlled to thicknesses ≤ 1 μm to minimize excess Li inventory. For some batteries, it is possible to reduce the excess Li content to zero by electroplating Li from the cathode directly onto the anode current collector.

Evolution of Lithium during Cycling

Anecdotally, the lithium microstructure evolves with deep and long cycling depending on confinement, but there are few studies openly addressing this issue. Two relevant observations in the literature include: X-ray tomography reveals lithium nodules after extended cycling with polystyrene-b-poly(ethylene oxide) block-copolymers,[33] and surface profilometry indicates gradual agglomeration of the lithium over thousands of cycles of some thin film batteries, depending on the cathode and the duty cycle.[34] Both of these processes eventually cause battery failure. Unreported are experiences from Polyplus using ceramic membranes, Infinite Power Solutions and other companies developing higher energy Lipon thin film batteries, and Bosch cycling optimized commercial polymer batteries at higher temperatures.

Several current investigations of the mechanical properties of lithium metal itself may provide measures of the elastic and plastic properties.[35,36] These are conducted under inert conditions using atomic force microscopy and nanoindentation tools. It is widely assumed that a certain stack pressure is needed to maintain a dense adherent lithium anode with the solid electrolyte, but to our knowledge, there are no relevant experiments or simulations to address this behavior for a high energy configuration with a limited volume of Li metal. It will be important to consider not only new solid electrolytes, but the consequences of interface properties and the anticipated evolution upon deep cycling of 80 to 100% of the metal. In particular, how does the lithium evolve upon either varying thickness of a thin coating, or the filling/emptying of a porous architecture?

Of course, solid state batteries are not limited to Li chemistry.[37] Solid-state Na, Ag, Cu, etc., batteries have been investigated starting from the heyday of β-alumina and the birth of the solid-state ionics community.

Technical and Cost Barriers

For solid state lithium batteries, the technical barriers are numerous and challenging. One reviewer notes that opinion of the future success is influenced by prejudice and misjudgments, leading one to be overly optimistic or overly pessimistic.[38] There are many examples of solids with excellent Li^+ ionic conductivity, so challenges lie elsewhere in taking these materials to functional cells. There are significant commercialization efforts to push solid state batteries into particular markets[39] driven by expectation of higher energy density, improved safety, and lower cost.

To outline the technological challenges, it may be useful to consider the pathway from solid electrolyte material to testing a full lithium battery:

bulk solid electrolyte → thin membrane →

Li half-cell → full cell → performance test

bulk Li anode → Li anode (3-30 μm volume) →

Most research is focused on the bulk ionic conductivity of the electrolyte, striving for the "highest on record." Other properties need to be measured and reported to clarify the practical tradeoffs. These include: the chemical stability (air, humidity, gases evolved), mechanical properties (intrinsic, bulk and thin membrane), microstructure (powders, compacted and sintered membrane, density, typical flaws), and electronic resistivity. If the electrolyte is not stable with Li, the possibility for Li alloys or anodes needs to be understood.

Similarly, it is important to consider and test the transition of what is known about the materials properties of bulk Li to what is expected for a thin film that is extremely dynamic with plating and stripping of essentially a 3-to-30 μm thick sheet, as a monolith or as filled into a porous or engineered host. No doubt properties such as bulk, grain boundary, and surface diffusion; creep and plastic flow; grain growth; impurity aggregation; and passivation are important and need further investigation. The stack pressure to maintain a dense Li anode needs to be tested with consideration of structure and interface properties.

For fabrication of the subassembly of Li and thin and dense solid electrolyte membrane, new scalable and practical processing needs to be investigated. Tradeoffs of using lamination versus liquid and vapor processing of the lithium need to be considered. It is important to begin limiting the amount of Li metal introduced for cycling tests.

It is important to study full cells in addition to symmetric Li/Li cells, as the potential gradients across the solid electrolyte will differ. The challenge of coupling to the cathode could be eased for the first generation of batteries, preparing "almost-all-solid-state" batteries to gain experience and speed development. With protection of the Li with a dense solid, a porous cathode could be wet with a gel or liquid or salt electrolyte, if this is easier than engineering a fully solid composite.

Performance tests need to include a wide variety of cycle and storage tests. This should be initiated by electrochemical tests of the bulk materials: for example, incorporating rest steps to assess stability and self-discharge, and using reference electrodes and post-cycling characterization to determine interface resistance and evolution with time. These and other evaluations that will impact the final product need to be initiated early for the most promising solid electrolytes to accelerate development and projections for successful outcomes with regard to safety, energy density, cost, and extended cycling and lifetime.

References

1 K. Brandt, Historical development of secondary lithium batteries, *Solid State Ionics,* 69 (1994) 173–183.

2 D. Lin, Y. Liu, and Y. Cui, Reviving the lithium metal anode for high-energy batteries, *Nat. Nanotech.,* 12 (2017) 194-206.

3 P. Albertus, personal communication.

4 P Hovington et al., New lithium metal polymer solid state battery for an ultrahigh energy: Nano C-$LiFePO_4$ versus nano $Li_{1.2}V_3O_8$, *ACS Nanolett.* 15 (2015) 2671-2678.

5 Infinite Power Solutions, *Performance Specifications for Ultrathin Batteries*.

6 NJ Dudney, Thin film micro-batteries, *The Electrochemical Society Interface*, (Fall 2008) 44-48; N.J. Dudney, Solid-state thin-film rechargeable batteries, *Mat. Sci. Eng. B* 116 (2005) 245-249.

7 D.T. Hallinan, Jr., and N.P. Balsara, Polymer electrolytes, *Annu. Rev. Mater. Res.,* 43 (2015) 503-525.

8 G.M. Stone et al., "Resolution of the modulus versus adhesion dilemma in solid polymer electrolytes for rechargeable lithium metal batteries, *J. Electrochem. Soc.,* 159 (2012) A222-A227.

9 K.J. Harry, K. Higa, V. Srinivasan, and N.P. Balsara, Influence of electrolyte modulus on the local current density at a dendrite tip on a lithium metal electrode, *J. Electrochem. Soc.,* 163 (2016) A2216-A2224.

10 J. C. Bachman et al., Inorganic solid-state electrolytes for lithium batteries: Mechanisms and properties governing ion conduction, *Chemical Reviews,* 116 (2016) 140-162.

11 Y. Wang et.al., Design principles for solid-state lithium superionic conductors, Nat. Mater. 14 (2015) 1026-1031.

12 N.D. Lepley, N.A. Holzwarth, and Y.A. Du, Computer modeling study of the solid electrolyte Li_3PS_4 and its phosphate analog Li_3PO_4, *ECS Transactions* (2013); Y.A. Du and N.A.W. Holzwarth, Effects of O vacancies and N or Si substitutions on Li^+ migration in Li_3PO_4 electrolytes from first principles, *Phys. Rev. B*, 78 (2008) 174301.

13 Y. Kato et al., High-power all-solid-state batteries using sulfide superionic conductors, *Nature Energy* 1 (2016) 1.

14 W. D. Richards et al., Interface stability in solid-state batteries, *Chem. Mat.,* 28 (2016) 266-273.

15 J. E. Trevey, J. R. Gilsdorf, S. W. Miller, and Se-Hee Lee, Li_2S-Li_2O-P_2S_5 solid electrolytes for all-solid state lithium batteries, *Sol. State Ionics* 214 (2013) 25-30.

16 Y Tao et al., Lithium superionic conducting oxysulfide solid electrolyte with excellent stability against lithium metal for all-solid-state cells, *J. Electrochem. Soc.* 163 (2016) A96-A101.

17 S. W. Martin, Glass and glass-ceramic sulfide and oxy-sulfide solid electrolytes, Ch.14 in *Handbook of Solid State Batteries*, *World Scientific*, pp. 433-501, 2.

18 W. Wang and P. Alexandridis, "Composite polymer electrolytes: Nanoparticles affect structure and properties, *Polymers*, 8 (2016) 387.

19 W. Zhou et al., Plating a dendrite-free lithium anode with a polymer/ceramic/polymer sandwich electrolyte, *J. Amer. Chem. Soc.,* 138 (2016) 9385-9388.

20 W. E. Tenhaeff et al., Impedance characterization of Li ion transport at the interface between laminated ceramic and polymeric electrolytes, *J. Electrochem. Soc.,* 159 (2012) A2118–23; W. E. Tenhaeff, et al., Ionic transport across interfaces of solid glass and polymer electrolytes for lithium ion batteries, *J. Electrochem. Soc.,* 158 (2011) A1143–9 (2011).

21 I. Villaluenga et al., Compliant glass–polymer hybrid single ion-conducting electrolytes for lithium batteries, *PNAS,* 113 (2016) 52–57.

22 J. M. Whiteley et al., Untra-thin solid-state Li-ion electrolyte membrane facilitated by a self-healing polymer matrix, *Adv. Mater.,* 27 (2015) 6922–7.

23 S. Kalnaus et al., Analysis of composite electrolytes with sintered reinforcement structure for energy storage applications, *J. Power Sources,* 241 (2013) 178–85.

24 K. Fun et al., Flexible, solid-state, ion-conducting membrane with 3D garnet nanofiber networks for lithium batteries, *PNAS*, 113 (2016) 7094-7099.

25 T. Thompson et al., Electrochemical window of the Li-ion solid electrolyte LLZO, *ACS Energy Mater.,* 2 (2017) 462-468.

26 Y.Zhu, X. He, and Y. Mo, Origin of outstanding stability in the lithium solid electrolyte materials: Insights from thermodynamic analyses based on first-principles calculations, *ACS Appl. Mater & Interfaces* 7 (2015) 23685-23693.

27 A. Sharafi et al., Characterizing the Li-$Li_7La_3Zr_2O_{12}$ interface stability and kinetics as a function of temperature and current density, *J. Power Sources*, 302 (2015) 135-139.

28 C. Wang et al., Conformal, nanoscale ZnO surface modification of garnet-based solid-state electrolyte for lithium metal anodes, *Nano Lett.,* 15 (2017) 565-571.

29 E. Jianfeng, A. Sharafi, and J. Sakamoto, Intergranular Li metal propagation through polycrystalline $Li_{6.25}Al_{0.25}La_3Zr_2O_{12}$ ceramic electrolyte, *Electrochim. Acta,* 223 (2017) 85-91.

30 L. Cheng et al., Effect of surface microstructure on electrochemical performance of garnet solid electrolytes, *ACS Appl. Mater. & Interfaces,* 7 (2015) 2073-2081.

31 F. Aguesse et al., Investigating the dendritic growth during full cell cycling of garnet electrolyte in direct contact with Li metal, *ACS Appl Mater & Interfaces,* 9 (2017) 3808-3816.

32 J.C. Li et al., Solid electrolytes: The key for high-voltage lithium batteries, *Adv. Energy Mater.,* 5 (2014) 1401408.

33 K.J. Harry, D.T. Hallinan, D.Y. Parkinson, A.A. MacDowell, and N.P. Balsara, Detection of subsurface structures underneath dendrites formed on cycled lithium metal electrodes, *Nat. Mater.*, 13 (2013) 69-73.

34 N.J. Dudney, Evolution of the lithium morphology from cycling of thin film solid-state batteries, *J. Electrocermics*, DOI: 10.1007/s10832-017-0073-2 (2017).

35 C Xu et al., Enhanced strength and temperature dependence of mechanical properties of Li at small scales and its implications for Li metal anodes, *PNAS* 114 (2017) 57-61.

36 E. Herbert, unpublished results.

37 N.J. Dudney, W.C. West, and J. Nanda, eds., *Handbook of Solid State Batteries*, E2nd edition, World Scientific (2016).

38 J Janek and W G. Zeier, A solid future for battery development, *Nature Energy* 1 (2016) 16141.

39 Samuel De-Leon Energy Ltd., *Solid Electrolyte Batteries, Technology, Applications & Market Review*, Version 6, Dec. 2015.

3.5 Li-S Systems

Lithium-sulfur (Li-S) batteries have potential for exceptionally high theoretical energy density based on the reversible reaction of $S+2Li \leftrightarrow Li_2S$ (Figure 3-5),[1, 2] with a theoretical specific capacity of 1670 mAh g^{-1} and energy of 2500 Wh kg^{-1}. However, Li-S batteries also have many fundamental challenges, including the formation of electronically insulating redox products of S/Li_2S and the dissolution of lithium polysulfide intermediates. As a result, Li-S batteries suffer from low sulfur utilization, low coulombic efficiency, and fast capacity fading. Over the last decade, great progress has been made on understanding the detailed electrochemical reaction pathways in the Li-S system and in developing strategies to extend the cycling life, but most of the efforts have been focused on the materials and component levels. Some key fundamental challenges have not been solved for practical applications and commercialization of the technology.

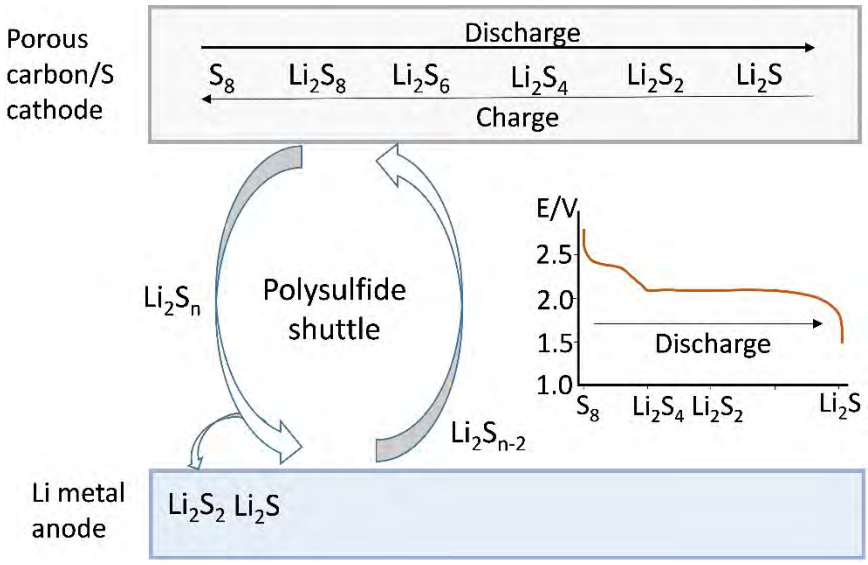

Figure 3-5. Schematic illustration of the charge and discharge processes in Li-S batteries. The polysulfides formed during charge and discharge dissolve into the electrolyte and are shuttled between the cathode and anode, causing capacity fading and self-discharge. Insoluble lithium sulfides also deposit on the electrode surface causing electrode degradation.

State of the Art

The Sulfur Cathode

Different from conventional Li-ion cathodes, sulfur is not a stable electrode material because of the dissolution of polysulfides formed during charge and discharge. For battery applications, the insulating nature of the sulfur and polysulfides is also a problem. To address these challenges, great efforts have been made to develop conducting sulfur composite cathode architectures to encapsulate the sulfur species and improve conductivity. Nazar et al. first explored mesoporous carbon to capture the sulfur species and demonstrated a high specific capacity of 1000 mAh/g.[3] Up to date, a wide range of high surface area carbon forms has been explored, demonstrating different levels of success. Examples include microporous and mesoporous carbon,[4] hollow carbon sphere,[5] graphene,[6] hollow carbon nanofibers,[7] metal-organic framework particles,[8] and conductive polymers.[9] Many different approaches have also been explored to functionalize the carbon surface and to incorporate additives in order to further improve the binding between the sulfur species and the host materials.

Recently, conducting sulfur host materials with a polar surface towards Li^+ and polysulfide anions S_x^{2-} were shown to be effective in trapping polysulfides through strong interfacial chemical interactions.[10] These materials

include Ti_4O_7[11], MXene phase Ti_2C,[12] and TiS_2.[13] This strategy is based on interfacial binding rather than physical confinements. Good stability and capacity retention (up to 2000 cycles) were reported. In addition, several groups reported the benefit of functional interlayers and membranes to reduce the polysulfide dissolution in the electrolyte and reduce diffusion of the products towards the lithium anode.[14]

The Electrolyte

Besides the cathode architecture, electrolytes also play a critical role in controlling polysulfide dissolution, the reaction kinetics and stability of sulfur cathode and lithium metal anode. The most widely used conventional electrolyte is based on ethers such as 1,2-dimethoxyethane (DME) and cyclic ether 1,3-dioxolane (DOL) as the co-solvents with lithium bis(trifluoromethane)sulfonimide (LiTFSI) as the supporting salt. The regular DOL:DME is a strong solvating system. Up to 6 M Li_2S_8 (based on atomic S concentration) can be dissolved. The soluble polysulfides provide fast reaction kinetics compared with solid-solid reactions. Nevertheless, without appropriate protection, the polysulfides will diffuse to the lithium anode during charge/discharge and cause shuttling reactions. An important strategy is to reduce the solubility of polysulfides in the electrolyte. Very recently, electrolytes with a low polysulfide solubility were studied to prevent dissolution and the shuttle effect. Such new electrolytes provide an alternative approach compared to traditional solvating electrolytes or solid state electrolytes for Li-S batteries.[15]

The Anode

The stability of the lithium anode is also a major challenge for long cycling Li-S batteries. Compared to what happens in Li-ion batteries, the lithium metal anode degradation in Li-S systems is caused by a complex reaction with the polysulfide species in the electrolytes. For example, soluble polysulfide intermediates formed during charge/discharge may migrate to the anode side and react with lithium metal, leading to anode corrosion, short cycle life, and low coulombic efficiency. Unstable passivation layers are formed on the lithium anode surface because of the presence of polysulfides and organic electrolytes. Various electrolyte additives, such as $LiNO_3$,[16] P_2S_5,[17] LiBOB,[18] LiI,[19] etc., are used to protect Li metal by forming a protection layer. So far, the $LiNO_3$ is the most effective additive to form a protection layer (LiN_xO_y decomposed from $LiNO_3$) on lithium metal, which alleviates the shuttle effect.[20] Interestingly, the $LiNO_3$ and polysulfide were reported to have a synergic effect that protects the lithium metal in Li-S batteries. However, the continuous consuming of $LiNO_3$ during cycling is still an unsolved problem for long-term cycling stability. Recently, concentrated electrolytes have been reported to help stabilize lithium metal by reducing the available solvent for chemical degradation. Numerous studies were also reported on using protection layers on the lithium metal surfaces. In addition, alternative anodes such as hybrid lithium, silicon, carbon, and alloys were explored to replace the lithium metal anode. However, such alternative anodes also suffer from other mechanisms of degradation and reduce the practical energy of Li-S batteries because of their lower capacity compared with lithium metal.

New Concepts

In order to stop polysulfide dissolution and prevent lithium metal anode failure, solid-state Li-S batteries have been studied in which the liquid electrolyte is replaced by a solid electrolyte. Sion Power has been developing a Li-S battery using a complicated protected lithium metal structure. High capacity (>1500 mAh g^{-1}) and stable cycling were reported using $Li_{1.5}PS_{3.3}$ as the solid electrolyte.[21] Recently, a new Li-S battery was developed with excellent cycling stability. It uses a gradient ceramic membrane with a dense Li-ion conducting layer in the middle and a porous layer on the cathode side to trap the sulfur species. Still, all-solid-state batteries are in early stages of development. In general, solid state electrolytes have poor ion conductivity compared with liquid electrolytes and thus give rise to sluggish reaction kinetics and low power. In addition, controlling interfacial structure and charge transport across the interfaces between the solid electrolyte and electrode materials remains a significant challenge. Furthermore, all-solid-state batteries are difficult to scale up for large scale manufacturing.

Rather than suppressing and reducing the dissolution of polysulfides, some new concepts take advantage of the solubility of polysulfide species. Several groups explored liquid electrolyte-based batteries such as Li-S redox flow batteries using polysulfide solutions or suspension in both organic- and water-based systems as the cathode.[22,23] In such systems, a high solubility of the active species is required. However, the low solubility and precipitation of small lithium sulfide molecules become a problem unless the discharge voltage is controlled. Furthermore, in most of the liquid-based electrode batteries, lithium metal degradation becomes more serious.

Technical Barriers

Although extended cycling life (up to 2000 cycles) has been reported in the literature, most studies were based on thin film sulfur electrodes, low sulfur loading (< 2 mg S cm^{-2}), and high carbon contents (30%-40 wt % in electrodes). The use of nanostructured carbon is critical in alleviating the polysulfide dissolution problem, but at the same time introduces a large amount of inactive materials and wasted space. Under these conditions, a large amount of electrolyte, typically electrolyte/sulfur (E/S; $\mu l_E/g_S$) ratio >10, is required to obtain good cycle life. These approaches significantly sacrifice the volumetric and gravimetric energy of the system.

Recent studies suggested that a high sulfur loading (>6 mg cm^{-2}), a low porosity and carbon content, and a low electrolyte amount are required to deliver a high energy density in Li-S battery systems.[24] The high sulfur utilization and low electrolyte amount present new fundamental and technological challenges. First, the low porosity and small pore sizes imply that the wetting of the electrolyte becomes difficult. The electrochemical reaction pathways, the distribution and transport of the liquid phases, and the reaction products could be different. Similarly, because of the insulating nature of the sulfur species, the reduced conducting carbon phase, low porosity, and small electrolyte amount, both the electronic and ion transport become much more difficult. This will cause high resistance, low sulfur utilization, and poor cycling performance, particularly with high currents. Furthermore, uncontrollable distribution and deposition of the reaction products on both the cathode and anode could cause the battery to fail. The stress associated with the thick electrode and the large volumetric change can also lead to breakdown of the electrode and the battery.

Perspective

From the above discussion, future high energy and high power Li-S batteries need to focus on the science of high sulfur utilization in thick electrodes with low porosity and minimum amount of electrolyte and additive. (1) There needs to be a better understanding of the polysulfide reaction mechanisms and the transport pathways of the reaction species under high sulfur utilization. (2) New thick electrode architectures are needed with stable and favorable interfaces between electrode and electrolyte and enhance electron and ion transport. (3) New electrolytes should be possible to control the solubility of different phases, reduce polysulfide dissolution, and optimize the reaction kinetics. (4) New concepts are needed to control the nucleation and deposition of the sulfur species in order to reduce the utilization of high surface carbon and the amount of electrolyte. (5) New electrode and battery design, such as solid and semi-solid batteries, could be developed to overcome the fundamental barriers in Li-S systems.

References

1 Armand, M.; Tarascon, J. M., Building better batteries, *Nature* **2008,** *451* (7179), 652-657.

2 Rauh, R. D.; Abraham, K. M.; Pearson, G. F.; Surprenant, J. K.; Brummer, S. B., A lithium/dissolved sulfur battery with an organic electrolyte, *J. Electrochem. Soc.***1979,** *126* (4), 523-527.

3 Ji, X.; Lee, K. T.; Nazar, L. F., A highly ordered nanostructured carbon-sulphur cathode for lithium-sulphur batteries, *Nat. Mater.* **2009,** *8* (6), 500-506.

4 (a) Schuster, J.; He, G.; Mandlmeier, B.; Yim, T.; Lee, K. T.; Bein, T.; Nazar, L. F., Spherical ordered mesoporous carbon nanoparticles with high porosity for lithium–sulfur batteries, *Angew. Chem. Int. Ed.* **2012,** *51* (15), 3591-3595; (b) Li, X.; Cao, Y.; Qi, W.; Saraf, L. V.; Xiao, J.; Nie, Z.; Mietek, J.; Zhang, J.-G.;

Schwenzer, B.; Liu, J., Optimization of mesoporous carbon structures for lithium-sulfur battery applications, *J. Mater. Chem.* **2011,** *21* (41), 16603-16610.

5 Zhang, C.; Wu, H. B.; Yuan, C.; Guo, Z.; Lou, X. W., Confining sulfur in double-shelled hollow carbon spheres for lithium–sulfur batteries, *Angew. Chem.* **2012,** *124* (38), 9730-9733.

6 (a) Cao, Y.; Li, X.; Aksay, I. A.; Lemmon, J.; Nie, Z.; Yang, Z.; Liu, J., Sandwich-type functionalized graphene sheet-sulfur nanocomposite for rechargeable lithium batteries, *Phys. Chem. Chem.Phys.* **2011,** *13* (17), 7660-7665; (b) Zhou, G.; Pei, S.; Li, L.; Wang, D.-W.; Wang, S.; Huang, K.; Yin, L.-C.; Li, F.; Cheng, H.-M., A graphene–pure-Sulfur sandwich structure for ultrafast, long-life lithium–sulfur batteries, *Adv. Mater.* **2014,** *26* (4), 625-631; (c) Wang, H.; Yang, Y.; Liang, Y.; Robinson, J. T.; Li, Y.; Jackson, A.; Cui, Y.; Dai, H., Graphene-wrapped sulfur particles as a rechargeable lithium–sulfur battery cathode material with high capacity and cycling stability, *Nano Lett.* **2011,** *11* (7), 2644-2647.

7 (a) Zheng, G.; Yang, Y.; Cha, J. J.; Hong, S. S.; Cui, Y., Hollow carbon nanofiber-encapsulated sulfur cathodes for high specific capacity rechargeable lithium batteries, *Nano Lett.* **2011,** *11* (10), 4462-4467; (b) Zheng, G.; Zhang, Q.; Cha, J. J.; Yang, Y.; Li, W.; Seh, Z. W.; Cui, Y., Amphiphilic surface modification of hollow carbon nanofibers for improved cycle life of lithium sulfur batteries, *Nano Lett.* **2013,** *13* (3), 1265-1270.

8 (a) Xu, G.; Ding, B.; Shen, L.; Nie, P.; Han, J.; Zhang, X., Sulfur embedded in metal organic framework-derived hierarchically porous carbon nanoplates for high performance lithium-sulfur battery, *J. Mater. Chem. A* **2013,** *1* (14), 4490-4496; (b) Zheng, J.; Tian, J.; Wu, D.; Gu, M.; Xu, W.; Wang, C.; Gao, F.; Engelhard, M. H.; Zhang, J.-G.; Liu, J.; Xiao, J., Lewis acid–base interactions between polysulfides and metal organic framework in lithium sulfur batteries, *Nano Lett.* **2014,** *14* (5), 2345-2352.

9 Xiao, L.; Cao, Y.; Xiao, J.; Schwenzer, B.; Engelhard, M. H.; Saraf, L. V.; Nie, Z.; Exarhos, G. J.; Liu, J., A soft approach to encapsulate sulfur: Polyaniline nanotubes for lithium-sulfur batteries with long cycle life, *Adv. Mater.* **2012,** *24* (9), 1176-1181.

10 Pang, Q.; Liang, X.; Kwok, C. Y.; Nazar, L. F., Advances in lithium–sulfur batteries based on multifunctionalcathodes and electrolytes, *Nature Energy* **2016,** *1*, 16132.

11 Pang, Q.; Kundu, D.; Cuisinier, M.; Nazar, L. F., Surface-enhanced redox chemistry of polysulphides on a metallic and polar host for lithium-sulphur batteries, *Nat.Commun.* **2014,** *5*, 4759.

12 Liang, X.; Garsuch, A.; Nazar, L. F., Sulfur cathodes based on conductive MXene nanosheets for high-performance lithium–sulfur batteries, *Angew. Chem. Int. Ed.* **2015,** *54* (13), 3907-3911.

13 Seh, Z. W.; Yu, J. H.; Li, W.; Hsu, P.-C.; Wang, H.; Sun, Y.; Yao, H.; Zhang, Q.; Cui, Y., Two-dimensional layered transition metal disulphides for effective encapsulation of high-capacity lithium sulphide cathodes, *Nat. Commun.* **2014,** *5*, 5017.

14 (a) Su, Y.-S.; Manthiram, A., Lithium–sulphur batteries with a microporous carbon paper as a bifunctional interlayer, *Nature Communications* **2012,** *3*, 1166; (b) Bai, S.; Liu, X.; Zhu, K.; Wu, S.; Zhou, H., Metal–organic framework-based separator for lithium–sulfur batteries, *Nature Energy* **2016,** *1*, 16094.

15 Cheng, L.; Curtiss, L. A.; Zavadil, K. R.; Gewirth, A. A.; Shao, Y.; Gallagher, K. G., Sparingly solvating electrolytes for high energy density lithium–sulfur batteries, *ACS Energy Lett.* **2016,** *1* (3), 503-509.

16 Xiong, S. Z.; Xie, K.; Diao, Y.; Hong, X. B., On the role of polysulfides for a stable solid electrolyte interphase on the lithium anode cycled in lithium-sulfur batteries, *J. Power Sources* **2013,** *236*, 181-187.

17 Lin, Z.; Liu, Z. C.; Fu, W. J.; Dudney, N. J.; Liang, C. D., Phosphorous pentasulfide as a novel additive for high-performance lithium-sulfur batteries, *Adv. Funct. Mater.* **2013,** *23* (8), 1064-1069.

18 Xiong, S.; Kai, X.; Hong, X.; Diao, Y., Effect of LiBOB as additive on electrochemical properties of lithium–sulfur batteries, *Ionics* **2012,** *18* (3), 249-254.

19 Wu, F.; Lee, J. T.; Nitta, N.; Kim, H.; Borodin, O.; Yushin, G., Lithium iodide as a promising electrolyte additive for lithium-sulfur batteries: Mechanisms of performance enhancement, *Adv. Mater.* **2015,** *27* (1), 101-108.

20 Cao, R.; Xu, W.; Lv, D.; Xiao, J.; Zhang, J.-G., Anodes for rechargeable lithium-sulfur batteries, *Adv. Energy Mater.* **2015,** *5* (16), DOI: 10.1002/aenm.201402273.

21 Nagata, H.; Chikusa, Y., All-solid-state lithium–sulfur battery with high energy and power densities at the cell level, *Energy Tech.* **2015,** *4* (4), 484-489.

22 (a) Yang, Y.; Zheng, G. Y.; Cui, Y., A membrane-free lithium/polysulfide semi-liquid battery for large-scale energy storage, *Energy Environ. Sci.* **2013,** *6* (5), 1552-1558; (b) Fan, F. Y.; Woodford, W. H.; Li, Z.; Baram, N.; Smith, K. C.; Helal, A.; McKinley, G. H.; Carter, W. C.; Chiang, Y.-M., Polysulfide flow batteries enabled by percolating nanoscale conductor networks, *Nano Lett.s* **2014,** *14* (4), 2210-2218; (c) Pan, H.; Wei, X.; Henderson, W. A.; Shao, Y.; Chen, J.; Bhattacharya, P.; Xiao, J.; Liu, J., On the way toward understanding solution chemistry of lithium polysulfides for high energy Li–S redox flow batteries, *Adv.Energy Mater.* **2015,** *5* (16), DOI: 10.1002/aenm.201500113.

23 http://ppbcadmin.webfactional.com/page/technology#_lithium-sulfur, accessed March 2017.

24 Eroglu, D.; Zavadil, K. R.; Gallagher, K. G., Critical link between materials chemistry and cell-level design for high energy density and low cost lithium-sulfur transportation battery, *J. Electrochem. Soc.* **2015,** *162* (6), A982-A990.

3.6 Lithium-Air Systems

Introduction

The Li-air (O_2) battery has recently received significant attention because of its high theoretical specific energy.[1,2] Currently, four Li-air cell configurations (outlined in Figure 3-6) are being pursued in an attempt to harness a modest fraction of this large specific energy.[2] In the nonaqueous, aprotic version (Figure 3-6A), and the version that employs a solid-state electrolyte and operates under dry conditions (Figure 3-6B), the Li-O_2 battery typically operates via the 2 e^- electrochemical formation and decomposition of lithium peroxide (Li_2O_2):

$$\text{Anode:} \quad Li(s) \rightarrow Li^+ + e^- \tag{1}$$

$$\text{Cathode:} \quad 2(Li^+ + e^-) + O_2 \rightarrow Li_2O_2(s), \ U=2.96 \text{ V vs. } Li/Li^+ \tag{2}$$

$$\text{Overall:} \quad 2Li(s) + O_2(g) \rightarrow Li_2O_2(s) \tag{3}$$

In cells where the Li metal anode is protected by using a Li^+ conductive/water impermeable ceramic membrane, an aqueous electrolyte can be employed in the cathode chamber (Figure 3-6C, D), and the active electrochemical reaction at the cathode changes to a 4 e^- process:

$$\text{Cathode:} \quad 4(Li^+ + e^-) + O_2 + 2H_2O \rightarrow 4LiOH, \ U=3.45 \text{ V vs. } Li/Li^+ \tag{4}$$

Overall: $4Li(s) + O_2 + 2H_2O \rightarrow 4LiOH$ (5)

No architecture shown in Figure 3-6 has proven to be more effective than others, and tradeoffs between possible performance, cell design complexity, safety, and energy density exist between each architecture. As an example, the aprotic version (Figure 3-6) may provide the highest possible theoretical energy density because water does not participate in the reversible reaction. However, Li_2O_2 is both insoluble in aprotic solvents and a wide bandgap insulator, and therefore, it deposits on and passivates the cathode during discharge. On the other hand, LiOH is soluble in aqueous electrolytes, such that passivation is less of a concern in aqueous Li-air batteries. Of the four architectures shown in Figure 3-6, the aprotic version has garnered the majority of research interest, likely because of the ease of cell assembly and design, as well as the potential to theoretically achieve the highest energy density. Specific challenges for each configuration are discussed more completely in the next section.

State of the Art

Despite their high theoretical specific energy, many significant challenges have so far limited all four configurations shown in Figure 3-6 from achieving commercial viability.[3] As such, Li-air batteries are still in the developmental stage (TRL 2-3), and researchers should pay particular attention to identifying solutions to the challenges listed in Section 2.1.3.

Nonaqueous (aprotic) Li-Air Batteries

Limited rechargeability due to cathode and electrolyte instabilities is perhaps the single largest hurdle facing Li-O_2 battery development. In fact, typical LIB liquid carbonate-based electrolytes cannot be used in aprotic Li-O_2 batteries due to their high reactivity with reduced oxygen species. A typical aprotic Li-O_2 cell composition includes a cathode consisting of porous carbon powder bound to a stainless steel mesh using polytetrafluoroethylene, an ether-based electrolyte (e.g., LiTFSI dissolved in monoglyme or tetraglyme) embedded into a porous glass fiber or polymer (e.g., Celgard) separator, and a Li metal anode. This cell has provided among the best coulombic efficiency measured, as defined by the ratio of O_2 evolved to O_2 consumed during an equal-capacity galvanostatic charge and discharge, respectively, at roughly 90% after one cycle[4] and ~50% after 50 cycles.[5] Noting that all organic electrolytes studied to date have limited stability in a Li-O_2 battery, a recent configuration in which an inorganic molten nitrate salt mixture (150°C, $LiNO_3/KNO_3$) was used as the electrolyte attained substantially better electrolyte stability compared to an organic-based electrolyte cell, and was able to achieve 50 cycles at 1-mAh/cm^2 depth of discharge at 0.25 mA/cm^2.[6] This cell's cyclability was ultimately limited by cathode carbon corrosion. New strategies will be necessary for all Li-air configurations, such as development of new methods to protect the carbon from parasitic reactions with reduced oxygen species, or the development of cost-effective, high-surface-area, stable alternatives to carbon.

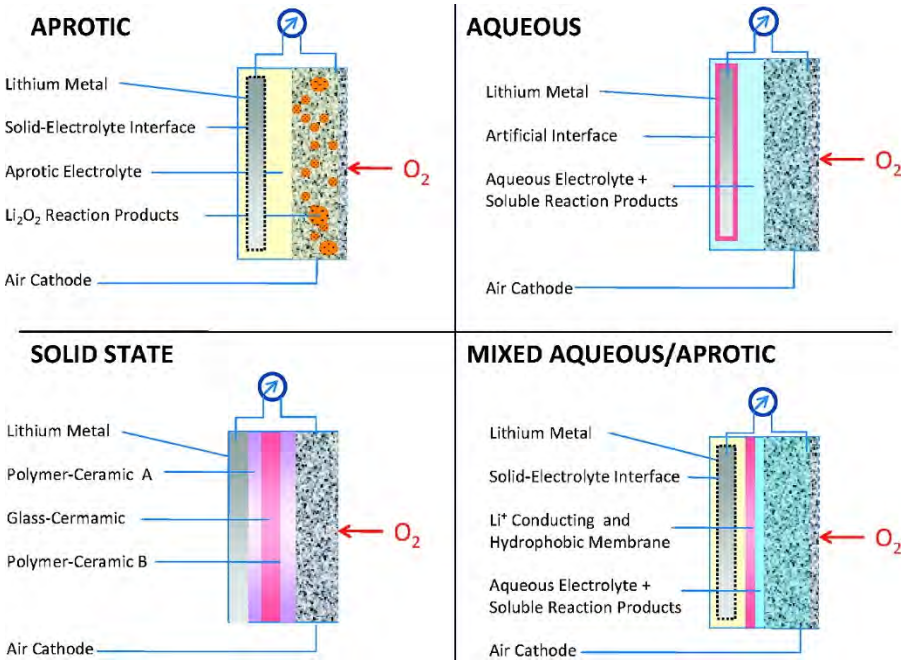

Figure 3-6. Four architectures of Li-air batteries. (A) Aprotic architecture in which an aprotic organic Li^+ electrolyte is in contact with both the Li metal anode and porous cathode. (B) Solid-state architecture in which a Li^+-conductive nonporous ceramic (e.g., LISICON, garnet, or Li_2S-P_2S_5 glass) "protects" the Li metal anode from O_2 crossover as it is being fed to the porous battery cathode. (C and D) Architectures in which Li metal is protected using a nonporous ceramic, and an aqueous electrolyte is used in the cathode chamber. Soluble LiOH is the primary discharge product at the cathode in these configurations, although Li_2O_2-hydrate has also been reported. Figure from ref. 2. Reproduced with permission of American Chemical Society.

Regarding the measurement of rechargeability, numerous instances of long-term Li-air battery cycling have been reported in the literature, with typical values being greater than 100 cycles at 1000 mAh per gram of carbon contained in the cathode. These reports are typically based on repeated galvanostatic discharge-charge cycles, with the ultimate rechargeability being inferred from how many cycles are achieved prior to cell failure (where substantial current can no longer be sustained). In cells where large electrolyte volumes or exceedingly small cathode carbon loadings are used (such that 1000 mAh/g of carbon is, in fact, an extremely small total capacity), it is difficult to decouple the coulombic efficiency of the reversible Li-O_2 electrochemistry from electrochemical degradation of the electrolyte and cathode using galvanostatic cycling without another quantitative measure of the Li-O_2 electrochemistry. In the aprotic system (Figure 3-6A), the electrolyte and cathode degradation are well-known challenges (as discussed above) that substantially contribute to electrochemical capacity decline if not appropriately controlled. True rechargeability in a system should be identified through quantitative measurements of O_2 consumption and evolution during discharge and charge, respectively. These measurements capture the coulombic efficiency of the battery reactions, and ideally, any O_2 consumed during discharge would be evolved during a charge of equal capacity, with O_2 consumed/evolved being equal over extended cycling. Unfortunately, very few reports of O_2 consumption and evolution are available, making it somewhat difficult to assess the current state-of-the-art in terms of rechargeability.

Another pressing challenge is Li_2O_2-induced electronic passivation of the oxygen electrode, which limits battery energy density to a small fraction of its theoretical energy density.[1] Since Li_2O_2 is a wide bandgap insulator, after the Li_2O_2 deposit reaches a critical thickness, the electronic conductivity of the cathode no longer can support an electrochemical current, and the battery suffers a "sudden-death" well before its theoretical maximum capacity. The cell capacity at which this "sudden death" occurs is also strongly dependent on

discharge current, as would be expected given that a higher rate of electron transport means that a smaller critical thickness for the Li_2O_2 deposit can support the electrochemistry.

Recent research has focused on electrolyte compositions that allow Li_2O_2 formation through a "solution mechanism," allowing it to form in large aggregates through a process that is less prone to electronic conductivity limitations, thereby dramatically enhancing the capacity of the cell. Using one of these strategies, Gao et al. reported an areal capacity of ~10 mAh/cm^2 at 0.2 mA/cm^2, which represents among the highest areal capacities known for a Li-air battery.[7] On charge, these Li_2O_2 aggregates pose a concern because Li_2O_2 is an insulator, disallowing charge transfer to Li_2O_2 not in intimate contact with the cathode surface. Soluble redox active molecules are being pursued as an interesting strategy to allow charge transfer to disconnected Li_2O_2 to occur through the solution, thereby reducing charge overpotential in cells where these aggregates form.[8]

Solid-State and Aqueous Electrolyte Configurations

In both aqueous and solid-state configurations of a Li-air battery, the Li metal electrode is separated from the oxygen electrode by a Li^+-conductive separator that is otherwise impermeable to all other matter. The development of the Li^+-conductive separator is critical to the success of both architectures, and associated challenges are described more completely in Section 2.1.3.

For wholly solid-state Li-air batteries, engineering the interfaces between the electrodes and the solid-state electrolyte is critically important. Lithium metal-induced reduction is a known problem with certain potential solid-state Li^+ conductors, which can result in the formation of a large impedance surface layer. Engineering a porous cathode that is both electronically and ionically conductive while reducing interfacial impedances with the solid-state electrolyte will also be a challenge. Preliminary results on solid-state Li-air batteries appear to be promising,[9] although many fundamental aspects of their operation are still left to be understood.

Aqueous Li-air batteries reduce issues associated with passivation at the cathode given the solubility of formed products in the aqueous electrolyte, which in theory could allow these batteries to achieve better areal capacities than aprotic Li-O_2 batteries. For example, a 25 mAh/cm^2 discharge was achieved at 1 mA/cm^2 in a concentrated LiOH electrolyte.[10] Of course, it is critical to ensure that no defects form in the Li^+ separator during aqueous cell operation given the high reactivity between water and Li metal. If such a design could be guaranteed, the aqueous cell would be substantially safer than an aprotic cell due to the elimination of the flammable organic electrolyte. The development of bifunctional 4e$^-$ oxygen reduction/evolution catalysts to reduce discharge and charge overpotentials is also necessary, as is typical for any device that utilizes oxygen electrochemistry.[3]

Technical Barriers and Needs

Technical barriers and needs for Li-air batteries are given below.

Technical barriers and needs	Component
• Electronically conductive cathode materials that are stable during Li_2O_2 formation and oxidation	• Cathode
• Oxygen reduction/evolution reaction bifunctional catalysts for aqueous Li-O_2 system	• Cathode
• Cathode design to optimize O_2 diffusion for high rates	• Cathode
• Cathode/electrolyte designs to circumvent Li_2O_2 passivation	• Cathode/Electrolyte
• Design to enable low impedance interface between porous cathode and solid electrolyte	• Cathode/electrolyte
• Nonaqueous/solid electrolyte stable to Li-O_2 cathode electrochemistry	• Electrolyte
• Electrolyte redox-active additives to improve battery capacity and/or to reduce charge transport limitations during charging	• Electrolyte
• Stable, thin, gas/water impermeable Li^+ conductors	• Electrolyte/anode
• High coulombic efficiency, safe (dendrite-free cycling) Li metal anode	• Anode
• Quantitative measurements of gas consumed and evolved during battery operation to gauge true reversibility in new battery architectures	• Cell
• Air purification system or new pressurized tank cell designs	• Pack/System

References

1 Luntz, A. C.; McCloskey, B. D., Nonaqueous Li-air batteries: a status report, *Chem. Rev.* **2014**, *114*, 11721.

2 Girishkumar, G.; McCloskey, B.; Luntz, A. C.; Swanson, S.; Wilcke, W., Lithium−air battery: Promise and challenges, *J. Phys. Chem. Lett.* **2010**, *1*, 2193.

3 Lu, J.; Li, L.; Park, J.-B.; Sun, Y.-K.; Wu, F.; Amine, K., Aprotic and aqueous Li-O_2 batteries, *Chem. Rev.* **2014**, *114*, 5611.

4 McCloskey, B. D.; Bethune, D. S.; Shelby, R. M.; Mori, T.; Scheffler, R.; Speidel, A.; Sherwood, M.; Luntz, A. C., Limitations in rechargeability of Li-O_2batteries and possible origins, *J. Phys. Chem. Lett.* **2012**, *3*, 3043.

5 Nasybulin, E. N.; Xu, W.; Mehdi, B. L.; Thomsen, E.; Engelhard, M. H.; Massé, R. C.; Bhattacharya, P.; Gu, M.; Bennett, W.; Nie, Z.; Wang, C.; Browning, N. D.; Zhang, J.-G., Formation of interfacial layer and long-term cyclability of Li-O_2 batteries, *ACS Appl. Mater. Interfaces* **2014**, *6*, 14141.

6 Giordani, V.; Tozier, D.; Tan, H.; Burke, C. M.; Gallant, B. M.; Uddin, J.; Greer, J. R.; McCloskey, B. D.; Chase, G. V.; Addison, D., A molten salt lithium-oxygen battery, *J. Am. Chem. Soc.* **2016**, *138*, 2656.

7 Gao, X.; Chen, Y.; Johnson, L.; Bruce, P. G., Promoting solution phase discharge in Li–O_2 batteries containing weakly solvating electrolyte solutions, *Nature Mater.* **2016**, *15*, 882.

8 Freunberger, S. A., Batteries: Charginf ahead rationally, *Nature Energy* **2016**, *1*, 16074.

9 Li, F.; Kitaura, H.; Zhou, H., The pursuit of rechargeable solid-state Li–air batteries, *Energy Environ. Sci.* **2013**, *6*, 2302.

10 Matsui, M.; Wada, A.; Matsuda, Y.; Yamamoto, O.; Takeda, Y.; Imanishi, N., A novel aqueous lithium-oxygen cell based on the oxygen-peroxide redox couple, *Chem. Commun.* **2015**, *51*, 3189.

3.7 Other Metal-Air System

Introduction

Metal-oxygen batteries are of great interest for energy storage because of their unparalleled theoretical energy densities.[1-4] They are assembled from a metal anode and an air-breathing cathode in a proper electrolyte. The metal anode can be alkali metals (e.g., Li, Na and K), alkaline earth metals (e.g., Mg), or first-row transition metals (e.g., Fe and Zn). The electrolyte can be aqueous or non-aqueous – depending on the nature of the anode employed. The air-breathing cathode often has an open porous architecture that permits continuous oxygen supply from surrounding air. *Metal-air batteries combine the design features of battery anodes and fuel cell cathodes.*

The first primary zinc-air battery was designed by Maiche dating back to 1878,[5] and its commercial products started to enter the market in 1932.[6] Following that, aqueous iron-air, aluminum-air, and magnesium-air batteries were developed in the 1960s.[7-9] Non-aqueous metal-air batteries first emerged about two decades ago, initially for Li-air, and more recently for Na-air and K-air.[1-3] Particularly attractive are the emerging superoxide-based Na-O_2 and K-O_2 batteries because they are based on the facile one-electron reduction/evolution of oxygen that forms sodium superoxide (NaO_2) or potassium superoxide KO_2) as the discharge product (Figure 3-7). The quasi-reversible one-electron redox reaction ($O_2 + e^- \leftrightarrow O_2^-$) eliminates the use of electrocatalysts and achieves low overpotentials, which are particularly beneficial during the charging process. These superoxide-based metal-air batteries provide promising solutions for energy storage applications with high energy efficiencies and low cost.

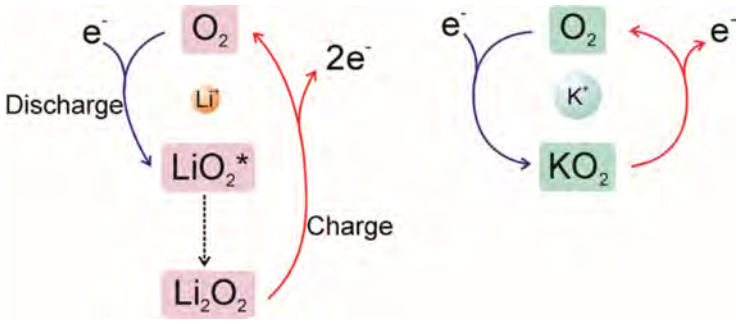

Figure 3-7. Comparison of the battery chemistry between Li-O_2 batteries and K-O_2 batteries.

State of the Art

Superoxide-Based Metal-Oxygen Batteries

Hartmann et al. reported the first rechargeable sodium superoxide battery in 2013.[2] Independently, Wu et al. reported the first potassium superoxide battery the same year.[3] Both studies elegantly show the benefits of the single-electron oxygen redox in reducing overpotentials even in the absence of electrocatalysts. Recently, a Li-O_2 battery with LiO_2 as the discharge product was reported.[10] It requires a specially designed cathode, Ir-rGO, to enable the stabilization of LiO_2. It was suggested that the Ir_3Li intermetallic compound that formed, which has a similar crystal structure with LiO_2, could act a template for the growth of LiO_2. Despite the similar operating principle of these superoxide batteries, only KO_2 is thermodynamically stable (Figure 3-8). The spontaneous decay of NaO_2 into Na_2O_2 was observed when the discharged cathode was rested.[11]

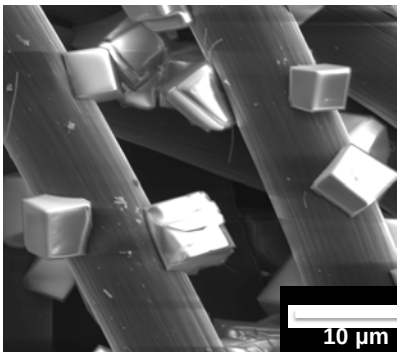

Figure 3-8. Scanning electron microscopy image of KO_2 crystals on carbon fibers. From Xiao et al., *ACS Applied Materials & Interfaces*, 2017, *9* (5), 4301–4308.

The above pioneering studies have stimulated further detailed investigations. For example, McCloskey et al. used the differential electrochemistry mass spectrometry technique to confirm that NaO_2 is the predominant discharge product in their Na-O_2 cell employing an ether-based electrolyte.[12] A theoretical calculation based on the surface energies of different sodium oxide crystals concluded that bulk Na_2O_2 is preferred under standard operating conditions while NaO_2 is more stable at the nanoscale and/or under elevated oxygen partial pressure.[13] In order to determine the reason behind the lower charging overpotential NaO_2 compared to Na_2O_2, Siegel et al. calculated the theoretical conductivity values for these species.[14] Nazar et al. investigated the role of phase-transfer catalysis in Na-O_2 cells by comparing the discharge capacity with electrolytes that contain different amounts of water.[15] It is shown that even trace amounts of water in the electrolyte can significantly increase the capacity of the Na-O_2 battery. Furthermore, they also demonstrated that other proton donors (such as anhydrous acetic acid and benzoic acid) also contribute to the growth of NaO_2 crystals.

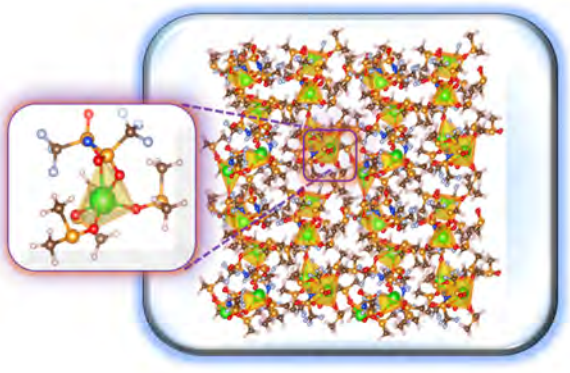

Figure 3-9. The unique solvated structure in superconcentrated DMSO/NaTFSI electrolyte. From He et al., *Angew. Chem. Int. Ed.*, 2016, *55*, 15310.

Developing electrolytes compatible with both the alkali metals and superoxide is crucial. The idea of superconcentrated electrolyte has been introduced for Na-O_2 batteries by Wu et al.[16] In their system, the high concentration of the organic salt, sodium trifluoromethanesulfonimide (NaTFSI), helps stabilize dimethyl sulfoxide (DMSO) molecules in the presence of sodium, where DMSO is known as a high-donor number solvent that benefits the electrochemical performance of Na-O_2 cells. Highly concentrated solutions (>3 mol/kg) result in a solvation structure of loosely crosslinked $Na(DMSO)_3TFSI$ units that binds up a large portion of the DMSO molecules as confirmed by ab-initio molecular dynamics simulation (Figure 3-9), leaving only few molecules available for reaction with Na metal. Sodium preferentially attacks the TFSI anions and forms a passivating protective layer that is composed of the inorganic side products.

The same group also found that a solvent- and O_2-impermeable layer can be formed in-situ on the K metal surface with 1M potassium bis(trifluoromethanesulfonyl)imide (KTFSI) in ether electrolyte. This protection layer is surprisingly effective in inhibiting the K anode decay by blocking ether molecules and O_2 crossover. As a result, K-O_2 batteries have obtained excellent cycle stability over 60 cycles (~ 700 hours) even under a pressurized O_2 environment, which is over 10 times better than that of the K-O_2 battery without the protection layer. This study highlights the importance of K anode protection and the potential of achieving long-life K anodes in K-O_2 batteries.

Aqueous Metal-Air Batteries

Metals such as Zn, Fe, Al, and Mg have been used in aqueous metal-air batteries.[4,17-19] Developing efficient and stable bifunctional electrocatalysts for oxygen reduction and evolution plays the decisive role to improving battery performance. The oxygen reduction reaction (ORR) mainly takes place at the triple-phase boundary where the solid electrode is simultaneously interfaced with liquid electrolyte and gaseous O_2. As a consequence, developing active air catalysts to expedite the ORR kinetics and designing proper electrode architecture to enlarge the triple-phase boundary would greatly benefit the battery discharge performance. Existing knowledge accumulated for alkaline fuel cells can be readily transplanted to aid the research of Zn-air batteries. Over the past several decades, a large variety of materials, ranging from precious metals (e.g., Pt and Ag) to non-precious metal oxides (e.g., MnO_x and CoO_x) or even metal-free carbonaceous materials (e.g., nitrogen-doped carbon nanotubes or graphene), have been investigated as the air catalyst.[4,20,21] A few high-performance bifunctional electrocatalysts have been successfully developed in just the last decade.[4,18,22-24] Alternatively, the bifunctionality of the air cathode can be achieved via the proper combination of multiple functional components.[25]

However, even with the combination of best available ORR and oxygen evolution reaction (OER) catalysts, the polarization of the air cathode between charge and discharge is still so large that the round-trip energy efficiency of rechargeable Zn-air batteries would unlikely go beyond 65% at current densities pertinent to practical applications. The durability of the catalysts under alternating reductive-oxidative environments during discharge-charge cycles also limits the cycling stability. Rational design of the air electrode in terms of an interfacial structure with optimal hydrophilicity and integration of catalysts into the air electrode is critical to optimize the catalytic activity and avoid flooding of the catalytic active sites. Furthermore, the metallic anode needs to be specifically engineered so as to suppress its corrosion and non-uniform dissolution/deposition. Without properly resolving this issue, the long-term cycling stability of rechargeable Zn-air batteries would not be achieved, but so far it is relatively overlooked.

Technical and Cost Barriers

The main barrier of superoxide batteries is suppressing metal dendrites and identifying an electrolyte system with good compatibility with the highly reactive alkali metals. Surface coating, replacing alkali metal with the alloy, optimizing electrolyte to form a stable protective layer on the metal surface, using membranes to block oxygen crossover are effective methods. The electrolyte should also be stable with reactive superoxide radicals (O_2^-). As an example, the cyclability of K-O_2 batteries with a KPF_6/DME electrolyte was found to be limited by the decay of the K anode due to oxygen crossover and the electrolyte decomposition on the anode.[26] The resultant overgrowth of the anode surface layer not only causes the huge increase of battery internal resistance, but also results in the depletion of both the anode and the electrolyte.[26] When using KTFSI salt in ether electrolyte, a solvent- and O_2-impermeable protection layer was in-situ formed on the K anode surface.[27] The excellent protection ability of this interfacial layer greatly enhanced the K anode stability, enabling very stable cycling over 700 hours even under pressurized O_2 environment. In future development, high-throughput screening is desirable to efficiently extract useful insights from a vast chemical space for electrolyte design and development.

Systematic studies of the ORR/OER kinetics are also needed. The ORR occurs at the three-phase interface (gaseous oxygen–liquid electrolyte–conductive electrode), while the OER involves electrochemical oxidation of superoxide that requires understanding the charge transport in the superoxide crystals and probably takes place at the three-phase interface of liquid electrolyte–superoxide crystal–conductive electrode. Thus, rational design of the oxygen electrode in terms of the porosity, pore size distribution, and surface wetting is critical to optimize the loading of discharge products and rate performance.

Safety is another concern due to the high reactivity of alkali metals. The reactive metal anode may be replaced by a more stable intercalation or alloy type electrode. For example, an antimony-based electrode exhibits a reversible storage capacity of 650 mAh/g corresponding to the formation of a cubic K_3Sb alloy. Layered MoS_2 can also be used as an alternative K^+ storage material. The formation of $K_{0.4}MoS_2$ was identified during the K^+ intercalation process. In addition, MoS_2 has been shown to have excellent stability for repetitive K^+ intercalation and de-intercalation.

Current superoxide batteries use pure oxygen instead of air. It is desirable for these batteries to breathe air directly. However, moisture and CO_2 will induce side reactions with both the metal electrode and the superoxide discharge product. The consumption of active materials will decrease coulombic efficiency and cycle life.

References

1 Abraham, K. M.; Jiang, Z., A polymer electrolyte-based rechargeable lithium/oxygen battery, *J Electrochem. Soc.,* **1996,** *143,* 1-5.

2 Hartmann, P.; Bender, C. L.; Vračar, M.; Dürr, A. K.; Garsuch, A.; Janek, J.; Adelhelm, P. A., Rechargeable room-temperature sodium superoxide (NaO_2) battery, *Nat. Mater.,* **2013,** *12,* 228-232.

3 Ren, X. D.; Wu, Y. Y., A low-overpotential potassium-oxygen battery based on potassium superoxide, *J. Am. Chem. Soc.,* **2013,** *135,* 2923-2926.

4 Li, Y.; Dai, H., Recent advances in zinc-air batteries, *Chem. Soc. Rev.,* **2014,** *43,* 5257-5275.

5 Maiche, L., French Patent 127,069 (1878).

6 George, W. H., U.S. Patent 1899615 (1933).

7 Ojefors, L.; Carlsson, L., An iron-air vehicle battery, *J. Power Sources,* **1978**, *2,* 287-296.

8 Zaromb, S., The use and behavior of aluminum anodes in alkaline primary batteries, *J. Electrochem. Soc.,* **1962,** *109,* 1125-1130, Doi 10.1149/1.2425257.

9 Carson, W. N.; Kent, C. E., The magnesium-air cell, in D. H. Collins (ed.) *Power Sources,* Pergamon (1966).

10 Lu, J.; Lee, Y. J.; Luo, X. Y.; Lau, K. C.; Asadi, M.; Wang, H. H.; Brombosz, S.; Wen, J. G.; Zhai, D. Y.; Chen, Z. H.; Miller, D. J.; Jeong, Y. S.; Park, J. B.; Fang, Z. Z.; Kumar, B.; Salehi-Khojin, A.; Sun, Y. K.; Curtiss, L. A.; Amine, K., A lithium-oxygen battery based on lithium superoxide, *Nature,* **2016,** *529,* 377.

11 Landa-Medrano, I.; Pinedo, R.; Bi, X. X.; de Larramendi, I. R.; Lezama, L.; Janek, J.; Amine, K.; Lu, J.; Rojo, T., New insights into the instability of discharge products in Na-O_2 batteries, *ACS Applied Materials & Interfaces,* **2016,** *8,* 20120-20127.

12 McCloskey, B. D.; Garcia, J. M.; Luntz, A. C., Chemical and Electrochemical differences in nonaqueous Li-O_2 and Na-O_2 Batteries, *J. Phys. Chem. Lett.,* **2014,** *5,* 1230-1235.

13 Kang, S.; Mo, Y. F.; Ong, S. P.; Ceder, G., Nanoscale stabilization of sodium oxides: Implications for Na-O_2 batteries, *Nano Lett.,* **2014, 14**, 1016-1020 (2014).

14 Yang, S.; Siegel, D. J., Intrinsic conductivity in sodium-air battery discharge phases: Sodium superoxide vs sodium peroxide, *Chem. Mater.,* **2015,** *27*, 3852-3860.

15 Xia, C.; Black, R.; Fernandes, R.; Adams, B.; Nazar, L. F., The critical role of phase-transfer catalysis in aprotic sodium oxygen batteries, *Nat. Chem.,* **2015,** *7,* 496-501.

16 He, M.; Lau, K. C.; Ren, X.; Xiao, N.; McCulloch, W. D.; Curtiss, L. A.; Wu, Y., Concentrated electrolyte for the sodium-oxygen battery: Solvation structure and improved cycle life, *Angew Chem. Int. Ed. Engl.,* **2016,** *55,* 15310-15314, doi:10.1002/anie.201608607.

17 Narayanan, S. R.; Prakash, G. K. S.; Manohar, A.; Yang, B.; Malkhandi, S.; Kindler, A., Materials challenges and technical approaches for realizing inexpensive and robust iron-air batteries for large-scale energy storage, *Solid State Ionics,* **2012,** *216,* 105-109, doi:DOI 10.1016/j.ssi.2011.12.002.

18 Fu, J.; Cano, Z. P.; Park, M. G.; Yu, A.; Fowler, M.; Chen, Z., Electrically rechargeable zinc-air batteries: Progress, challenges, and perspectives, *Adv. Mater.*, **2016,** 10.1002/adma.201604685.

19 Egan, D. R.; de Leon, C. P.; Wood, R. J. K.; Jones, R. L.; Stokes, K. R.; Walsh, F. C., Developments in electrode materials and electrolytes for aluminum-air batteries, *J. Power Sources,* **2013,** *236,* 293-310, doi:DOI 10.1016/j.jpowsour.2013.01.141.

20 Lee, J. S.; Kim, S. T.; Cao, R.; Choi, N. S.; Liu, M.; Lee, K. T.; Cho, J. Metal-air batteries with high energy density: Li-air versus Zn-Air, *Adv. Energy Mater.,* **2011,** *1,* 34-50, DOI 10.1002/aenm.201000010.

21 Cheng, F. Y.; Chen, J., Metal-air batteries: From oxygen reduction electrochemistry to cathode catalysts, *Chem. Soc. Rev.* **2012,** *41,* 2172-2192, doi: 10.1039/C1cs15228a.

22 Cheng, F.; Shen, J.; Peng, B.; Pan, Y.; Tao, Z.; Chen, J., Rapid room-temperature synthesis of nanocrystalline spinels as oxygen reduction and evolution electrocatalysts, *Nat. Chem.,* **2011,** *3,* 79-84.

23 Liang, Y.; Li, Y.; Wang, H.; Zhou, J.; Wang, J.; Regier, T.; Dai, H., Co_3O_4 nanocrystals on graphene as a synergistic catalyst for oxygen reduction reaction, *Nat. Mater.,* **2011,** *10,* 780-786.

24 Zhang, J.; Zhao, Z.; Xia, Z.; Dai, L., A metal-free bifunctional electrocatalyst for oxygen reduction and oxygen evolution reactions, *Nat. Nanotechnol.,* **2016,** *10,* 444-452.

25 Li, Y.; Gong, M.; Liang, Y.; Feng, J.; Kim, J.-E.; Wang, H.; Hong, G.; Zhang, Z.; Dai, H., Advanced zinc-air batteries based on high-performance hybrid electrocatalysts, *Nat. Commun.,* **2013,** *4,* 1805.

26 Ren, X.; Lau, K. C.; Yu, M.; Bi, X.; Kreidler, E.; Curtiss, L. A.; Wu, Y., Understanding side reactions in K–O_2 batteries for improved cycle life, *ACS Applied Materials & Interfaces,* **2014,** *6,* 19299-19307, doi:10.1021/am505351s.

27 Ren, X. D.; He, M. F.; Xiao, N.; McCulloch, W. D.; Wu, Y. Y., Greatly enhanced anode stability in K-oxygen batteries with an in situ formed solvent- and oxygen-impermeable protection layer, *Adv. Energy Mater.,* **2016,** *7,* DOI: 10.1002/aenm.201601080.

3.8 Next Generation Systems (Na-ion, Mg-ion, Zn-ion: aqueous and non-aqueous)

Introduction

In the last several decades, LIB systems have achieved notoriety as the archetypal working ion for reversible electrochemical intercalation (or insertion) in batteries. However, LIBs are not ideal for certain applications due to cost or stored energy density limits,[1] thereby requiring new technologies to be developed. For instance, alternative intercalation working ions, such as sodium, magnesium, and zinc, are receiving considerable attention as potential next-generation intercalation batteries due to their conceptual similarity with Li-ion batteries as well as potential cost ($ kWh^{-1}), stored energy (Wh kg^{-1} or Wh L^{-1}), or power (W kg^{-1}) benefits.

Various degrees of commercialization have been achieved with next-generation intercalation working ions; however, most effort to date has been limited to R&D. Several significant challenges must be overcome before full market integration is realized for these potential battery technologies. Aqueous systems are typically considered more feasible for grid-scale applications when cost, discharge rate, and cycle life are prioritized; whereas, non-aqueous systems typically provide higher energy densities consistent with transportation and portable electronics. Some cost and energy densities are compared in Figure 3-10 for non-aqueous systems, which were determined by adapting Argonne National Laboratory's Lithium Ion BatPaC Model for Electric-Drive Vehicles[2] using calculated voltage, capacity, and rate capability estimates from the Materials Project.[3]

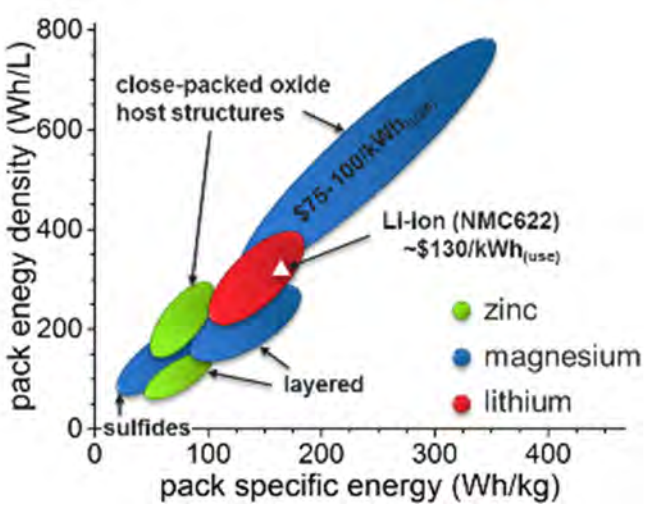

Figure 3-10. Pack-level comparison of non-aqueous intercalation energy storage chemistries considering cathode structure types, working ion, and metallic anodes (graphite, in the case of LIBs). Values are estimated by the Battery Performance and Cost Model[2] with materials properties input from the Materials Project.[3] Useable energy is identified for EV applications.

Like LIBs, sodium-ion batteries (SIBs) rely on a monovalent cation but introduce several additionally attractive features and tradeoffs for specific applications.[4,5] Most notably, SIBs have low cost projections, particularly due to utilization of inexpensive materials that are non-variant in market pricing. The theoretical energy density for non-aqueous SIBs is ~250 Wh kg^{-1} (pouch cell) when utilizing high capacity electrodes as determined by the BatPaC model.[2] Additionally, safety concerns, relative to LIBs, are mitigated. For example, SIBs negate the need of cobalt in the cathode material, which is considered a health concern. Also, SIBs have shown high durability and can be discharged to 0 V, stored for months, and cycled well for hundreds of cycles when

restarted. They can be shipped in zero-charge state, unlike LIBs, which are shipped at 30% state of charge, resulting in safety concerns, particularly in large size formats. Finally, the thermal stability of SIBs is superior to charged $LiFePO_4$ (LIB), according to data compiled from accelerating rate calorimetry results by Faradion Ltd.

Nonaqueous multivalent metal cells are promising for advanced energy storage technologies due to their enhanced theoretical coulometric capacity, limited dendrite formation, and low cost. From Figure 3-10, the proposed next-generation batteries based on multivalent ions can surpass the current performance of LIB technology in terms of specific energy and cost. Non-aqueous Mg-ion batteries, for example, are very interesting as next-generation batteries and present a number of promising features, including high volumetric capacities,[6] similar ionic radius compared with Li^+ ions,[7] relatively low migration activation barrier energy for diffusion in certain cathode materials,[8] and highly-efficient reversible Mg deposition on metal anodes.[9]

State of the Art

Sodium-Ion Batteries

At present, SIBs come in non-aqueous and aqueous electrolyte media. For both, the electrochemical storage reactions rely principally on the intercalation reaction mechanism for sodium cations into host electrodes.[4,5] Both aqueous and non-aqueous SIBs are currently in the mature device stage.

Non-aqueous SIBs can provide nominally 3.3 V voltage and modest power capability in prismatic and 18650 cells based on hard carbon as the anode and either $NaVPO_4F$ or layered sodium transition metal oxides as the cathode. The working energy density of prototypes designed for the e-mobility application is 140-150 Wh kg^{-1} (prismatic cell) developed by Faradion Ltd. in the UK and 95 Wh kg^{-1} for the 18650 cylindrical cell developed in France by RS2E and CEA organizations. These cells have been cycled to 3000 cycles at rates demonstrating good power. The U.S. is notably absent in involvement with these chemistries.

Aqueous SIBs are dominated in the U.S. by Aquion Energy (~25 kWh module size) for grid storage applications, utilizing a hard carbon or sodium titanium phosphate anode material coupled with sodium manganese oxide cathode and sodium sulfate water-based electrolyte. Energy density is not quoted, but is likely low (< 30 Wh kg^{-1}); however, the cost is anticipated to be very low due to sustainable inexpensive precursors such as manganese, carbon, water, and sodium sulfate salt. Cycle life and safety are excellent. In Korea, grid storage sodium-seawater aqueous batteries are under mature development. These designs use a dual electrolyte in which a sodiated Sn anode is bathed in non-aqueous electrolyte that is separated by a NASICON ceramic membrane. These are paired with a carbon cathode (air electrode) loaded with catalyst for oxygen reduction/evolution reactions (ORR/OER) using seawater flowing across the electrode. Sodium cations are extracted from seawater and transported through NASICON and alloy with Sn-based anode at voltages approximately 2.8 V; reversibility is excellent. This high-energy-density grid storage battery is in the process of being scaled up and has a planned commercialized future in Asia, as an example of an aggressive pursuit of SIB.

Zn-Ion Batteries

Non-aqueous zinc-ion batteries (naq-ZIBs) are limited to research-level development and are not currently reduced to practice or commercially available; however, several systems consisting of Zn metal anode and a reversible intercalation cathodes have recently been reported. Zinc non-aqueous electrolytes have been identified to electrochemically deposit reversibly on Zn metal anodes and possess a wide electrochemical stability window (~3.8 V vs. Zn^{2+}/Zn), which has enabled a pathway toward a multivalent rechargeable battery with high voltage cathode material.[10] Fully reversible naq-ZIB chemistries have been established in research laboratories: hydrated Zn/nanostructured bilayered V_2O_5[11] or δ–MnO_2 cells with acetonitrile-$Zn(TFSI)_2$ electrolytes demonstrate good reversibility and stability for 120+ cycles with nearly 100% coulombic efficiency and energy densities of ~170 mAh g^{-1} and ~100 mAh g^{-1}, respectively (albeit operating at low cell voltages of only 0.8 V and 1.2 V, respectively, vs. Zn/Zn^{2+}).

Aqueous ZIBs have been considered primarily as low cost opportunities for grid storage applications. As with their naq-ZIB cousins, development of aq-ZIBs is limited to research-scale activities with no known commercialization due to a limited choice of functioning positive intercalation/insertion electrodes. Several cathodes have been investigated and shown to have underperforming performance (metal-hexacyanoferrates and MnO_2),[12,13,14,15,16] although conversion reactions in aq-ZIB cathodes (MnO_2) have been reported with reasonable efficiency and lifetime.[17] A recent report proposed a feasible intercalation cathode: vanadium oxide bronze pillared by interlayer Zn^{2+} ions and water ($Zn_{0.25}V_2O_5{\cdot}nH_2O$) achieved a capacity of 300 mAh g^{-1} at high rates.[18]

Mg-Ion Batteries

Magnesium-ion batteries (MIBs) were first considered two decades ago[19,20] and have garnered newfound attention with the first successfully demonstrated reversible MIB reported in 2000 based on a molybdenum sulfide cathode, Mg-metal anode, and a Grignard reagent-based electrolyte.[21] To date, MIBs are not commercially available primarily due to the significant scientific challenges being faced, e.g., electrolyte reductive stability, availability of high-voltage Mg insertion cathodes, and slow kinetics. As such, MIB research is still in a nescient stage; however, significant progress in understanding has been accomplished in recent years as highlighted in several review articles.[21,22,23,24,25,26,27,28]

To improve Mg deposition, electrolyte development has seen the replacement of Grignard reagents with all-Mg complexes, non-polarizing anion species in various solvents, and ionic liquids[21,23,24,25,28]; however, reductive stability at high voltages is still a challenge.[29] The relationship between the electrolyte and Mg-metal anode toward efficient and reversible electrochemical magnesium deposition has been investigated.[30] To date, demonstration of feasible cathode materials has been limited to sulfides, with inherent low voltages (< 1.2 V vs. Mg/Mg^{2+}), and layered oxides, with cycle lifetime limitations.[27] Several high-voltage (2.8-3.8 V vs. Mg/Mg^{2+}) dense oxide materials have been predicted to have sufficient Mg mobility for MIB applications, suggesting they may be important Mg insertion materials.[26,27] Despite these reports and the high potential for naq-MIBs, to date, no reversible Mg insertion at high voltages capable of obtaining theoretical energy densities in excess of LIBs has been established.

Technical and Cost Barriers

Across all potential next-generation rechargeable batteries with working ion intercalation, the technical barriers are fundamentally tied to materials discovery, i.e., identifying functional active materials (especially cathodes), developing chemically and electrochemically stable (e.g., corrosion) active and inactive components, and determining charge transport rates in bulk components and across interfaces. A significant potential market for energy storage products, unsatisfied by existing technology for multivalent working ions, can be realized by solving these challenges. A summary of technical barriers broadly applicable to these systems is provided below.

Note that the technology readiness level of MIBs and ZIBs is relatively low (level 2-3), so more analysis is required to accurately predict the cost barriers for market infiltration; however, aqueous systems are very promising, as is naq-MIB, for cost per kWh competitiveness. The more advanced SIB technology is less limited by existing materials, but rather optimization and cost structures. For example, $NaPF_6$, the current salt used in SIB electrolyte, is costly but is expected to decrease in price with market growth.

Anodes

- Enhance coulombic efficiency of reversible metal deposition.

Electrolytes

- Expand electrochemical stability window up to 4 V (vs. M/M^{2+}) while maintaining oxidative stability.
- Establish anodic decomposition mechanisms and mitigation strategies.
- Improve low-temperature (<30 °C) performance.
- Identify electrolyte additives or other strategy for enhancing interface stability.
- Lower cost of salts/solvents.
- Potentially replace solvent-based electrolytes with ionic liquids or solid polymer electrodes with sufficient transport and stability properties.

Cathodes

- Identify and engineer material with high specific capacity, rate capabilities, and stability for high-voltage >3.0 V operation.
- Modify interfacial surface for enhanced stability
- Increase working ion transport (bulk and interface).

References

1 Whittingham, M.S., Ultimate limits to intercalation reactions for lithium batteries, *Chem. Rev.* **2014**, *114* (23), 11414–11443.

2 *BatPaC: A Lithium-Ion Battery Performance and Cost Model for Electric-Drive Vehicles,* http://www.cse.anl.gov/batpac.

3 *Materials Project,* https://www.materialsproject.org.

4 Slater, M.D.; Kim, D.; Lee, E.; Johnson, C.S., Sodium-ion batteries, *Adv. Funct. Mater.,* **2013**, *23* (8), 947–958.

5 Huang, L.; Cheng, J.; Li, X.; Wang, B., Electrode nanomaterials for room temperature sodium-ion batteries: A review, *J. Nanosci. Nantotech*., **2015**, *15* (9), 6295.

6 Muldoon, J.; Bucur, C.B.; Gregory, T., Quest for nonaqueous multivalent secondary batteries: Magnesium and beyond, *Chem. Rev.* **2014**, *114* (23), 11683–11720.

7 Shannon, R.D., Revised effective ionic radii and systematic studies of interatomic distances in halides and chalcogenides, *Acta Cryst. A*, **1976,** *32* (5), 751–767.

8 Rong, Z.; Kitchaev, D.; Canepa, P.; Huang, W.; Ceder, G., An efficient algorithm for finding the minimum energy path for cation migration in ionic materials, *J. Chem. Phys.,* **2016**, *145* (7), 074112.

9 See, K.A.; Chapman, K.W.; Zhu, L.; Wiaderek, K.M.; Borkiewicz, O.J.; Barile, C.J.; Chupas, P.J.; Gewirth, A.A., The interplay of Al and Mg speciation in advanced Mg battery electrolyte solutions, *J. Am. Chem. Soc.* **2016**, *138* (1), 328–337.

10 Han, S.-D.; Rajput, N.N.; Qu, X.; Pan, B.; He, M.; Ferrandon, M.S.; Liao, C.; Persson, K.A.; Burrell, A. K., Origin of electrochemical, structural, and transport properties in nonaqueous zinc electrolytes, *ACS Appl. Mater. Interfaces,* **2016**, *8* (5), 3021–3031.

11 Senguttuvan, P.; Han, S.-D.; Kim, S.; Lipson, A.L.; Tepavcevic, S.; Fister, T.T.; Bloom, I.D.; Burrell, A.K.; Johnson, C.S., A high power rechargeable nonaqueous multivalent Zn/V_2O_5 battery, *Adv. Energy Mater.* **2016**, *6* (24), 1600826.

12 Chen, L.; Zhang, L. Y.; Zhou, X. F.; Liu, Z.P., Aqueous batteries based on mixed monovalence metal ions: A new battery family, *ChemSusChem,* **2014**, *7*, 2295.

13 Zhang, L.; Chen, L.; Zhou, X.; Liu, Z., Towards high-voltage aqueous metal-ion batteries beyond 1.5 V: The zinc/zinc hexacyanoferrate system, *Adv. Energy Mater.,* **2015,** *5,* 1400930.

14 Jia, Z.; Wang, B.; Wang, Y., Copper hexacyanoferrate with a well-defined open framework as a positive electrode for aqueous zinc ion batteries, *Mater. Chem. Phys.* **2015,** *149*, 601–606.

15 Gupta, T.; Kim A.; Phadke S.; Biswas S.; Luong T.; Hertzberg B.J.; Chamoun M.; Evans-Lutterodt K.; Steingart D.A., Improving the cycle life of a high-rate, high-potential aqueous dual-ion battery using hyper-dendritic zinc and copper hexacyanoferrate, *J. Power Sources,* **2016**, *305*: 22–29.

16 Lee, B.; Lee, H.R.; Kim, H.; Chung, K.Y.; Cho, B.W.; Oh, S.H., Elucidating the intercalation mechanism of zinc ions into α-MnO_2 for rechargeable zinc batteries, *Chem. Comm.,* **2015,** *51*, 9265-9268.

17 Pan, H.; Shao, Y.; Yan, P.; Cheng, Y.; Han, K.S.; Nie, Z.; Wang, C.; Yang, J.; Li, X.; Bhattacharya, P.; Mueller, K.T.; Liu, J., Reversible aqueous zinc/manganese oxide energy storage from conversion reactions, *Nature Energy* 2016, 1, 16039.

18 Kundu, D.; Adams, B.D.; Duffort, V.; Vajargah, S. H.; Nazar, L.F., A high-capacity and long-life aqueous rechargeable zinc battery using a metal oxide intercalation cathode, *Nature Energy,* **2016**, *1*, 16119.

19 Gregory, T.D.; Hoffman, R.J.; Winterton, R.C., Nonaqueous electrochemistry of magnesium: Applications to energy storage, *J. Electrochem. Soc.,* **1990**, *137* (3), 775–780.

20 Novák, P.; Scheifele, W.; Haas, O. Magnesium insertion batteries — an alternative to lithium? *J. Power Sources,* **1995**, *54* (2), 479–482.

21 Aurbach, D.; Lu, Z.; Schechter, A.; Gofer, Y.; Gizbar, H.; Turgeman, R.; Cohen, Y.; Moshkovich, M.; Levi, E., Prototype systems for rechargeable magnesium batteries, *Nature,* **2000**, *407* (6805), 724–727.

22 Huie, M.M.; Bock, D. C.; Takeuchi, E.S.; Marschilok, A.C.; Takeuchi, K.J., Cathode materials for magnesium and magnesium-ion based batteries, *Coord. Chem. Rev.* **2015**, *287*, 15–27.

23 Yoo, H.D.; Shterenberg, I.; Gofer, Y.; Gershinsky, G.; Pour, N.; Aurbach, D., Mg rechargeable batteries: An on-going challenge, *Energy Environ. Sci.,* **2013**, *6* (8), 2265–2279.

24 Song, J.; Sahadeo, E.; Noked, M.; Lee, S. B. Mapping the challenges of magnesium battery, *J. Phys. Chem. Lett.* **2016**, *7* (9), 1736–1749.

25 Saha, P.; Datta, M. K.; Velikokhatnyi, O. I.; Manivannan, A.; Alman, D.; Kumta, P.N., Rechargeable magnesium battery: Current status and key challenges for the future, *Progress in Materials Science* **2014**, *66*, 1–86.

26 Massé, R. C.; Uchaker, E.; Cao, G., Beyond Li-ion: Electrode materials for sodium- and magnesium-ion batteries, *Sci. China Mater.* **2015**, *58* (9), 715–766.

27 Canepa, P.; Gautam, G.S.; Hannah, D.C.; Malik, R.; Liu, M.; Gallagher, K.G.; Persson, K.A.; Ceder, G., Odyssey of multivalent cathode materials: Open questions and future challenges, *Chem. Rev.* **2017**, *117* (5), 4287–4341.

28 Huie, M.M.; Cama, C.A.; Smith, P.F.; Yin, J.; Marschilok, A.C.; Takeuchi, K.J.; Takeuchi, E.S., Ionic liquid hybrids: Progress toward non-corrosive electrolytes with high-voltage oxidation stability for magnesium-ion based batteries, *Electrochimica Acta,* **2016**, *219*, 267–276.

29 Lipson, A.L.; Han, S.-D.; Pan, B.; See, K.A.; Gewirth, A.A.; Liao, C.; Vaughey, J.T.; Ingram, B.J., Practical stability limits of magnesium electrolytes, *J. Electrochem. Soc.,* **2016**, *163* (10), A2253–A2257.

30 Rajput, N.N.; Qu, X.; Sa, N.; Burrell, A.K.; Persson, K.A., The coupling between stability and ion pair formation in magnesium electrolytes from first-principles quantum mechanics and classical molecular dynamics, *J. Am. Chem. Soc.,* **2015**, *137* (9), 3411–3420.

3.9 New Cell Designs (3D batteries, thin-film batteries, bi-polar batteries)

Introduction

Improvements in electrochemical power sources are absolutely critical for enabling innovation in a wide range of applications. For any particular energy storage chemistry, the design, synthesis, and discovery of new materials is paramount, but innovations in new materials is not a linear process. Therefore, innovation in cell design is critical for extracting the maximum performance from known materials used for energy storage. For almost any cell chemistry, new cell construction can be used to maximize electrical contact to active materials, as well as to minimize diffusion lengths between anodes and cathodes to increase power density and to extend cycle life. The overall goal is to develop a device that has the high energy density of a battery but with the high power density of an ultracapacitor, while extending cycle life and safety.[1,2] This is a tall order.

Whereas thin film (2D) batteries can be used to great effect for small devices (such as for IOT applications), they are not likely to be able to provide reasonable capacities or power densities required for large-scale applications. Three-dimensional (3D) batteries, on the other hand, are challenging to make reproducibly with low cost and high throughput.[3] This section of the report will discuss new designs for electrode morphologies, as well as overall cell construction with a particular emphasis on Li-ion battery chemistry as one of the most advanced examples on the market, with a very large overall market share.

State of the Art: Nanostructure Electrodes

Incorporation of small particles of active material into slurry-based 2D electrodes has had enormous success in the manufacture of conventional Li-ion batteries, but limitations in energy and power densities are rapidly approaching.[4] As new materials are incorporated into cells, attention to the relevant surface reactions that are possible, as well as diffusion processes and interfacial resistances, is becoming increasingly important. It is well known that increasing the surface area of electrodes can be used to increase the accessible capacity as well as the cycle life of many candidate materials,[5] particularly high-energy-density conversion materials that exhibit large volume change,[6] but increasing the amount of active material loaded onto a current collector, with excellent electrical contact, is still a challenge. Advances in the synthesis and surface chemistry of

nanostructured electrodes are being made (Figure 3-11).[7] Current methods for making nanostructured electrodes include solution phase synthesis, chemical vapor deposition, and electrodeposition, and these synthetic methods are each being exploited for improving the morphology of the active materials such that there is controlled porosity with continuous electrical conductivity.[8] In theory, these methods could be scaled for large-scale manufacturing. However, often these materials are simply incorporated into conventional slurry-based electrodes, and the energy and power density at the full cell level are still intimately tied to each other.

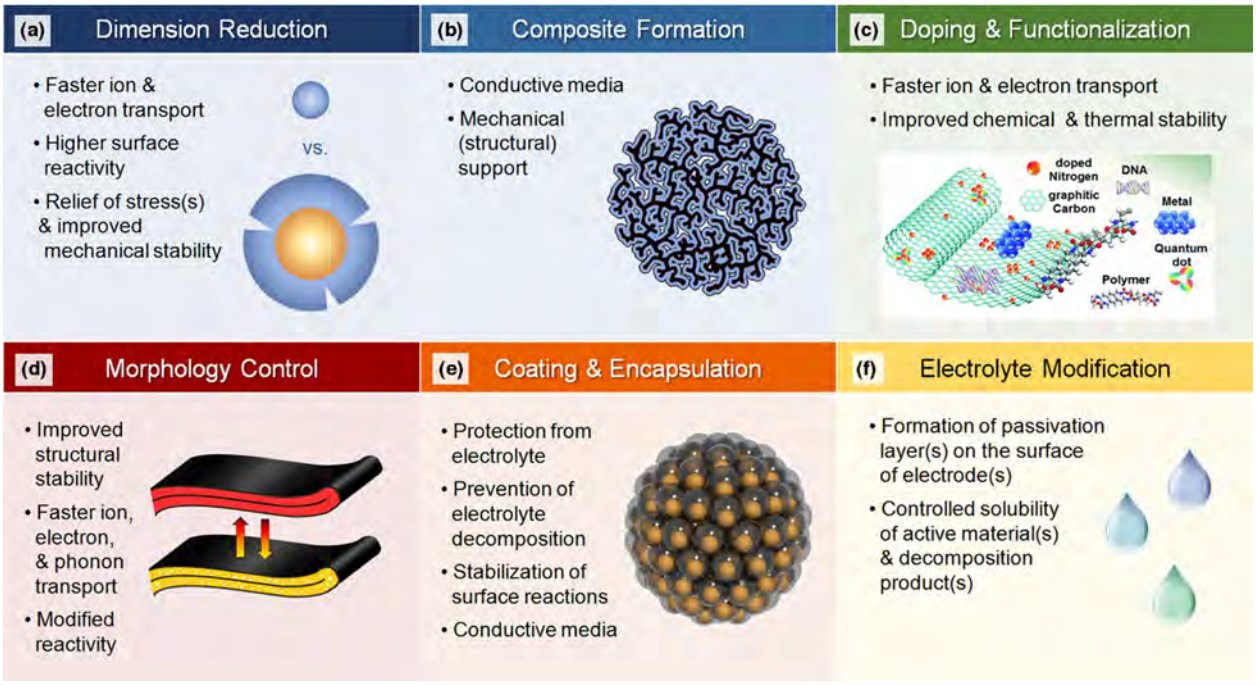

Figure 3-11. General strategies for performance enhancement and their rationale: (a) reduction of dimensions of active materials, (b) formation of composites, (c) doping and functionalization, (d) tuning of particle morphology, (e) formation of coatings or shells around active materials, and (f) modification of electrolyte.[7]

Traditional battery designs with 2D geometries require fairly large footprint areas to achieve practical capacities. The common strategy for increasing capacity is to increase the areal loading of the active materials (making the electrodes thicker). However, this strategy is not a viable approach because the mechanical integrity of the film decreases with increasing thickness (due to expansion and contraction of the active materials during cycling)[9], and also because thicker films reduce the power density of the device. Although reducing the particle size of the active material to nanostructured dimensions is helpful, the incorporation of those particles into conventional electrodes still results in a 2D battery. In general, 2D battery designs result in a compromise between energy density and power density because of the limitation in footprint area. Three-dimensional batteries, in comparison, should achieve an order of magnitude more capacity per footprint. Moreover, with 3D configurations, there is also the promise that these batteries can achieve both high energy density and high power density within a small footprint area.

A true 3D battery should have all three components interdigitated such that the Li-ion diffusion path into and between electrodes is short. A recent example is shown in Figure 3-12,[10] and several other possible architectures have been proposed.[11] The most significant challenge to realizing a 3D battery reproducibly is the application of conformal, pinhole-free electrolytes that can be deposited with controlled thickness.[12]

Technical and Cost Barriers

Although a range of synthetic methods can be used to make nanostructured electrodes, integrating all three components of a battery into a 3D battery is still a significant challenge. The most significant challenge to realizing a 3D battery reproducibly is the application of conformal, pinhole-free electrolytes that can be deposited with controlled thickness.[13] Another significant challenge is that surface-mediated parasitic reactions (such as uncontrolled SEI formation) are exaggerated on high-surface-area electrodes.[14] There is still much to learn about interfacial chemistry, particularly since very little is known about how conventional liquid electrolytes form solid-electrolyte interphases on new high energy density materials. Often conventional additives are used (additives that have been developed for graphite), with very few guiding hypotheses for why such additives are used.

Finally, manufacturing methods are critically needed for mesostructured materials that are low cost and highly controlled. The use of techno-economic modeling in academic work is very welcome; however, these models are typically based on conventional manufacturing. Some new work spanning different battery types is being developed,[15] and there are a few companies striving to commercialize 3D electrodes or full batteries using novel manufacturing methods (M24, Prieto Battery Inc., and Xerion Advanced Battery Corp.). The barrier to entry for these technologies into the market place will hinge on the success of developing novel manufacturing methods that can be scaled effectively to meet the very large markets waiting for advances in high energy density, high power density batteries that are safe and have long cycle lives.

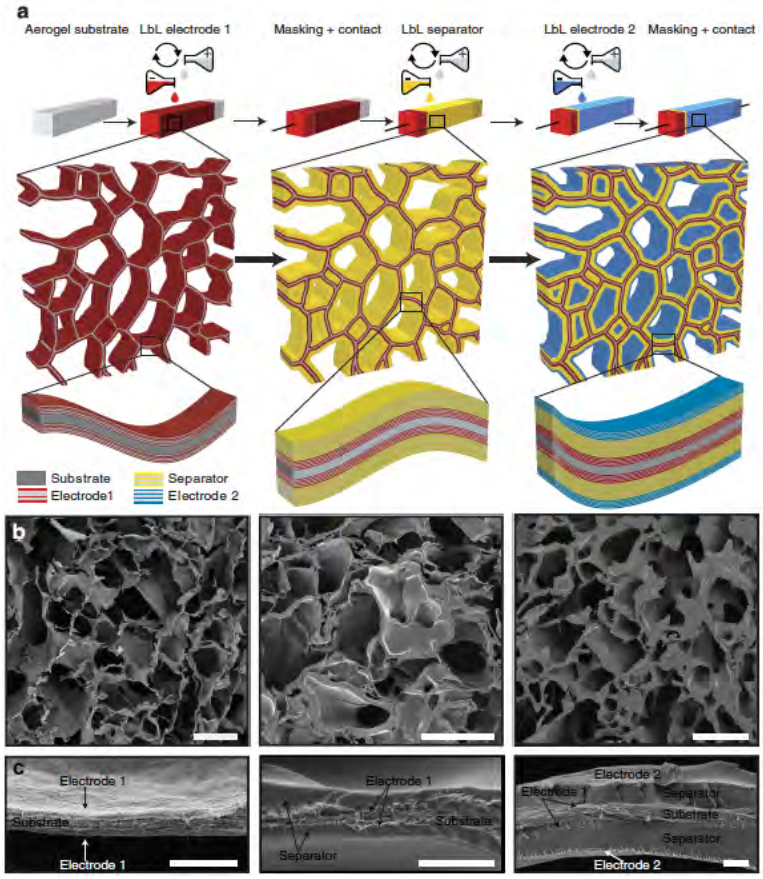

Figure 3-12. Device assembly and structural architecture. (a) Schematics of the layer-by-layer process used to assemble 3D devices in an aerogel and (b,c) cross-section SEM images of the first polyethyleneimine/ carbon nanotube (PEI/CNT) electrode (left column), the PEI/CNT electrode with separator (middle column), and the full device (right column). Scale bars: (b) 50 mm and (c) 2 mm. From Ref. 10.

References

1 Zhang, H.; Yu, X.; Braun, P.V., Three-dimensional bicontinuous ultrafast-charge and –discharge bulk battery electrodes, *Nature Nanotechnology,* **2011**, *6*, 277-281.

2 Simon, P.; Gogotsi, Y.; Dunn, B. Where do batteries end and supercapacitors begin? *Science*, **2014**, *343*, 1210**–**1211.

3 Arthur, T.S.; Bates, D.J.; Cirigliano, N.; Johnson, D.C.; Malati, P.; Mosby, J.M.; Perre, E.; Rawls, M.T.; Prieto, A.L.; Dunn, B., Three-dimensional electrodes and battery architectures, *MRS Bulletin*, **2011**, *36(7)*, 523-531.

4 Tarascon, J.M.; Armand, M., Issues and challenges facing rechargeable lithium batteries, *Nature***, 2001**, *414***,** 359-367.

5 Sides, C.R.; Martin, C.R., Nanostructured electrodes and the low-temperature performance of Li-ion batteries, *Advanced Materials*, **2005**, *17*, 125-128.

6 Chan, C.K.; Peng, H.; Liu, G.; McIlwrath, K.; Zhang, X.F.; Huggins, R.A.; Cui, Y., High-performance lithium battery anodes using silicon nanowires, *Nature Nanotechnology,* **2008**, *3*, 31-35.

7 Mitta, N.; Wuw, F.; Lee, J.T.; Yushin, G., Li-ion battery materials: Present and future, *Materials Today*, **2015**, *18 (5)*, 252-264.

8 Ye, J.; Baumgaertel, A.C.; Wang, Y.M.; Biener, J.; Biener, M.M., Structural optimization of 3D porous electrodes for high rate performance, *ACS Nano*, **2015**, *9(2)*, 2194**–**2202.

9 Jackson, E.D.; Mosby, J.M.; Prieto, A.L., Evaluation of the electrochemical properties of crystalline copper antimonide thin film anodes for lithium ion batteries produced by single step electrodeposition, *Electrochimica Acta*, **2016**, *214,* 253-264.

10 Nystrom, G.; Marais, A.; Karabulut, E.; Wagberg, L.; Cui, Y.; Hamedi, M.M., Self-assembled three-dimensional and compressible interdigitated thin-film supercapacitors and batteries, *Nature Communications,* **2015**, *6*, 1-8.

11 Long, J.W.; Dunn, B.; Rolison, D.R.; White, H.S., Three-dimensional battery architectures, *Chemical Reviews,* **2004**, *104*, 4463-4492.

12 Cho, J. Chang, J.P., Prieto, A.L.; Dudney, N., Thin film lithium electrolytes, *Handbook of Solid State Batteries,* **2015**, *6,* 307.

13 Cho, J.; Chang, J.P.; Prieto, A.L.; Dudney, N., Thin film lithium electrolytes, *Handbook of Solid State Batteries,* **2015**, *6,* 307.

14 Jackson, E.D., Prieto, A.L.,. Copper antimonide nanowire array lithium ion anodes stabilized by electrolyte additives, *ACS Appl. Mater. Interfaces*, **2016,** *8* (44), 30379–30386.

15 Hopkins, B.J.; Smith, K.C.; Slocum, A.H.; Chiang, Y.M., Component-cost and performance based comparison of flow and static batteries, *Journal of Power Sources*, **2015**, *293*, 1032 - 1038.

3.10 Electrochemical Capacitive Systems

Introduction

Electrochemical capacitive systems (colloquially referred to as “supercapacitors”) are a class of energy storage devices characterized by specific power and energy densities that bridge the gap between the high power density of dielectric capacitors and the high energy density of batteries. Electrochemical capacitive systems are classified by their mechanism of charge storage: non-faradaic (electrical double-layer capacitors), faradaic (pseudocapacitors), and a combination of the two (hybrid devices).

Dielectric capacitors store charge in the electric field between parallel conductive plates. The energy stored is proportional to the capacitance, *C*, and the square of the voltage, *V*:

$$E = \frac{1}{2}CV^2 \quad (1)$$

$$C = \frac{\varepsilon A}{d} \quad (2)$$

where ε is the permittivity of the dielectric, *A* is the surface area of the parallel plate, and *d* is the charge separation distance (here the distance between plates). Charge storage is non-faradaic because the process is electrostatic and does not involve redox reactions.

Electrical double-layer capacitors (EDLCs) are based on the double layer that forms at the electrode-electrolyte interface from the electrostatic attraction between the ions of an electrolyte and the charges present on the electrode surface. Electrochemical cells consist of activated carbon electrodes with high surface area (SA, 1000-2000 $m^2\ g^{-1}$) and organic solvents containing solvated ions (e.g., quaternary ammonium salts in acetonitrile).[1] The effective thickness of the double layer, *d*, is typically less than 1 nm, and the electrical double-layer capacitance is ~10-20 $\mu F\ cm^{-2}$.[2] The electrochemical cell is modeled as two capacitors in series with a total capacitance equal to:

$$\frac{1}{C_{total}} = \frac{C_p C_n}{C_p + C_n} \quad (3)$$

where C_p and C_n are equal to the capacitances of the cathode and anode, respectively. The combination of high SA and atomically small separation distance leads to orders of magnitude improvement in energy density over dielectric capacitors. Typical values of ~200 $F\ g^{-1}$ have been reported for activated carbon electrodes.[2] Commercial devices demonstrate a lower specific capacitance of ~100 $F\ g^{-1}$ (4-5 $Wh\ kg^{-1}$ as a packaged device) as not all surfaces are accessible to the electrolyte, especially when using practical levels of mass loading.[3]

Pseudocapacitance arises from redox reactions whose electrochemical features appear capacitive (Figure 3-13). There are several faradaic mechanisms that can lead to pseudocapacitance: underpotential deposition, redox pseudocapacitance, and intercalation pseudocapacitance.[4] Electrochemical capacitive research has focused on redox and intercalation pseudocapacitance in recent years, as underpotential deposition is unsuitable for high-rate energy storage due to the formation of metal dendrites.

Several metal oxides, such as RuO_2 and MnO_2, as well as conjugated polymers, have been studied extensively for their promising redox pseudocapacitance.[5,6,7,8] The pseudocapacitance of metal oxide systems is known to originate from successive electron-transfer redox reactions at cation sites, particularly in aqueous systems. The multi-electron redox process in these materials leads to high specific capacitances (1450 $F\ g^{-1}$ for hydrous RuO_2, 1233 $F\ g^{-1}$ for MnO_2). However, the high cost of RuO_2 has prevented its commercialization, whereas the inability to utilize the sub-surface sites of MnO_2 has limited its use to thick-film, practical applications.[9]

Conducting polymers (CPs) can either be p- or n-doped with anions or cations, respectively, and exhibit good performance due their combination of conductivity, porosity, and SA. Polyaniline (PANI) is an especially promising CP because of its variable oxidation states and low cost, as well as the ease with which electrical properties can be manipulated. Electrodeposited PANI films with high specific capacitance of ~2300 F g^{-1} and good retention up to 1,000 cycles have been reported.[10] Polypyrrole, polythiophene, and their derivatives not only demonstrate excellent capacitive storage properties but also mechanical flexibility, low cost, and environmental stability. When CPs are used in bulk, however, they suffer from poor cyclability, which restricts their practical utilization. The focus of CPs in supercapacitor applications has, therefore, been directed toward fabricating hybrid systems to maximize the combined advantages of both conducting polymers and metal oxides.

State of the Art

Carbon is an ideal electrode material for EDLCs because of its high conductivity, large surface area, and low density. Various carbon allotropes have been investigated in EDLCs. [11,12,13] The low specific capacitance of commercial carbon-based EDLCs compared to values obtained in research settings is often attributed to the high SA contributed by micropores (<2 nm), which are unable to accommodate solvated ions. The traditional view of electrolyte accessibility and pore size has recently been altered, as a 100% increase in normalized capacitance (~15 μF cm^{-2}) can be achieved when the pore size is equal to the crystallographic diameter of the ion.[14] This behavior is due to the closer approach of the ion to the electrode surface, thereby decreasing the effective thickness of the double layer. As in battery electrodes, electrolyte access is an important factor in transitioning from thin to thick films for practical applications. Commercially available activated carbon has a high specific SA but low mesoporosity (2-50 nm), which has been targeted as a critical feature for electrolyte access.[15] The utilization of high SA carbon with porosity tailored to EDLC applications has become a topic of considerable interest and has prompted the investigation of carbon nanotubes and graphene. One of the most promising systems to date is based on the facile synthesis of high SA holey-graphene (1560 m^2 g^{-1}), which achieves nearly 300 F g^{-1} at 250 W kg^{-1}.[16]

Recent developments in electrolytes, specifically ionic liquids and redox-active electrolytes, are also leading to advances in EDLCs, Commercial EDLCs are limited to a nominal operating voltage of 3 V due to the oxidative and reductive degradation of the organic electrolyte. Room-temperature ionic liquids have been utilized with high SA carbon electrodes in an effort to increase the device operating voltage. Ionic liquids are composed solely of ions and offer large electrochemical stability windows, chemical stability, and negligible vapor pressure. $[Pyr_{13}][PF_6]$ offers a window from ~2 to 8 V vs. standard hydrogen electrode (-1 to 5 V vs. Li), and an energy density of ~50 Wh kg^{-1} has been reported for a symmetric conductive carbon cell.[17,18] Furthermore, the use of redox-active electrolytes can provide an additional increase in energy density. Potassium iodide in aqueous electrolyte can increase the specific capacitance of high SA carbon electrodes from 100 to 1,200 F g^{-1} while undergoing up to a six-electron process.[19] A common problem with the use of redox-active electrolytes is that the oxidized or reduced products can diffuse and lead to self-discharge of the device. The functionalization of both the cation and anion of ionic liquids with redox-active moieties combines higher operating voltages with increased capacitance.[20] By tethering additives to the ions, the solubility of redox-active species is increased and the oxidized/reduced species are doubly charged, leading to strong electrosorption in the charged state and negligible self-discharge.

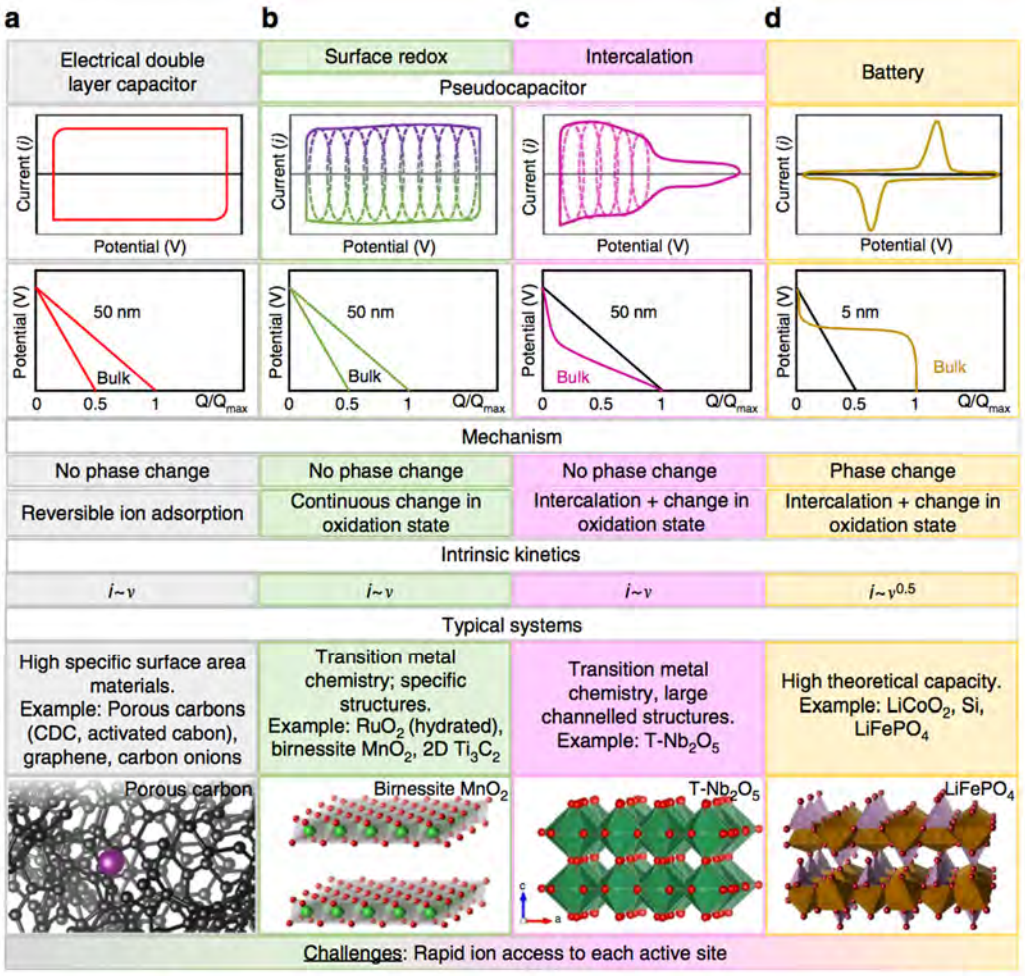

Figure 3-13. Comparison of electrochemical features and materials for EDLCs, redox pseudocapacitors, intercalation pseudocapacitors, and batteries.[19]

Pseudocapacitive materials based on rapid Li-ion insertion have also generated significant interest because redox materials can be designed and engineered for high energy and power densities. In some cases, these pseudocapacitive materials have crystalline features that allow for facile ion-transport (intrinsic pseudocapacitors). For example, *T*-phase niobium oxide possesses relatively open crystallographic pathways for Li-ion transport, which leads to specific capacitances of ~400 F g^{-1}.[21] In other cases, traditional lithium-ion battery materials can be nanostructured to exhibit pseudocapacitance (extrinsic pseudocapacitors).[9] This is due to the ability of nanoparticles to accommodate strain during intercalation/de-intercalation and suppress phase transformations. Lithium cobalt oxide achieves ~75 mAh g^{-1} for particles of <20 nm at specific currents typically used in supercapacitor devices.[22] Two-dimensional materials such as transition metal dichalcogenides have also been of interest as pseudocapacitive materials because their layered structures enable facile ion transport and high rate capabilities. This behavior is observed in nano-sized TiS_2 and MoS_2 where capacities of ~120 mAh g^{-1} at high rates are demonstrated.[23,24]

Hybrid devices that combine a pseudocapacitor or battery electrode with a high SA carbon electrode can overcome the intrinsic energy density limits for EDLCs. The inclusion of a pseudocapacitor electrode with a specific capacitance greater than that of activated carbon will increase the energy density of the hybrid according to Eq. 3. For lithium-ion pseudocapacitor or battery electrodes, the greater the difference between

the lithiation window/potential of the active material and the chemical potential of carbon vs. Li (~3 V), the greater the increase in the operating voltage of the device. This results in a large increase in energy density and is realized even at low states of charge, where the full capacity of the redox-active electrode is not utilized (Figure 3-14).[25] Lithium titanate (LTO) has been investigated for its use as an anode in hybrid devices. The operating potential of LTO (1.55 V vs. Li) avoids the reductive decomposition of electrolyte, and its theoretical capacity (175 mAh g^{-1}) offers four times the specific energy density of activated carbon. The LTO is particularly well-suited for cycling at high charge/discharge rates with respectable energy density in the hybrid device (~35 Wh kg^{-1}).[26] Hybrid devices that utilize traditional battery electrodes can offer even greater energy densities than that of pseudocapacitive electrodes. For example, graphite has a high theoretical capacity (372 mAh g^{-1}) and low lithiation potential vs. Li (0.01 V vs. Li), resulting in an energy density of 30 Wh kg^{-1} for commercial devices.[25] However, the active material must be pre-doped with lithium for appreciable rate capability, and since the lithiation potential lies in the decomposition region of organic electrolytes, SEI formation reduces rate capabilities.

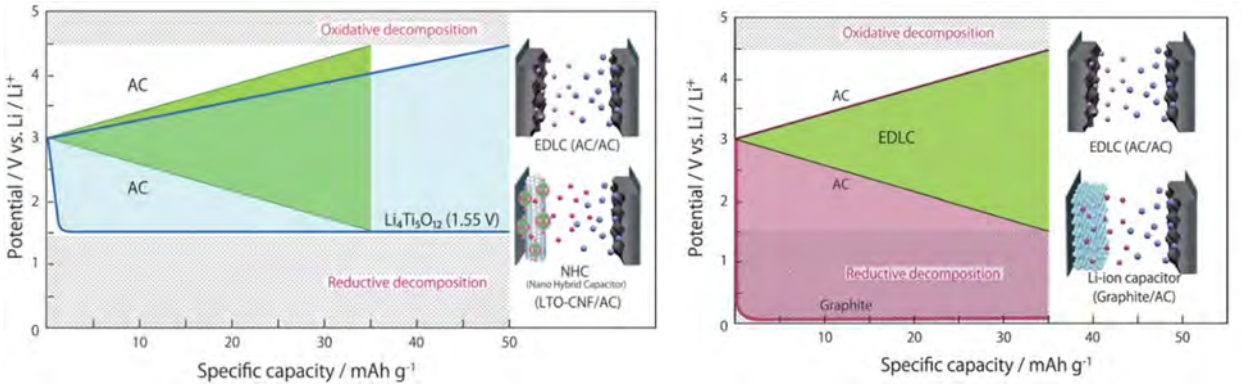

Figure 3-14. Voltage profiles of lithium-ion hybrid devices using battery electrodes.[25]

Technical and Cost Barriers

As electrochemical capacitor (EC) systems continue to increase in both specific and volumetric energy densities, their commercial applications and market values do as well. The global supercapacitor market, evaluated near 500 million dollars in 2015, is expected to become a multibillion dollar market by 2022 with compound annual growth rates estimated at 20%-29%.[27,28]

Much of the current market is for the automotive industry. Through their essentially unlimited cycle life and fast charge/discharge times, ECs can provide sufficient power density for peak current situations and regenerative braking in hybrid buses/automobiles and trains. When used in conjunction with traditional battery systems, ECs can extend the lifetime of vehicle energy storage systems by reducing the number of cycles and maximum current seen by the battery. An additional benefit of ECs is that they are much less susceptible to poor performance from large temperature fluctuations. For this reason, ECs are frequently used in heavy-duty vehicles, such as large trucks and cranes in cold temperatures in order to provide short bursts of power. For grid-level applications, ECs are used for frequency smoothing to ameliorate large deviations from 60 Hz. Other uses of ECs include intermittent storage mechanisms for wind and solar power, as well as uninterruptible power systems, where backup power is provided to preserve critical functions.[4,29]

References

1 El-Kady, M. F; Strong, V.; Dubin, S.; Kaner, R. B., Laser scribing of high-performance and flexible graphene-based electrochemical capacitors, *Science,* **2012,** 335, 1326–1330.

2 Zhang, Y.; Feng, H.; Wu, X.; Wang, L.; Zhang, A.; Xia, T.; Dong, H.; Li, X.; Zhang, L., Progress of electrochemical capacitor electrode materials: A review, *Int. J. Hydrogen Energy,* **2009,** *34***,** 4889-4899.

3 Chen, T.; Dai, L., Carbon nanomaterials for high-performance supercapacitors, *Mat. Tod.,* **2013,** *16***,** 272–280.

4 Conway, B. E., *Electrochemical Supercapacitors: Scientific Fundamentals and Technological Applications*, Springer Science & Business Media (2013).

5 Zheng, J.P.; Cygan, C.J.; Jow, T.R., Hydrous ruthenium oxide as an electrode material for electrochemical capacitors, *J. Electrochem. Soc.,* **1995,** *142,* 2699-2703.

6 Wu, N.L., Nanocrystalline oxide supercapacitors, *Mater. Chem. Phys*., **2002,** *75,* 6–11.

7 Brousse, T.; Toupin, M.; Dugas, R.; Athouël, L.; Crosnier, O.; Bélanger, D., Crystalline MnO_2 as possible alternatives to amorphous compounds in electrochemical supercapacitors, *J. Electrochem. Soc*., **2006,** *153,* A2171–A2180.

8 Wang, K.; Wu, H.; Meng, Y.; Wei, Z., Conducting polymer nanowire arrays for high performance supercapacitors, *Small*, **2014,** *10,* 14–31.

9 Augustyn, V.; Simon, P.; Dunn, B., Pseudocapacitive oxide materials for high-rate electrochemical energy storage, *Energy Environ. Sci.*, **2014, *7*,** 1597-1614.

10 Girija, T.C.; Sangaranarayanan, M.V., Polyaniline-based nickel electrodes for electrochemical supercapacitors—Influence of Triton X-100, *J. Power Sources,* **2006,** *159,* 1519–1526.

11 Harris, P.; Liu, Z.; Suenaga, K., Imaging the atomic structure of activated carbon, *J. Phys.: Condens. Matter,* **2008,** *20,* 362201.

12 Hartmann, R.; Kono, J.; Portnoi, M., Terahertz science and technology of carbon nanomaterials, *Nanotechnology,* **2014***, 25,* 322001.

13 Delgado, J.; Ángeles Herranz, M.; Martín, N., The nano-forms of carbon, *J. Mater. Chem.,* **2008,** *18,* 1417-1426.

14 Chmiola, J.; Yushin, G.; Gogotsi, Y.; Portet, C.; Simon, P.; Taberna, P., Anomalous increase in carbon capacitance at pore sizes less than 1 nanometer, *Science,* **2006,** *313,* 1760–1763.

15 Frackowiak, E.; Béguin, F., Carbon materials for the electrochemical storage of energy in capacitors, *Carbon,* **2001,** *39,* 937–950.

16 Xu, Y.; Lin, Z.; Zhong, X.; Huang, X.; Weiss, N.; Huang, Y.; Duan, X. Holey graphene frameworks for highly efficient capacitive energy storage, *Nat. Commun.,* **2014,** *5***,** 4554.

17 Ong, S. P.; Andreussi, O.; Wu, Y.; Marzari, N.; Ceder, G., Electrochemical windows of room-temperature ionic liquids from molecular dynamics and density functional theory calculations, *Chem. Mater.,* **2011,** *23,* 2979–2986.

18 Lewandowski, A.; Olejniczak, A.; Galinski, M.; Stepniak, I., Performance of carbon-carbon supercapacitors based on organic, aqueous and ionic liquid electrolytes, *J. Power Sources,* **2010,** *195,* 5814-5819.

19 Lukatskaya, M. R.; Dunn, B.; Gogotsi, Y., Multidimensional materials and device architectures for future hybrid energy storage, *Nat. Commun*., **2016, 7,** 12647.

20 Mourad, E.; Coustan, L.; Pierre, L.; Zigah, D.; Mehdi, A.; Vioux, A.; Freunberger, S.A.; Favier, F.; Fontaine, O., Biredox ionic liquids with solid-like redox density in the liquid state for high-energy supercapacitors, *Nat. Mater.,* **2017,** *16,* 446-453.

21 Come, J.; Augustyn, V.; Kim, J.; Rozier, P.; Taberna, P.L.; Gogotsi, P.; Long, J.; Dunn, B.; Simon P., Electrochemical kinetics of nanostructured Nb_2O_5 electrodes, *J. Electrochem. Soc.,* **2014,** *161*, A718-A725.

22 Okubo, M.; Hosono, E.; Kim, J.; Enomoto, M.; Kojima, N.; Kudo, T.; Zhou, H.; Honma, I., Nanosize effect on high-rate Li-ion intercalation in $LiCoO_2$ electrode, *J. Am. Chem. Soc.,* **2007,** *129,* 7444-7452.

23 Muller, G.; Cook, J.; Kim, H.S.; Tolbert, S.; Dunn, B., High performance pseudocapacitor based on 2D layered metal chalcogenide nanocrystals, *Nano Lett.,* **2015,** *15,* 1911−1917.

24 Cook, J.; Kim, H.S.; Lin, T.; Lai, C.H.; Dunn, B.; Tolbert, S., Pseudocapacitive charge storage in thick composite MoS_2 nanocrystal-based electrodes, *Adv. Energy Mater*., **2017,** *7***,** 1601283.

25 Naoi, K.; Ishimoto, S.; Miyamoto, J.; Naoi, W., Second generation “nanohybrid supercapacitor”: Evolution of capacitive energy storage devices, *Energy Environ. Sci.,* **2012,** *5,* 9363–9373.

26 Du Pasquier, A.; Plitz, I.; Menocal, S.; Amatucci, G., A comparative study of Li-ion battery, supercapacitor, and nonaqueous hybrid devices for automotive applications, *J. Power Sources,* **2003,** *115,* 171-178.

27 Allied Market Research, *Global Supercapacitor Market by Module Type (Less than 10 Volts Modules, 10-25 Volts Modules, 25-50 Volts Modules, 50-100 Volts Modules, and Above 100 Volts Modules) and Application (Automotive, Industrial, Energy, and Electronics) - Global Opportunities Analysis & Industry Forecast, 2014-2022*.

28 MarketsandMarket, *Supercapacitor Market by Type (Double Layer, Pseudocapacitor, and Hybrid) – 2022*.s.

29 Wang, Y.; Song, Y.; Xia, Y., Electrochemical capacitors: mechanism, materials, systems, characterization and applications, *Chem. Soc. Rev*., **2016,** *45***,** 5925–5950.

3.11 Redox Flow Batteries

Introduction

Redox flow batteries were introduced during the energy crises of the 1970s.[1] Flow batteries store energy using redox couples dissolved in electrolytic solutions that are circulated through electrochemical reactors to alternately charge or discharge the battery. For example, in the all-vanadium flow battery, an aqueous solution containing sulfuric acid and V(II)/V(III) circulates through the negative electrode while a solution containing acid and V(IV)/V(V) circulates through the positive electrode. The following reactions occur when the battery is discharged:

Negative: $V^{2+} \rightarrow V^{3+} + e^-$

Positive: $VO_2^+ + 2H^+ + e^- \rightarrow VO^{2+} + H_2O$

Cell voltage: 1.26 V; gravimetric energy density: 29 Wh kg^{-1}

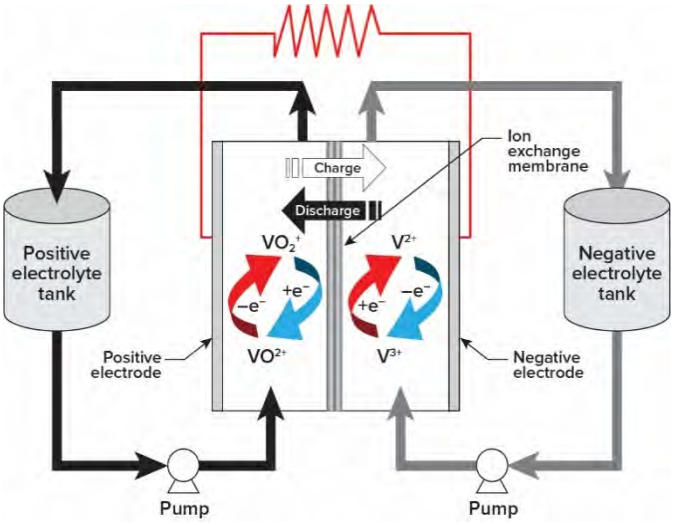

Figure 3-15. Schematic diagram of an all-vanadium redox flow cell. Adapted from Ref. 2.

The architecture of flow batteries, depicted schematically in Figure 3-15,[2] is distinct from conventional batteries like Pb-acid and Li-ion because the energy is stored outside of the electrode structures. This arrangement allows flow batteries to utilize active materials with low energy density cost effectively by minimizing the ratio of inactive to active material. Flow batteries are particularly suited to stationary applications that require MW of power to be discharged over four or more hours.[3] The reactors in an MWh battery may contain 200 or more bipolar cells, each with an area of up to 1 m^2. A cell consists of a solid bipolar separator plate surrounded by an electrically insulating frame and two porous electrodes separated by an ion exchange membrane. Typically, the separator plate is a carbon composite, the frame is plastic, the porous electrodes are carbon papers or felts, and the ion-exchange membrane is similar to a fluorinated polymer such as Nafion. The redox reactions in most flow batteries do not stress the electrode materials because they only require electron transfer and not morphological or structural changes. Efficiently delivering the electrolyte from the storage tanks to the flow cells by minimizing pumping and shunt current losses is an important aspect of system design. Shunt currents are a particularly acute problem because the electrolyte solutions in most flow batteries are very conductive. The forced convection inherent to flow batteries leads to much greater areal power densities than is possible in conventional enclosed batteries, where diffusion and migration are the dominant modes of transport in the electrolyte.

State of the Art

Table 3-4 is an incomplete list of inorganic couples that have been studied for flow batteries. In a cost effective flow battery, the potential difference between the positive and negative couples should be large, all four oxidation states should be very soluble, and the redox compounds should be inexpensive. The necessity of attaining a large potential difference is hindered by the need to avoid oxygen and hydrogen evolution in aqueous electrolytes, especially when charging. This limits the maximum open-circuit voltage of flow batteries with aqueous electrolytes to ~1.5 V. Flow batteries that have been demonstrated at scale include: iron-chrome, all-vanadium, zinc-bromine, and sodium-polysulfide. Systems that plate a metal like Zn or Fe on a stationary electrode are hybrid flow batteries that lack the distinct separation of power and energy that flow batteries relying solely on dissolved redox compounds possess.

TABLE 3-4: Inorganic redox couples studied for flow batteries.

Negative Couples					**Positive Couples**			
Zn/Zn^{2+}	Cr^{2+}/Cr^{3+}	V^{2+}/V^{3+}	H_2/H^+		Fe^{2+}/Fe^{3+}	VO^{2+}/VO_2^+	Br^-/Br_2	Ce^{3+}/Ce^{4+}
-0.76	-0.42	-0.26	0.00		0.77	1.00	1.08	1.74
←Increasing hydrogen evolution					Oxygen evolution, carbon corrosion→			

All-vanadium flow batteries, invented in the 1980s,[4] have been commercially deployed at >100 kW scale since 1996 in Japan, Europe, Australia, and the USA. The all-vanadium system possesses many compelling attributes, including an open-circuit voltage of ~1.5 V, vanadium ion solubilities exceeding 1.6 mol/L, and the ability to completely recover from cross contamination of the positive and negative electrolytes. Sumitomo Electric offers 20 years of life with an unlimited number of cycles.[5] Unfortunately, vanadium is currently $29/kg, which corresponds to $73/kWh, a large fraction of the $150/kWh target stated by DOE for four hours of storage.[6] The price of vanadium has fluctuated from $14/kg to $84/kg over the last decade.

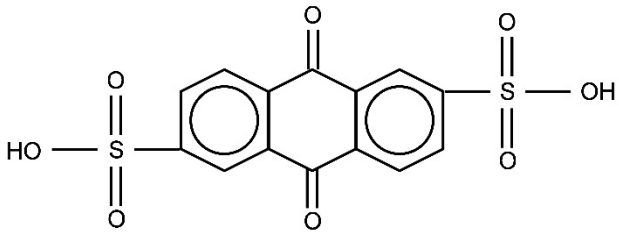

Figure 3-16. Anthraquinone-2,6-disulfonate.

There has been a recent resurgence of research into flow batteries driven by the growing deployment of wind and solar, which generate power intermittently. One thrust has been into the design and synthesis of tailored organic redox compounds like the anthraquinone-2,6-disulfonate molecule depicted in Figure 3-16.[7] The redox potential and solubility of organics can be tuned by the addition of electron donating and withdrawing groups.[8] Another recent approach combines larger active molecules, ranging from oligomers to polymers and colloids, with separators having pores with molecular dimensions to eliminate crossover.[9] The replacement of water with organic solvents opens routes to higher cell voltages and higher solubility of organic active species.[10] These theoretical advantages need to offset the higher solvent and salt costs in order to lead to a net cost benefit. Dramatic improvements in the areal power density of electrochemical reactors through changes to electrode, flow field, and membrane design have been described recently.[11] These improvements translate directly to lower reactor cost.

Redox flow batteries can be used to store energy from wind and solar when conditions favor production, and release energy when production is low, in order to maintain constant, reliable output. Redox flow batteries are also suitable for load-leveling and grid support. They offer the capability to prevent service interruptions in the event of failure and to prevent voltage spikes, voltage sags, and power outages that last for periods from a few cycles (less than a second) to minutes, protecting production and data for customers. The use of flow batteries for electric power transmission applications provides effective use of existing plant investment, flexibility in operation, and better response to price changes. Stored electricity can be made readily available to meet immediate changes in demand, allowing effective operation of base load units at high and essentially constant levels of power. Redox flow batteries use off-peak power for pumping and charging. This stabilizes operations and provides flexibility for buying or selling electricity during peak or off-peak periods. Modular construction allows high power rating, long energy storage time, and excellent response time; full power can be delivered in a few seconds. Such characteristics are important in the competitive electricity market. At the generation level, energy storage can be used to increase the load factor, helping utilities cope with load increases and covering operating and contingency reserves. Thus, there is a significant potential market for energy storage products.

Presently, installations of flow batteries on the grid lag those of lithium-ion batteries. Flow batteries are best suited to applications requiring MW of power discharged over the course of more than four hours. To date, most installations of batteries on the grid have been for frequency regulation, which does not require long discharge times. The market for hours of energy storage is nascent and fragmented. Furthermore, the prices of lithium-ion batteries have fallen sharply in recent years to $145/kWh for cells in transportation applications,[12] making them more competitive for projects with long discharge times. Finally, flow battery technology is relatively new and unfamiliar, while customers are gaining familiarity with lithium-ion.

Technical Barriers

A significant potential market for energy storage products, unsatisfied by existing technology, exists within the range from several hundred megawatts and several hours of storage to the multi-megawatt level. The nascent market for electricity storage systems is in conjunction with renewable energy sources, such as photovoltaic generation and wind power energy systems. Capital cost is the largest barrier preventing widespread adoption of flow batteries. The technically strong all-vanadium system is hampered by the high cost of vanadium. Replacing vanadium with tailored organic molecules offers the promise of significantly lower costs. These tailored molecules should be based on inexpensive precursors, and need to match the voltage and solubilities achieved with vanadium. The active species in an all-vanadium battery do not decay, and tailored molecules will need to demonstrate a path to decades of durability. Expensive fluorinated ion-exchange membranes, like Nafion, contribute significantly to reactor cost. Replacement with simpler polymers that can, in conjunction with large active species, prevent crossover could address this cost. The durability of carbon electrodes and bipolar plates at the potential of the positive electrode needs to be confirmed. Improving the catalytic activity of the electrode materials will also play a role in lower cost.

References

1 Thaller, L. H., U.S. Patent 3,996,064, 1976.

2 Li, X.; Zhang, H.; Mai, Z.; Zhang, H.; Vankelecom, I., Ion exchange membranes for vanadium redox flow battery (VRB) applications, *Energy Environ. Sci.,* **2011**, 4, 1147-1160.

3 Skyllas-Kazacos, M.; Chakrabarti, M.H.; Hajimolana, S.A.; Mjalli, F.S.; Saleem, M., Progress in flow battery research and development, *J. Electrochem. Soc.,* **2011,** *158* (8), R55-R79.

4 Skyllas-Kazacos, M.; Robins, R., U. S. Patent 4,786,567, 1986.

5 S. Electric, http://global-sei.com/products/redox [accessed October 3, 2017].

6 Rastler, D., "Market Driven Distributed Energy Storage System Requirements for Load Management Applications," Palo Alto, CA, 2007.

7 Huskinson, B.; Marshak, M.P.; Suh, C.; Er, S.; Gerhardt, M.R.; Galvin, C.J.; Chen, X.; Aspuru-Guzik, A.; Gordon, R.G.; Aziz, M.J., A metal-free organic–inorganic aqueous flow battery, *Nature,* **2014,** *505*, 195-198.

8 Er, S.; Suh, C.; Marshak, M.P.; Aspuru-Guzik, A., Computational design of molecules for an all-quinone redox flow battery, *Chem. Sci.,* **2015,** *6*, 885-893.

9 Doris, S.E.; Ward, A.L.; Baskin, A.; Frischmann, P.D.; Gavvalapalli, N.; Chenard, E.; Sevov, C.; Prendergast, D.; Moore, J.S.; Helms, B.A., Macromolecular design strategies for preventing active-material crossover in non-aqueous all-organic redox-flow batteries, **2017,** *56*, 1595-1599.

10 Liu, T.; Wei, X.; Nie, Z.; Sprenkle, V.; Wang, W., A total organic aqueous redox flow battery employing a low cost and sustainable methyl viologen anolyte and 4-HO-TEMPO catholyte, *Adv. Energy Mater.,* **2016,** *6,* 1501449.

11 Liu, T.; Wei, X.; Nie, Z.; Sprenkle, V.; Wang, W., A total organic aqueous redox flow battery employing a low cost and sustainable methyl viologen anolyte and 4-HO-TEMPO catholyte, *Adv. Energy Mater.,* **2016,** *6,* 1501449.

12 King, D., autoblog, http://www.autoblog.com/2015/10/08/gm-li-ion-battery-cost-per-kwh-already-down-to-145, August 10, 2015.

3.12 Reversible Fuel Cells

Introduction

Reversible or regenerative fuel cells first received attention in the 1960s as energy-storage devices for the space program.[1,2] Generally, reversible fuel cells discharge by converting stored hydrogen and oxygen to water and charge by converting water to oxygen and hydrogen. Figure 3-17 shows a schematic diagram of the major components in a reversible fuel cells system. The arrangement in the diagram is referred to as discrete because the fuel cell and electrolyzer are distinct modules. When a single component accomplishes the functions of both the fuel and the electrolyzer, the system is called "unitized." A single device should increase energy density, critical in aerospace applications, and reduce capital cost. Unfortunately, this approach significantly increases durability challenges because electrodes are exposed to much wider voltage ranges. The system depicted in Figure 3-17 is closed as the fuel, oxidant, and water are all stored. A completely closed system is necessary for some aerospace applications. In terrestrial applications, the water and oxygen do not necessarily need to be stored, as indicated by the hatched lines. The oxygen feed to the fuel cell can be replaced with ambient air, and the oxygen generated by the electrolyzer can be vented. Similarly, the water feed to the electrolyzer can be taken from an external supply and the water generated by the fuel cell can be vented. For grid energy storage, the hydrogen would probably be stored in stainless steel tanks at <20 MPa. Electrical work, *IV*, is supplied to the electrolyzer to split water and charge the system. The fuel cell generates a smaller amount of electrical work and heat when the system is discharged. The electrolysis reaction can be either exothermic or endothermic. Low temperature systems based on cationic or anionic exchange membranes are invariably exothermic because of the sluggish kinetics of the oxygen evolution reaction, but electrolysis at high temperatures in solid oxide systems can be endothermic.

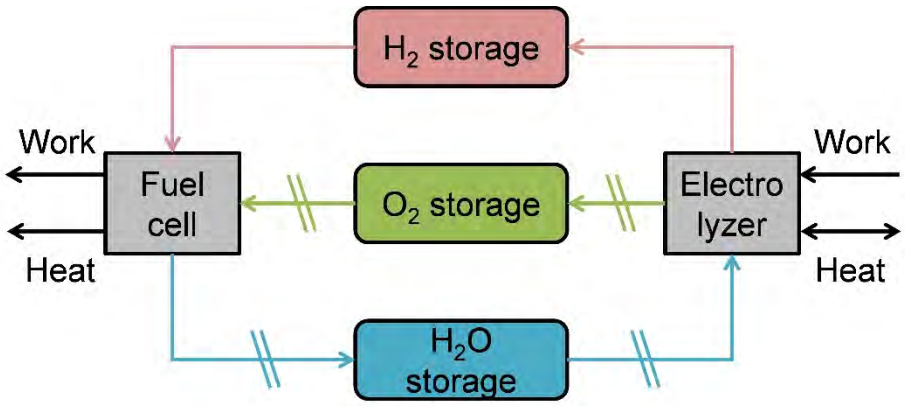

Figure 3-17. Schematic diagram of a reversible fuel cell system showing major components.

State of the Art

The most mature reversible fuel cells are based on polymer cation exchange membranes. These systems are severely hindered by the sluggish kinetics of water oxidation and oxygen reduction at normal operating temperatures even with precious metal catalysts (<80°C). Round trip efficiencies range from 40% to 50% (see

Table 3-5), which means that a large difference between peak and off-peak electricity prices is necessary to generate positive net revenue. Adoption is also hindered by high capital costs driven by the high cost of commercial fluorinated cation exchange membranes and precious metal catalysts. Unitizing the fuel cell and electrolyzer has proven to be difficult largely because of catalyst layer degradation driven by the large electrode potential changes encountered when switching from charging to discharging. Water management is another challenge because fuel cells need to reject product water, which is usually accomplished with hydrophobic structures, while electrolyzers need to feed water to the anode catalyst layer, which tends to necessitate open, hydrophilic structures.

TABLE 3-5: Representative round trip efficiencies for reversible fuel cells.[1]

System	Charge carrier	Round trip efficiency
Cation exchange membrane	H^+	40-50%
Anion exchange membrane	OH-	30-40%
Solid oxide	O^{2-}	60-80%
Solid oxide	H^+	60-80%

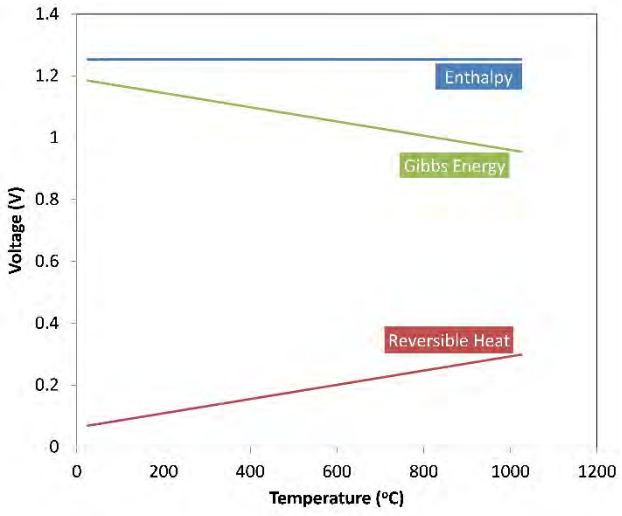

Figure 3-18. Thermodynamic voltages for electrolysis as a function of temperature.

Reversible fuel cells using anion exchange membranes are theoretically appealing because oxygen reduction and water oxidation can be accomplished without noble metal catalysts in basic media. However, anion exchange membranes are not as mature as cation exchange membranes like Nafion. Furthermore, poisoning by carbon dioxide is an issue for open systems. Reported peak power densities for reversible fuel cells with anion exchange membranes are less than half of those reported for cation exchange membranes. Round trip efficiencies ranging from 30% to 40% have been demonstrated. Water management challenges are similar for cation and anion exchange membrane systems.

Solid oxide fuel cells have been under development for decades because they promise high efficiency and compatibility with hydrocarbon fuels. Interest in solid oxide electrolyzers is more recent. Oxygen reduction and water oxidation are much more efficient in solid oxide cells at high temperature (>750°C for O^{2-} conductors) than they are in low temperature cells with polymer membranes. This, in combination with thin electrolyte and electrode layers, leads to peak power densities that can surpass systems with cation exchange membranes. Round trip efficiencies range from 60% to 80%. Figure 3-18 shows the

thermoneutral (enthalpy), reversible (Gibbs energy), and reversible heat voltages for the reaction: $H_2 + ½ O_2 \leftrightarrow H_2O$ (g).

Electrolysis of water becomes endothermic when the operating voltage is between the thermoneutral and reversible voltages. The efficiency of electrolysis, defined as the lower heating value of the hydrogen produced divided by the electrical energy input, is greater than one under these conditions. The necessary heat input could be provided by a high temperature source of waste heat or it could be returned from the fuel cell, which is exothermic. This would require efficient storage of thermal energy and careful thermal integration. Solid oxide systems can also electrolyze simple hydrocarbons like methane and methanol, opening the possibility of cycles not based on water.[2]

High temperature proton conductors (500-750^{o}C) are a relatively new class of solid oxide fuel cells. They tend to be less efficient than higher temperature oxide conducting solid oxide cells. However, the lower temperature offers access to a wider variety of materials of construction, including potentially stainless steels. Another benefit of proton conductors for electrolysis is that the product water is generated on the oxygen side, which eliminates the need for separation in open systems.

Technical Barriers

A significant potential market for energy storage products, unsatisfied by existing technology, exists within the range from several hundred megawatts and several hours of storage to the multi-megawatt level. The nascent market for electricity storage systems is in conjunction with renewable energy sources, such as photovoltaic generation and wind power energy systems. The adoption of low temperature reversible fuel cells with either cationic or anionic exchange membranes is hindered by high capital costs and low round trip efficiencies. The prospects for achieving efficiencies that are competitive with conventional batteries in low temperature systems appear to be low given the long-standing issues of sluggish oxygen reduction and evolution kinetics.

Considerable resources have been directed at improving the kinetics of these reactions over several decades, and breakthroughs that results in an increase of >10% in round-trip efficiency are unlikely. Solid oxide systems have demonstrated higher efficiencies, in large part because oxygen evolution and reduction are less problematic at elevated temperature. Durability, especially of electrolyzers, remains a significant challenge for solid oxide systems. Thermal integration is important, since thermal cycles are known to degrade solid oxide fuel cells, and the system is likely to be exothermic when discharging and endothermic when charging.

References

1 Wang, Y.; Leung, D. Y. C.; Xuan, J.; Wang, H., A review of unitized regenerative fuel cell technologies, part-A: Unitized regenerative proton exchange membrane fuel cells, *Renewable and Sustainable Energy Reviews*, **2016,** *65*, 961-977.

2 Wang, Y.; Leung, D. Y. C.; Xuan, J.; Wang, H., A review on unitized regenerative fuel cell technologies, part B: Unitized regenerative alkaline fuel cell, solid oxide fuel cell, and microfluidic fuel cell, *Renewable and Sustainable Energy Reviews*, **2017**, *75*, 775-795.

4 STATUS OF SCIENCE AND TECHNOLOGY OF ENERGY STORAGE

4.1 Electrochemistry Theory

This section encapsulates the state of the art in electrochemistry, with emphasis on advances in areas relevant to electrochemical energy storage (EES) since the last DOE EES workshop in 2007.[1] Electrochemistry stands as the basis for EES technologies. These technologies may be broadly classified into chemical and capacitive storage. Though this distinction is somewhat blurred in some cases (e.g., conducting polymer-based supercapacitors), the electrochemical tools used to characterize such systems are often similar. The period between roughly 1990 and 2007 was characterized by tremendous advances in the development of "hyphenated" techniques, in which various spectroscopies, spectrometries, and other methods (including scanning probe-based methods) were combined with electrochemical experiments. These developments provided a new level of understanding of both the interface(s) in electrochemical systems and the materials being examined. These advances have continued and are summarized below. In addition, the application of theory to electrochemical experiments began in earnest during that time period, and has advanced considerably since. Some of these "theory" topics, including molecular dynamics, quantum chemical and similar methods, are reviewed in other chapters of this report. Those are excluded from this discussion. Also not discussed is the use of finite element tools (such as the commercial program COMSOL™) for simulation of electrochemical systems, which has propagated widely through the field.[2] This chapter offers opinions about areas that would benefit from more work or seem ripe to have more impact, especially those that are directly relevant to EES.

4.1.1 CHARGE TRANSFER

The transfer of charge across an interface remains one of the fundamental events in many EES systems. The study of electron and ion transfer has a long history in electrochemistry. Recent advances that are relevant to EES have offered new understanding for this key step. Savéant recently reviewed the area of multi-electron transfer in electrocatalysis. This work is ultimately relevant both to multi-step electrocatalytic processes and to multi-step redox processes that have high-energy, single-electron intermediates, such as will be relevant for next generation batteries based on multi-electron redox systems.[3] Xu and coworkers studied the barrier to Li^+ transfer across the electrolyte/graphite interface, offering a rare understanding of how desolvation can influence ion transfer across such an interface.[4] Bazant recently offered an important new understanding of how non-equilibrium thermodynamics can influence the kinetics of charge transfer in phase-change battery materials.[5] He demonstrated the importance of redox-driven phase transformations in controlling charge transfer rates, where, for example, reaction rates may be influenced by chemical potential gradients, phase separation, large electric fields, or mechanical stresses. These findings are relevant for insertion materials, and will be especially relevant for conversion materials and any battery anodes or cathodes comprised of multi-phase active materials. Application of this model in concert with synchrotron-based liquid scanning transmission X-ray microscopy has provided the first thorough description of the interplay between charge transfer kinetics, lithiation, and phase separation/transformation in Li_xPO_4.[6] Figure 4-1 shows an example of the experimentally determined dependence of phase separation in Li_xPO_4 as a function of lithiation rate.

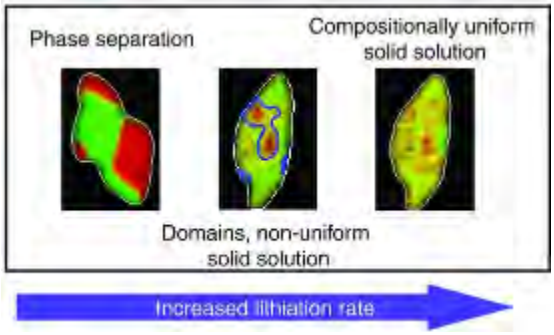

Figure 4-1. Dependence of Li_xPO_4 phase separation on lithiation rate.[6]

The rate dependence of phase separation is ultimately the result of a non-monotonic dependence of local current density on degree of lithiation, as proposed by Bazant using a general phase-field theory of chemical kinetics based on nonequilibrium thermodynamics. These results point to the opportunity for electrode engineering and battery management based on fundamental principles.

4.1.2 NEW LIQUID AND SOLID ELECTROLYTES AND NEW MATERIALS AND ARCHITECTURES

Most energy storage technologies rely on either aqueous or "traditional" non-aqueous supporting electrolyte systems. The non-aqueous systems tend to be focused on organic solvents such as propylene carbonate, dialkyl carbonates, etc. There has been a recent surge of interest in ionic liquids (ILs) as possible electrolytes for energy storage systems.[7] These materials have low volatility, a broad range of physical properties (viscosity, conductivity, acid-base character, etc.), and chemical properties that should be tunable. Recent work shows that the chemical properties of ILs can strongly influence the reversibility of electrodeposition at multi-electron metal anodes.[8] There also are solid-state analogues, some of which are polymeric, that also have attractive properties. Some of these materials show promise as anion exchange membranes suitable for redox flow battery systems.[9] To the extent that ILs are relevant to EES, much remains to be done to develop new ILs and explore their chemical and physical properties. A very large, new area that has emerged since the last EES workshop involves various uses of graphene-based materials. Graphene and graphene oxide have been used widely both as "electrode" materials and as additives in various formulations relevant to EES.[10] Much remains to be done in this emerging area. Finally, nanomaterials have become a mainstream staple, being used in a wide variety of formulations relevant to EES systems. Several reviews relevant to EES have covered metallic nanoparticles,[11] metal oxide nanoparticles,[12] metal sulfide nanoparticles,[13] polymeric nanomaterials,[14] and a range of carbonaceous nanomaterials.[15] The use of architecture at the nanoscale has been emphasized as a way to control transport of electrons and molecular species (ionic and neutral), a key attribute of highly functioning energy storage materials.[16] Methods for mesoscopic control of architecture have allowed control of the electrochemical behavior of EES systems.[17] Finally, a resurgence of interest in redox active polymeric materials (e.g., redox active polymers and colloids) has enabled new approaches to redox flow batteries.[18]

4.1.3 DOUBLE LAYER STUDIES

Studies of the electrochemical double layer have a long history in electrochemical science. For "traditional" aqueous and non-aqueous (organic) electrolytes, double layer models are well-established and tested, making such systems reasonably well understood. For newer media, such as ILs, theory has been developed,[19] but there remains a paucity of experimental tests of these newer models.[20] As mentioned above, to the extent that ILs are relevant to EES, studies of their interfacial, chemical, and physical properties could be an area of emphasis.

4.1.4 CHARACTERIZATION OF THE ELECTRODE-ELECTROLYTE INTERFACE AND ELECTROCHEMICAL MATERIALS

As discussed above, for much of the past three decades, electrochemists have worked to develop new and better tools to characterize electrochemical interfaces—in many cases, under *in situ* or *operando* conditions. Much of the key work focused on use of X-ray spectroscopies due to the ability of X-rays to penetrate into and through electrochemical interfaces. By now, synchrotron X-ray experiments have become a common tool for understanding both electrochemical interfaces and the bulk materials used in many EES applications. The area has transitioned from development of the tools [e.g. X-ray absorption near edge spectroscopy (XANES) and extended X-ray absorption fine structure (EXAFS)] to their application to a wide range of different EES materials and systems. A recent review focuses on methods employing photons and neutrons, including the important synchrotron-based tools.[21] Recent work has expanded the repertoire of available methods. Meng and coworkers showed that *in situ* strain measurements, revealed by coherent X-ray diffractive imaging (available at synchrotron light sources), can provide an understanding of interparticle disconnects between single nanoparticles.[22] Many other techniques also have been used: scanning probe methods (atomic force microscopy, scanning tunneling microscopy, and scanning electrochemical microscopy), reflection infrared

spectroscopy, Raman spectroscopy, sum-frequency generation, etc. A recent review covers some of these various techniques as applied to obtaining a molecular level view of the solid-liquid interface.[23] Other methods continue to be advanced. For example, Shao-Horn and coworkers have described the use of ambient pressure photoelectron spectroscopy in understanding electrochemical materials.[24] Grey and coworkers have pioneered the use of nuclear magnetic resonance (NMR) techniques to characterize battery materials. A recent review offers an excellent survey of the use of NMR for a variety of nuclei, describes what can be learned from the technique, and provides illustrative examples of the application of NMR to several battery materials.[25] With the continued technological improvements in NMR spectrometers suitable for solid state techniques, this method has the potential to be much more widely used, especially since it offers a detailed look at battery materials in an element-selective way.

A new area that has emerged since the last EES workshop uses high resolution electron microscopy (EM) for *in situ* studies of electrochemical processes. A recent review discusses the use of EM for specimens in liquid environments.[26] Huang and coworkers described the use of high resolution EM to monitor the lithiation of a single SnO_2 nanowire electrode.[27] Zheng and coworkers combined *in situ* transmission EM with X-ray microscopy and X-ray absorption spectroscopy to study Mg electrodeposition in a chloride-containing electrolyte.[28] These studies show the unique power of direct observation of interfacial and phase transformation processes in EES systems. As more high resolution EM instruments are made available, especially aberration-corrected ones capable of sub-Ångstrom resolution, these techniques will prove their worth in the EES area.

A new frontier in electrochemistry is its application to stochastic events, such as electrochemical studies of single molecules, single nanoparticles, and single nanopores.[29] Van Duyne and coworkers combined the power of tip-enhanced Raman spectroscopy with the sensitivity of nanoscale electrochemical measurements to detect single redox events.[30] Measurements focused on single (nano)particles are becoming more common in the study of redox systems relevant to EES.[31,32] For example, electrocatalytic properties of individual nanoparticles have been studied on the basis of their collisions with catalytically inert microelectrodes.[33,34] Also, there are recent reports of electrochemical measurements on catalytic centers comprised of individual atomic species.[35] These reports suggest that electrocatalytic materials can be deposited in an atom-by-atom manner. Finally, in an important development, the electrochemical evolution of gas is becoming better understood, based on pioneering efforts by the White group to understand the nucleation and growth of single nanobubbles.[36] These studies will be critical to the first-principles design of efficient, next-generation, gas-evolving electrodes, which are key to air-breathing batteries.

4.1.5 SUMMARY

The evolution of the field over the past few decades from new tool development toward tool refinement and application of these tools to specific EES systems has continued. In our opinion, the field is more focused on the science and technology of EES than ever before. Further, the practitioners of electrochemistry engaged in EES research are no longer all trained as electrochemists, but rather range from materials scientists to synthetic and physical chemists. Because of this, and because of the sophistication of the electrochemical, spectroscopic, and other types of tools now available for studying EES systems, collaborative efforts are more important than ever before.

References

1 U.S. Department of Energy, *Basic Research Needs for Electrical Energy Storage,* https://science.energy.gov/~/media/bes/pdf/reports/files/Basic_Research_Needs_for_Electrical_Energy_Storage_rpt.pdf, 2007.

2 Dickinson, E. J. F.; Ekstrom, H.; Fontes, E., COMSOL Multiphysics (R): Finite element software for electrochemical analysis: A mini-review, *Electrochem. Commun.*, **2014**, *40*, 71-74.

3 Savéant, J. M., Molecular electrochemistry: Recent trends and upcoming challenges, *ChemElectroChem,* **2016**, *3*, 1967-1977.

4 Xu, K., Electrolytes and interphases in Li-ion batteries and beyond, *Chem. Rev.*, **2014**, *114*, 11503-11618.

5 Bazant, M. Z., Theory of chemical kinetics and charge transfer based on nonequilibrium thermodynamics, *Accounts Chem. Res.*, **2013**, *46*, 1144-1160.

6 Lim, J.; Li, Y. Y.; Alsem, D. H.; So, H.; Lee, S. C.; Bai, P.; Cogswell, D. A.; Liu, X. Z.; Jin, N.; Yu, Y. S.; Salmon, N. J.; Shapiro, D. A.; Bazant, M. Z.; Tyliszczak, T.; Chueh, W. C., Origin and hysteresis of lithium compositional spatiodynamics within battery primary particles, *Science*, **2016**, *353*, 566-571.

7 MacFarlane, D. R.; Forsyth, M.; Howlett, P. C.; Kar, M.; Passerini, S.; Pringle, J. M.; Ohno, H.; Watanabe, M.; Yan, F.; Zheng, W. J.; Zhang, S. G.; Zhang, J., Ionic liquids and their solid-state analogues as materials for energy generation and storage, *Nat. Rev. Mater.* **2016**, *1*, 15005.

8 Watkins, T.; Kumar, A.; Buttry, D. A., Designer ionic liquids for reversible electrochemical deposition/dissolution of magnesium, *J. Am. Chem. Soc.*, **2016**, *138*, 641-650.

9 Hickner, M. A.; Herring, A. M.; Coughlin, E. B., Anion exchange membranes: Current status and moving forward, *J. Polym. Sci. Pt. B-Polym. Phys.*, **2013**, *51*, 1727-1735.

10 Bonaccorso, F.; Colombo, L.; Yu, G. H.; Stoller, M.; Tozzini, V.; Ferrari, A. C.; Ruoff, R. S.; Pellegrini, V., Graphene, related two-dimensional crystals, and hybrid systems for energy conversion and storage, *Science*, **2015**, *347*, 1246501.

11 Kleijn, S. E. F.; Lai, S. C. S.; Koper, M. T. M.; Unwin, P. R., Electrochemistry of nanoparticles, *Angew. Chem.-Int. Edit.*, **2014**, *53*, 3558-3586.

12 Jiang, J.; Li, Y. Y.; Liu, J. P.; Huang, X. T.; Yuan, C. Z.; Lou, X. W., Recent advances in metal oxide-based electrode architecture design for electrochemical energy storage, *Adv. Mater.*, **2012**, *24*, 5166-5180.

13 Xu, X.; Liu, W.; Kim, Y.; Cho, J., Nanostructured transition metal sulfides for lithium ion batteries: Progress and challenges, *Nano Today,* **2014**, *9*, 604-630.

14 Xu, Y. H.; Jin, S. B.; Xu, H.; Nagai, A.; Jiang, D. L., Conjugated microporous polymers: Design, synthesis and application, *Chem. Soc. Rev.*, **2013**, *42*, 8012-8031.

15 Simon, P.; Gogotsi, Y., Materials for electrochemical capacitors, *Nat. Mater.*, **2008**, *7*, 845-854.

16 Rolison, D. R.; Long, J. W.; Lytle, J. C.; Fischer, A. E.; Rhodes, C. P.; McEvoy, T. M.; Bourga, M. E.; Lubers, A. M., Multifunctional 3D nanoarchitectures for energy storage and conversion, *Chem. Soc. Rev.*, **2009**, *38*, 226-252.

17 Walcarius, A., Mesoporous materials and electrochemistry, *Chem. Soc. Rev.* **2013**, *42*, 4098-4140.

18 Burgess, M.; Moore, J. S.; Rodriguez-Lopez, J., Redox active polymers as soluble nanomaterials for energy storage, *Accounts Chem. Res.,* **2016**, *49*, 2649-2657.

19 Bazant, M. Z.; Storey, B. D.; Kornyshev, A. A., Double layer in ionic liquids: Overscreening versus crowding, *Phys. Rev. Lett.*, **2011**, *106*, 046102.

20 Hayes, R.; Warr, G. G.; Atkin, R., *Structure and nanostructure in ionic liquids, Chem. Rev.*, **2015**, *115*, 6357-6426.

21 Itkis, D. M.; Velasco-Velez, J. J.; Knop-Gericke, A.; Vyalikh, A.; Avdeev, M. V.; Yashina, L. V., Probing operating electrochemical interfaces by photons and neutrons, *ChemElectroChem*, **2015**, *2*, 1427-1445.

22 Ulvestad, A.; Clark, J. N.; Singer, A.; Vine, D.; Cho, H. M.; Harder, R.; Meng, Y. S.; Shpyrko, O. G., In situ strain evolution during a disconnection event in a battery nanoparticle, *Phys. Chem. Chem. Phys.,* **2015**, *17*, 10551-10555.

23 Zaera, F., Probing liquid/solid interfaces at the molecular level, *Chem. Rev.*, **2012**, *112*, 2920-2986.

24 Stoerzinger, K. A.; Hong, W. T.; Crumlin, E. J.; Bluhm, H.; Shao-Horn, Y., Insights into electrochemical reactions from ambient pressure photoelectron spectroscopy, *Accounts Chem. Res.*, **2015**, *48*, 2976-2983.

25 Pecher, O.; Carretero-Gonzalez, J.; Griffith, K. J.; Grey, C. P., Materials' methods: NMR in battery research, *Chem. Mat.*, **2017**, *29*, 213-242.

26 de Jonge, N.; Ross, F. M., Electron microscopy of specimens in liquid, *Nat. Nanotechnol.*, **2011**, *6*, 695-704.

27 Huang, J. Y.; Zhong, L.; Wang, C. M.; Sullivan, J. P.; Xu, W.; Zhang, L. Q.; Mao, S. X.; Hudak, N. S.; Liu, X. H.; Subramanian, A.; Fan, H. Y.; Qi, L. A.; Kushima, A.; Li, J., In situ observation of the electrochemical lithiation of a single SnO_2 nanowire electrode, *Science*, **2010**, *330*, 1515-1520.

28 Wu, Y. M. A.; Yin, Z. W.; Farmand, M.; Yu, Y. S.; Shapiro, D. A.; Liao, H. G.; Liang, W. I.; Chu, Y. H.; Zheng, H. M., In-situ multimodal imaging and spectroscopy of Mg electrodeposition at electrode-electrolyte interfaces, *Sci. Rep.* **2017**, *7*, 42527.

29 Oja, S. M.; Fan, Y. S.; Armstrong, C. M.; Defnet, P.; Zhang, B., Nanoscale electrochemistry revisited, *Anal. Chem.*, **2016**, *88*, 414-430.

30 Zaleski, S.; Wilson, A. J.; Mattei, M.; Chen, X.; Goubert, G.; Cardinal, M. F.; Willets, K. A.; Van Duyne, R. P., Investigating nanoscale electrochemistry with surface- and tip-enhanced Raman spectroscopy, *Accounts Chem. Res.*, **2016**, *49*, 2023-2030.

31 Jebaraj, A. J. J.; Scherson, D. A., Microparticle electrodes and single particle microbatteries: Electrochemical and in situ microRaman spectroscopic studies, *Accounts Chem. Res.*, **2013**, *46*, 1192-1205.

32 Kirshenbaum, K. C.; Bock, D. C.; Brady, A. B.; Marschilok, A. C.; Takeuchi, K. J.; Takeuchi, E. S., Electrochemical reduction of an $Ag_2VO_2PO_4$ particle: Dramatic increase of local electronic conductivity, *Phys. Chem. Chem. Phys.*, **2015**, *17*, 11204-11210.

33 Alligrant, T. M.; Anderson, M. J.; Dasari, R.; Stevenson, K. J.; Crooks, R. M., Single nanoparticle collisions at microfluidic microband electrodes: The effect of electrode material and mass transfer, *Langmuir,* **2014**, *30*, 13462-13469.

34 Kim, J.; Renault, C.; Nioradze, N.; Arroyo-Curras, N.; Leonard, K. C.; Bard, A. J., Electrocatalytic activity of individual Pt nanoparticles studied by nanoscale scanning electrochemical microscopy, *J. Am. Chem. Soc.,* **2016**, *138*, 8560-8568.

35 Kim, J.; Dick, J. E.; Bard, A. J., Advanced electrochemistry of individual metal clusters electrodeposited atom by atom to nanometer by nanometer, *Accounts Chem. Res.*, **2016**, *49*, 2587-2595.

36 German, S. R.; Edwards, M. A.; Chen, Q. J.; Liu, Y. W.; Luo, L.; White, H. S., Electrochemistry of single nanobubbles. Estimating the critical size of bubble-forming nuclei for gas-evolving electrode reactions, *Faraday Discuss.,* **2016**, *193*, 223-240.

4.2 Structure-Processing-Property Relationships

Understanding structure-processing-property relationships for anodes, cathodes, and electrolytes is critical to the rational design and development of next generation energy storage technologies. Appropriate structures can emphasize high power, high energy, or long lifetime. To access every electroactive particle and maximize utilization, internal pathways for both electrons and ions must be low-resistance and continuous, connecting all regions of the battery electrode.[1] Appropriate processing can maximize beneficial and minimize detrimental aspects of material structures, promoting desired properties for functional systems. For example, scientifically informed design of thin electrodes with selected architectures has been proposed to protect electrodes from parasitic reactions, accommodate mechanical stress due to volumetric changes, and optimize charge carrier mobility.[2]

Some structure-processing approaches apply to the anode, cathode, and electrolyte in concert. There has been recent progress in processing methods where each battery component can be deposited sequentially (e.g., printing methods[3,4] and physical vapor deposition[5]). Other approaches apply specifically to the electrodes (anode or cathode). Within an electrode, mass transport limitations can affect structures over various length scales (encompassing crystallite and aggregate size).[6,7] Even conventional processing methods such as electrode slurry preparation can benefit from deliberate control of process variables to achieve desired mesoscale structures.[8] Notably, non-redox active components (e.g., binders) can play a critical role in processing, where the functional capacity and capacity retention can be dramatically impacted with formation of highly conductive and hierarchically porous networks, which promote both electronic and ionic transport.[9,10] While recognizing some overlap, specific structure-processing-property relationships most relevant to anodes, cathodes, or electrolytes are highlighted below.

4.2.1 ANODES

Nanostructuring to reduce path lengths is an approach which has been applied broadly for high capacity anode materials.[11] A potential disadvantage of using nanoparticles as anodes is the inherent high resistance due to weak interparticle contact limiting the electron collection efficiency in the current collector. Many researchers have addressed this by using anisotropic nanostructures (Figure 4-2).[12] Emerging structural designs for anodes have been categorized as low-dimensional, inter-spatial, or composite with ordered-array, cross-aligned, alternating-layer, or 3D porous as representative heterostructures.[13]

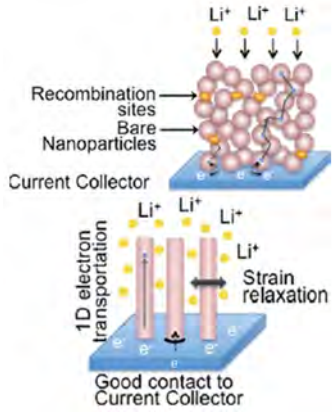

Figure 4-2. Schematic of isotropic (top) and anisotropic (bottom) nanoparticle anodes.[12] Reproduced with permission of Royal Society of Chemistry.

While graphite has been a dominant anode material historically for lithium-ion batteries, more recently carbon nanotubes,[14,15,16] graphene,[17,18,19] and their resulting heterostructures have been of interest both as active materials (for anodes) and conductive additives (for anodes and cathodes) due to their unique morphology and high conductivity. In carbon nanotubes, intercalation capacity is no longer limited to LiC_6 as structural defects can significantly affect the morphologies of the nanotubes and influence their capacities.[14] For sodium-ion battery systems there is a structural mismatch of the graphite interlayer spacing and Na^+ ion radius. Therefore, hard carbons are a preferred anode,[20] and particle size is critical to achieve reversibility.[21]

$Li_4Ti_5O_{12}$ (LTO) has a defect spinel structure that can be written as $Li[Li_{1/3}Ti_{5/3}]O_4$ and can reversibly accommodate lithium to yield the rock salt-type phase $Li_2[Li_{1/3}Ti_{5/3}]O_4$ in a zero-strain insertion process.[22] Large-pore mesoporous LTO thin film electrodes have shown excellent rate capability and stable cycling due to the combined benefits of their crystallographic, nanoscale, and mesoscale structures,[23] where the importance of void volume and structure was demonstrated via synthesis and electrochemical evaluation of 3D ordered microporous LTO materials from poly(methylmethacrylate) colloidal crystal templates and metal organic aqueous precursors with controlled filling fractions.[24]

Materials which reversibly alloy lithium, with low operating potentials and large theoretical capacities (i.e., Si, Ge, and Sn), are also of interest as potential alternative anode materials with theoretical capacities exceeding those of graphite. However, large volume changes during electrochemical alloying (up to 320% for Si) can lead to structural degradation.[25] Decreasing Si particle size to the nanoscale can mitigate the large volume expansion.[26,27] Conductive polymer or carbon-coated nanomaterials have shown electrochemical stability by maintaining internal electrical contact and stable SEI upon cycling.[28,29,30] For example, a pomegranate-inspired structure comprised of clusters of carbon-coated silicon nanoparticles with defined void space (Figure 4-3)[28] provided excellent capacity retention.

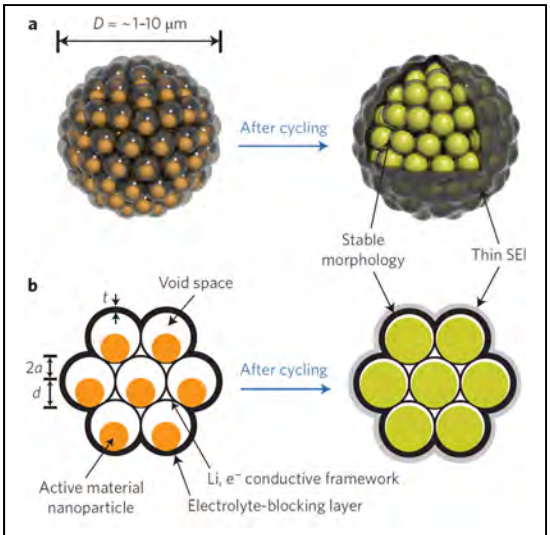

Figure 4-3. Schematic of the pomegranate-inspired C/Si composite structure.[28]

Lithium metal is the most appealing anode from an energy density perspective due to its high specific capacity (3860 mAh/g). Recent work has focused on understanding the lithium dendrite formation mechanism[31] and interfacial engineering[32,33] to impede lithium dendrite formation. Additional advances in electrolytes relevant to

lithium metal anodes are discussed below. A layered reduced graphene oxide has been proven to be a good lithium metal host material, showing stable lithium deposition/stripping without dendrite-induced short circuits.[33] It may one day be possible to safely utilize lithium metal in secondary batteries by understanding interfacial structure-property relationships.

4.2.2 CATHODES

Intercalation cathodes, in which guest ions can be inserted into and removed from the host network reversibly, are categorized by their crystallographic structure (e.g., layered, spinel, or olivine).[34] Modern intercalation cathode research centers are investigating transition metal oxide and polyanion compounds due to their high operating voltage and large energy density, with an impressive diversity of materials studied. Examples are provided here to illustrate structure-processing-property relationships over various length scales.

An atomic-level investigation of the role of defects and dopants on lithium transport in the olivine-type $LiFePO_4$ structure determined the lowest Li migration energy to be the pathway along the [010] channel, with a nonlinear, curved trajectory between Li sites.[35] Lower favorable energies were predicted only for divalent dopants on the Fe site (such as Mn), consistent with experimental observations. Structural disorder has also been shown to have a significant effect on electrochemistry in micrometer-sized spinel structured $LiNi_xMn_{2-x}O_4$ ($0.3 \leq x \leq 0.5$). The single crystals with (111) surface facets were shown to be triggered by an increase in Mn^{3+} content, due to change in the chemical composition or post-synthesis thermal processing.[36] Increased disorder led to increased solid solution behavior, reduced two-phase transformation domains, and improved transport properties during Li insertion and extraction. At the crystallite size level, a diffusion model was developed to explain the experimental correlation between capacity and crystallite size/lattice defect density in nickel metal hydride batteries, where the high nickel utilization of small crystallite nickel hydroxide was attributed to the high mobility of protons and electrons along grain boundaries and disordered lattice areas.[37]

$LiMn_2O_4$ is a spinel structured cathode material prone to capacity fade due to dissolution of Mn^{2+}.[38] As ample material and composite designs have been explored for this material, it can illustrate several useful structure-processing-property relationships. Sometimes, structural modification at the atomic level can have a follow-on impact at larger length scales. For example, doping with Al^{3+} improved capacity retention of $LiMn_2O_4$, by suppressing Jahn-Teller distortion by increasing the manganese oxidation state while simultaneously increasing the material surface area relative to the undoped analog.[39] At the particle level, various sizes and morphologies of $LiMn_2O_4$ were studied such as nanoparticles, nanowires, nanorods, hollow spheres, and thin films,[38] where porous nanospheres exhibited better high rate capability than their non-porous analogs attributed to formation of tunnels for Li^+ diffusion,[40] and the intermediate-sized particles exhibited the highest functional capacity attributed to better interaction with the conductive additive.[41] Surface coating with TiO_2,[42] CeO_2,[43] and $LiMn_{1.912}Ni_{0.072}Co_{0.016}O_4$[44] to minimize direct interaction with electrolyte showed benefit, attributed to inhibition of Mn^{2+} dissolution and HF generation.

In a conventional electrode design, the electroactive material is combined with a conductive additive where each material plays a distinct role. The design and implementation of multifunctional materials where each metal center contributes to electrode function in a distinctive manner can conceptually reduce or eliminate the contribution of passive materials to the size and mass of the final system. Upon electrochemical discharge, bimetallic oxide (MM'O) or phosphate (MM'PO) materials can undergo reactions where one metal ion (M^{m+}) is reduced to the metallic state (M^0) and repositioned externally to the original crystal through a reduction-displacement process, while the other metal ion (M'^{n+}) is partially reduced and structurally contributes to the crystal framework.[45] In silver vanadium phosphorus oxides, such as $Ag_2VO_2PO_4$, *in situ* reduction-displacement of silver has been demonstrated to generate a conductive Ag^0 network with an accompanying 15,000-fold decrease in impedance.[46] Since the conductive network is generated *in situ* upon electrochemical reduction, the rate of initial discharge is the processing method dictating formation of the percolation network.[47] Stable

crystallographic structures for the M'O or M'PO framework have resulted in reversible redox at the M'^{n+} center for this material class.[48,49,50]

Materials which undergo a conversion reaction (e.g., M_xO and MX_2) can often accommodate more than one lithium atom per transition-metal cation, making them promising candidates for high-capacity electrodes. In such systems, the relation between the structure of the parent material and the structures of the reduction products is a critical deterministic factor toward the reversibility of the conversion process. For example, while both FeF_2 and CuF_2 react with lithium via a direct conversion process with no intercalation step, the FeF_2 material shows good reversibility while CuF_2 is inactive after the first discharge.[51] Upon reduction of FeF_2, small metallic iron nanoparticles (<5 nm in diameter) nucleate in close proximity to the converted LiF phase as a result of the low diffusivity of iron, forming a bicontinuous interconnected network for transport through the insulating LiF phase. In contrast, the CuF_2 electrode is converted to Cu segregates which form large particles (5–12 nm in diameter) during the first discharge; this segregation may be partially responsible for the lack of reversibility. For Fe_3O_4, the cubic-close-packed (ccp) O-anion array is sustained throughout the lithiation and delithiation processes, enabling multiple lithium intercalation and conversion reactions between metallic Fe and FeO-like phases.[52] Lithiation of a model electrode consisting of well defined, vertically aligned layers of Cr and CrO_x was recently reported, revealing the combination of confining lithiation to nanoscale sheets of Li_2O and the availability of reaction sites in the metal layers in the layered structure to be a strategy for improving the reversibility and mass transport properties in conversion systems.[53] It is important to note that while both are discussed in this section, conversion-type metal oxides and metal fluorides are typically described as anode and cathode materials, respectively. Metal oxide conversion materials are typically anodes due to their low potentials (~1.0 V). With a higher potential for conversion (~2.0 V), metal fluorides can be described as cathode materials due to the more ionic character in MF induced by the fluoride ion.

Cathodes that function through chemical transformation processes (e.g., metal air and metal sulfur) offer opportunity for unprecedented energy densities if their complex structure-process-property relationships can be understood and controlled. For example, sulfur has a high theoretical capacity of 1675 mAh/g and energy density of ~2600 Wh/kg, yet the application of sulfur materials to commercial batteries is significantly impeded by its poor cycle stability, which is attributed to soluble discharge intermediate products.[54] Research efforts to date have emphasized use of porous carbon materials to physically trap and prevent dissolution of soluble polysulfides.[55,56] However, more sulfiphilic transition metal oxides or sulfides, with stronger surface binding affinities to polysulfides, can further improve long-term cycle life.[57] Recently, transition metal sulfides,[58,59] oxides,[59,60,61] and nitrides,[62,63] have shown the capability to support extended cycling. Further development of suitable polysulfide trapping structures will be critical to further advance lithium/sulfur battery technology.

Considering the new developments in both intercalation and conversion cathodes over the recent years, many new strategies and critical observations have shown increased stability and high power capabilites in battery techology. Synergetic effects between the cathode, anode, and electrolyte will be crucial as researchers continue to push the limits of energy density, power, and cycle life for energy storage systems.

4.2.3 ELECTROLYTES

The most common electrolytes in state-of-the-art energy storage technologies are liquids containing dissolved salts. While empirical[64,65] and computational[66,67] studies used to identify promising chemistries are important areas of research, particularly for beyond lithium-ion systems (e.g., magnesium-ion,[68,69] sodium-ion,[70] lithium sulfur,[71,72] metal-air,[73] and redox flow[74]), this section will emphasize structure and processing approaches to electrolyte development.

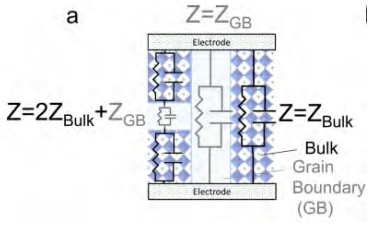

Figure 4-4. Schematic of conduction pathways in polycrystalline material.[75] Reproduced with permission of American Chemical Society.

An emerging trend in electrolyte technology is the integration of solid-state electrolytes. The interest in these materials evolved due to their potential to improve battery lifetime and safety owing to greater electrochemical stability voltage windows, enhanced thermal stability and lower flammability relative to conventional electrolytes. Historically, the main issues for solid-state electrolytes have been low ionic conductivities relative to organic liquid solvents and the stability of the electrode-electrolyte interface. Inorganic solid-state ion conductors are comprised of metal and nonmetal ions that create polyhedra with ligands to create an open crystal structure that allows for ion migration. Structure-tuning techniques have been employed to improve cation mobility,[75] where electrolytes with body-centered cubic anion sublattices and structures in which the mobile species is not in its preferred coordination environment can provide high ionic conductivity. Structural studies focused on limiting grain boundaries through various synthetic approaches have been effective in increasing ion conduction (Figure 4-4).[75] Bulk solid-state electrolytes (hundreds of μm thick, as in LISICON and NASICON based electrolyte) are typically synthesized through milling, sintering, and compaction while thin films (hundreds of nm to several μm thick, as in LiPON) are produced from pulsed laser deposition or spark plasma sintering.[76]

Another promising alternative to current electrolytes are ionic liquids (ILs) with bulky cations and anions preventing room temperature crystallization. These are desirable due to their low melting points, negligible vapor pressures, and low flammability.[77] Some ILs display stabilities up to 6 V vs. Li/Li^+. Typical ILs employ a quaternary ammonium cation like imidazolium, pyridinium, pyrrolidinium, piperidnium, or ammonium derivatives combined with anions such as BF_4^-, PF_6^-, $[(FSO_2)(CF_3SO_2)N)]^-$, $[(CF_3SO_2)(CF_3SO_2)_2N]^-$, $[(C_3SO_2)_2N]^-$ or $[(C_2F_5SO_2)_2N]^-$. A study of low-melting point ILs based on the small aliphatic quaternary ammonium cations $[R^1R^2R^3NR]^+$ (where R^1, R^2, R^3 = CH_3 or C_2H_5, R = C_3H_7, C_4H_9, C_6H_{13}, C_8H_{17}, $CF_3C_3H_6$) and imide anions showed small alkyl chain length or fluorination promoted higher oxidative stability.[78] Hybrids of ILs and organic solvent (e.g., vinylene, ethylene, or chloroethylene carbonate) additives show promise for synergistically combining the stability of ILs and the low viscosities of organic solvents,[79] with potential for future application to magnesium electrolyte systems.[80]

Polymer electrolytes are appealing for future safe and flexible batteries as they do not contain flammable, liquid, organic solvents.[81,82] There are two main structure-processing approaches: 1) dry or solid polymer electrolytes without any additional solvent where the polymer must be an ion conductor (e.g., poly(ethylene oxide)(PEO)/lithium salt complexes), and 2) blended electrolytes made from combinations of solid polymers and organic solvents where the polymer does not necessarily need to conduct ions (polymer-gel). The solid polymer electrolytes are generated from complexing polymers with an inorganic salt to achieve low lattice energy and high stability (e.g., poly(ethylene oxide) (PEO) electrolytes, such as PEO-$LiCF_3SO_3$ and PEO-$LiBF_4$). They offer ease of fabrication and good compatibility with lithium salts.[83] Lowering the glass transition temperature of these electrolytes by using branched copolymers with multiple chain ends has been shown to enhance ion mobility. Other polymer-gel electrolytes such as poly(vinylidene difluoride-co-hexafluoropropylene) soaked with $LiPF_6$ and carbonates utilize their polymer matrix to provide mechanical strength and flexibility while the solvent provides Li^+ diffusive properties, an approach which can reduce the need for a polymer separator. Recent structural studies have introduced polymers that can enhance Li^+ ion transport with polar elements in their skeleton such as oxygen or nitrogen.

Designing electrolytes to promote favorable Li-metal surface-electrolyte interfaces for stable, dendrite-free deposition of lithium metal is critical to enable lithium metal batteries with high energy density. While a uniform and stable interfaces can passivate the Li surface, spontaneously formed SEIs on Li with conventional liquid electrolytes are typically inhomogeneous (providing nucleation sites for dendrite formation at any current

density) or mechanically fragile (depleting the electrolyte continually through exposure of fresh Li).[84] Physical protection of lithium metal with thin layers (e.g., LiPON deposited via radio frequency magnetron sputter-coating[85] and Al_2O_3 introduced via atomic layer deposition[86]) has shown significant benefit. Liquid electrolytes can also be hosted in the pores of ceramic membranes with a high areal density of nanometer-sized pores, smaller than typical Li dendrite sizes, which provide a novel electrolyte design approach for achieving dendrite-free lithium metal batteries.[87]

References

1 Dudney, N. J.; Li, J., Using all energy in a battery, *Science,* **2015**, *347*, 131.

2 Noked, M.; Liu, C.; Hu, J.; Gregorczyk, K.; Rubloff, G. W.; Lee, S. B., Electrochemical thin layers in nanostructures for energy storage, *Accounts of Chemical Research,* **2016**, *49*, 2336-2346.

3 Gaikwad, A. M.; Arias, A. C.; Steingart, D. A., Recent progress on printed flexible batteries: Mechanical challenges, printing technologies, and future prospects, *Energy Technology,* **2015**, *3*, 305-328.

4 Fu, K.; Yao, Y.; Dai, J.; Hu, L., Progress in 3D printing of carbon materials for energy-related applications, *Advanced Materials,* **2017**, *29*, DOI: 10.1002/adma.201603486.

5 Talin, A. A.; Ruzmetov, D.; Kolmakov, A.; McKelvey, K.; Ware, N.; El Gabaly, F.; Dunn, B.; White, H. S., Fabrication, testing, and simulation of all-solid-state three-dimensional Li-ion batteries, *ACS Applied Materials & Interfaces,* **2016**, *8*, 32385-32391.

6 Knehr, K. W.; Brady, N. W.; Cama, C. A.; Bock, D. C.; Lin, Z.; Lininger, C. N.; Marschilok, A. C.; Takeuchi, K. J.; Takeuchi, E. S.; West, A. C., Modeling the mesoscale transport of lithium-magnetite electrodes using insight from discharge and voltage recovery experiments, *Journal of the Electrochemical Society,* **2015**, *162*, A2817-A2826.

7 Abraham, A.; Housel, L. M.; Lininger, C. N.; Bock, D. C.; Jou, J.; Wang, F.; West, A. C.; Marschilok, A. C.; Takeuchi, K. J.; Takeuchi, E. S., Investigating the complex chemistry of functional energy storage systems: The Need for an integrative, multiscale (molecular to mesoscale) perspective, *ACS Central Science,* **2016**, *2*, 380-387.

8 Kraytsberg, A.; Ein-Eli, Y., Conveying advanced Li-ion battery materials into practice: The impact of electrode slurry preparation skills, *Advanced Energy Materials,* **2016**, *6*, DOI: 10.1002/aenm.201600655.

9 Shi, Y.; Zhou, X.; Zhang, J.; Bruck, A. M.; Bond, A. C.; Marschilok, A. C.; Takeuchi, K. J.; Takeuchi, E. S.; Yu, G., Nanostructured conductive polymer gels as a general framework material to improve electrochemical performance of cathode materials in Li-ion batteries, *Nano Letters,* **2017**, *17*, 1906-1914.

10 Kwon, Y. H.; Minnici, K.; Huie, M. M.; Takeuchi, K. J.; Takeuchi, E. S.; Marschilok, A. C.; Reichmanis, E., Electron/ion transport enhancer in high capacity Li-ion battery anodes, *Chemistry of Materials,* **2016**, *28*, 6689-6697.

11 Goriparti, S.; Miele, E.; De Angelis, F.; Di Fabrizio, E.; Proietti Zaccaria, R.; Capiglia, C., Review on recent progress of nanostructured anode materials for Li-ion batteries, *Journal of Power Sources,* **2014**, *257*, 421-443.

12 Roy, P.; Srivastava, S. K., Nanostructured anode materials for lithium ion batteries, *Journal of Materials Chemistry A,* **2015**, *3*, 2454-2484.

13 Zhong, Y.; Yang, M.; Zhou, X.; Zhou, Z., Structural design for anodes of lithium-ion batteries: emerging horizons from materials to electrodes, *Materials Horizons,* **2015**, *2*, 553-566.

14 Sehrawat, P.; Julien, C.; Islam, S. S. Carbon nanotubes in Li-ion batteries: A review, *Materials Science and Engineering B-Advanced Functional Solid-State Materials,* **2016**, *213*, 12-40.

15 Landi, B. J.; Ganter, M. J.; Cress, C. D.; DiLeo, R. A.; Raffaelle, R. P., Carbon nanotubes for lithium ion batteries, *Energy & Environmental Science,* **2009**, *2*, 638-654.

16 Wang, L.; Li, Y. R.; Li, J.; Zou, S.; Stach, E. A.; Takeuchi, K. J.; Takeuchi, E. S.; Marschilok, A. C.; Wong, S. S., Correlating preparative approaches with electrochemical performance of $Fe3O_4$-MWNT composites used as anodes in Li-ion batteries, *ECS Journal of Solid State Science and Technology,* **2017**, *6*, M3122-M3131.

17 Kucinskis, G.; Bajars, G.; Kleperis, J., Graphene in lithium ion battery cathode materials: A review, *Journal of Power Sources,* **2013**, *240*, 66-79.

18 Mori, T.; Chen, C. J.; Hung, T. F.; Mohamed, S. G.; Lin, Y. Q.; Lin, H. Z.; Sung, J. C.; Hu, S. F.; Liu, R. S., High specific capacity retention of graphene/silicon nanosized sandwich structure fabricated by continuous electron beam evaporation as anode for lithium-ion batteries, *Electrochimica Acta,* **2015**, *165*, 166-172.

19 Yu, S.-H.; Conte, D. E.; Baek, S.; Lee, D.-C.; Park, S.-K.; Lee, K. J.; Piao, Y.; Sung, Y.-E.; Pinna, N., Structure-properties relationship in iron oxide-reduced graphene oxide nanostructures for Li-ion batteries, *Advanced Functional Materials,* **2013**, *23*, 4293-4305.

20 Balogun, M.-S.; Luo, Y.; Qiu, W.; Liu, P.; Tong, Y., A review of carbon materials and their composites with alloy metals for sodium ion battery anodes, *Carbon,* **2016**, *98*, 162-178.

21 Doeff, M. M.; Ma, Y.; Visco, S. J.; De Jonghe, L. C., Electrochemical insertion of sodium into carbon, *Journal of the Electrochemical Society,* **1993**, *140*, L169-L170.

22 Palacin, M. R., Recent advances in rechargeable battery materials: A chemist's perspective, *Chemical Society Reviews,* **2009**, *38*, 2565-2575.

23 Haetge, J.; Hartmann, P.; Brezesinski, K.; Janek, J.; Brezesinski, T., Ordered large-pore mesoporous $Li_4Ti_5O_{12}$ spinel thin film electrodes with nanocrystalline framework for high rate rechargeable lithium batteries: Relationships among charge storage, electrical conductivity, and nanoscale structure, *Chemistry of Materials,* **2011**, *23*, 4384-4393.

24 Sorensen, E. M.; Barry, S. J.; Jung, H.-K.; Rondinelli, J. M.; Vaughey, J. T.; Poeppelmeier, K. R., Three-dimensionally ordered macroporous $Li_4Ti_5O_{12}$: Effect of wall structure on electrochemical properties, *Chemistry of Materials,* **2006**, *18*, 482-489.

25 Zamfir, M. R.; Nguyen, H. T.; Moyen, E.; Lee, Y. H.; Pribat, D., Silicon nanowires for Li-based battery anodes: a review, *Journal of Materials Chemistry A,* **2013**, *1*, 9566-9586.

26 Chan, C. K.; Peng, H.; Liu, G.; McIlwrath, K.; Zhang, X. F.; Huggins, R. A.; Cui, Y., High-performance lithium battery anodes using silicon nanowires, *Nature Nano,* **2008**, *3*, 31-35.

27 Wu, H.; Chan, G.; Choi, J. W.; Ryu, I.; Yao, Y.; McDowell, M. T.; Lee, S. W.; Jackson, A.; Yang, Y.; Hu, L.; Cui, Y., Stable cycling of double-walled silicon nanotube battery anodes through solid-electrolyte interphase control, *Nature Nano,* **2012**, *7*, 310-315.

28 Liu, N.; Lu, Z.; Zhao, J.; McDowell, M. T.; Lee, H.-W.; Zhao, W.; Cui, Y., A pomegranate-inspired nanoscale design for large-volume-change lithium battery anodes, *Nature Nano,* **2014**, *9*, 187-192.

29 Yao, Y.; Liu, N.; McDowell, M. T.; Pasta, M.; Cui, Y., Improving the cycling stability of silicon nanowire anodes with conducting polymer coatings, *Energy & Environmental Science,* **2012**, *5*, 7927-7930.

30 Wu, H.; Yu, G.; Pan, L.; Liu, N.; McDowell, M. T.; Bao, Z.; Cui, Y., Stable Li-ion battery anodes by in-situ polymerization of conducting hydrogel to conformally coat silicon nanoparticles, *Nature Communications* **2013**, *4*, 1943.

31 Bhattacharyya, R.; Key, B.; Chen, H.; Best, A. S.; Hollenkamp, A. F.; Grey, C. P., In situ NMR observation of the formation of metallic lithium microstructures in lithium batteries, *Nature Materials,* **2010**, *9*, 504-510.

32 Zheng, G.; Lee, S. W.; Liang, Z.; Lee, H.-W.; Yan, K.; Yao, H.; Wang, H.; Li, W.; Chu, S.; Cui, Y., Interconnected hollow carbon nanospheres for stable lithium metal anodes, *Nature Nano,* **2014**, *9*, 618-623.

33 Lin, D.; Liu, Y.; Liang, Z.; Lee, H.-W.; Sun, J.; Wang, H.; Yan, K.; Xie, J.; Cui, Y., Layered reduced graphene oxide with nanoscale interlayer gaps as a stable host for lithium metal anodes, *Nature Nano,* **2016**, *11*, 626-632.

34 Nitta, N.; Wu, F.; Lee, J. T.; Yushin, G., Li-ion battery materials: Present and future, *Materials Today,* **2015**, *18*, 252-264.

35 Islam, M. S.; Driscoll, D. J.; Fisher, C. A. J.; Slater, P. R., Atomic-scale investigation of defects, dopants, and lithium transport in the $LiFePO_4$ olivine-type battery material, *Chemistry of Materials,* **2005**, *17*, 5085-5092.

36 Duncan, H.; Hai, B.; Leskes, M.; Grey, C. P.; Chen, G., Relationships between Mn^{3+} content, structural ordering, phase transformation, and kinetic properties in $LiNi_xMn_{2-x}O_4$ cathode materials, *Chemistry of Materials,* **2014**, *26*, 5374-5382.

37 Gille, G.; Albrecht, S.; Meese-Marktscheffel, J.; Olbrich, A.; Schrumpf, F., Cathode materials for rechargeable batteries—preparation, structure–property relationships and performance, *Solid State Ionics,* **2002**, *148*, 269-282.

38 Dou, S. M., Review and prospects of Mn-based spinel compounds as cathode materials for lithium-ion batteries, *Ionics,* **2015**, *21*, 3001-3030.

39 Wang, J. L.; Li, Z. H.; Yang, J.; Tang, J. J.; Yu, J. J.; Nie, W. B.; Lei, G. T.; Xiao, Q. Z., Effect of Al-doping on the electrochemical properties of a three-dimensionally porous lithium manganese oxide for lithium-ion batteries, *Electrochimica Acta,* **2012**, *75*, 115-122.

40 Wang, Y. Z.; Shao, X.; Xu, H. Y.; Xie, M.; Deng, S. X.; Wang, H.; Liu, J. B.; Yan, H., Facile synthesis of porous $LiMn_2O_4$ spheres as cathode materials for high-power lithium ion batteries, *Journal of Power Sources,* **2013**, *226*, 140-148.

41 Xiao, L.; Guo, Y. L.; Qu, D. Y.; Deng, B. H.; Liu, H. X.; Tang, D. P., Influence of particle sizes and morphologies on the electrochemical performances of spinel $LiMn_2O_4$ cathode materials, *Journal of Power Sources,* **2013**, *225*, 286-292.

42 Zhang, J. Y.; Shen, J. X.; Wang, T. L.; Wei, C. B.; Ma, Y.; Zhu, C. F.; Yue, Y. Z., Improvement of capacity and cycling performance of spinel $LiMn_2O_4$ cathode materials with TiO_2-B nanobelts, *Electrochimica Acta,* **2013**, *111*, 691-697.

43 Michalska, M.; Hamankiewicz, B.; Ziolkowska, D.; Krajewski, M.; Lipinska, L.; Andrzejczuk, M.; Czerwinski, A., Influence of $LiMn_2O_4$ modification with CeO_2 on electrode performance, *Electrochimica Acta,* **2014**, *136*, 286-291.

44 Wen, W. C.; Chen, S. H.; Fu, Y. Q.; Wang, X. Y.; Shu, H. B., A core-shell structure spinel cathode material with a concentration-gradient shell for high performance lithium-ion batteries, *Journal of Power Sources,* **2015**, *274*, 219-228.

45 Durham, J. L.; Poyraz, A. S.; Takeuchi, E. S.; Marschilok, A. C.; Takeuchi, K. J., Impact of multifunctional bimetallic materials on lithium battery electrochemistry, *Accounts of Chemical Research,* **2016**, *49*, 1864-1872.

46 Takeuchi, E. S.; Marschilok, A. C.; Tanzil, K.; Kozarsky, E. S.; Zhu, S.; Takeuchi, K. J., Electrochemical reduction of silver vanadium phosphorus oxide, $Ag_2VO_2PO_4$: The formation of electrically conductive metallic silver nanoparticles, *Chemistry of Materials,* **2009**, *21*, 4934-4939.

47 Kirshenbaum, K.; Bock, D. C.; Lee, C.-Y.; Zhong, Z.; Takeuchi, K. J.; Marschilok, A. C.; Takeuchi, E. S., In situ visualization of $Li/Ag_2VP_2O_8$ batteries revealing rate-dependent discharge mechanism, *Science,* **2015**, *347*, 149-154.

48 Zhang, Y.; Kirshenbaum, K. C.; Marschilok, A. C.; Takeuchi, E. S.; Takeuchi, K. J., Battery relevant electrochemistry of $Ag_7Fe_3(P_2O_7)_4$: Contrasting contributions from the redox chemistries of Ag^+ and Fe^{3+}, *Chemistry of Materials,* **2016**, *28*, 7619-7628.

49 Durham, J. L.; Kirshenbaum, K.; Takeuchi, E. S.; Marschilok, A. C.; Takeuchi, K. J., Synthetic control of composition and crystallite size of silver ferrite composites: Profound electrochemistry impacts, *Chemical Communications,* **2015**, *51*, 5120-5123.

50 Marschilok, A. C.; Kim, Y. J.; Takeuchi, K. J.; Takeuchi, E. S., Silver vanadium phosphorous oxide, $Ag_{0.48}VOPO_4$: Exploration as a cathode material in primary and secondary battery applications, *Journal of the Electrochemical Society,* **2012**, *159*, A1690-A1695.

51 Wang, F.; Robert, R.; Chernova, N. A.; Pereira, N.; Omenya, F.; Badway, F.; Hua, X.; Ruotolo, M.; Zhang, R.; Wu, L.; Volkov, V.; Su, D.; Key, B.; Whittingham, M. S.; Grey, C. P.; Amatucci, G. G.; Zhu, Y.; Graetz, J., Conversion reaction mechanisms in lithium ion batteries: Study of the binary metal fluoride electrodes, *Journal of the American Chemical Society,* **2011**, *133*, 18828-18836.

52 Zhang, W.; Bock, D. C.; Pelliccione, C. J.; Li, Y.; Wu, L.; Zhu, Y.; Marschilok, A. C.; Takeuchi, E. S.; Takeuchi, K. J.; Wang, F., Insights into ionic transport and structural changes in magnetite during multiple-electron transfer reactions, *Advanced Energy Materials,* **2016**, *6*, DOI: 10.1002/aenm.201502471.

53 Fister, T. T.; Hu, X.; Esbenshade, J.; Chen, X.; Wu, J.; Dravid, V.; Bedzyk, M.; Long, B.; Gewirth, A. A.; Shi, B.; Schlepütz, C. M.; Fenter, P., Dimensionally controlled lithiation of chromium oxide, *Chemistry of Materials,* **2016**, *28*, 47-54.

54 Manthiram, A.; Fu, Y.; Su, Y.-S., Challenges and prospects of lithium–sulfur batteries, *Accounts of Chemical Research,* **2012**, *46*, 1125-1134.

55 Ji, X.; Lee, K. T.; Nazar, L. F., A highly ordered nanostructured carbon–sulphur cathode for lithium–sulphur batteries, *Nature Materials,* **2009**, *8*, 500-506.

56 Jayaprakash, N.; Shen, J.; Moganty, S. S.; Corona, A.; Archer, L. A., Porous hollow carbon@ sulfur composites for high-power lithium–sulfur batteries, *Angewandte Chemie,* **2011**, *123*, 6026-6030.

57 Peng, H. J.; Zhang, Q., Designing host materials for sulfur cathodes: From physical confinement to surface chemistry, *Angewandte Chemie International Edition,* **2015**, *54*, 11018-11020.

58 Seh, Z. W.; Yu, J. H.; Li, W.; Hsu, P.-C.; Wang, H.; Sun, Y.; Yao, H.; Zhang, Q.; Cui, Y., Two-dimensional layered transition metal disulphides for effective encapsulation of high-capacity lithium sulphide cathodes, *Nature Communications,* **2014**, *5.*

59 Liu, X.; Huang, J.-Q.; Zhang, Q.; Mai, L., Nanostructured metal oxides and sulfides for lithium–sulfur batteries, *Advanced Materials,* **2017**, 1601759.

60 Seh, Z. W.; Li, W.; Cha, J. J.; Zheng, G.; Yang, Y.; McDowell, M. T.; Hsu, P.-C.; Cui, Y., Sulphur–TiO_2 yolk–shell nanoarchitecture with internal void space for long-cycle lithium–sulphur batteries, *Nature Communications,* **2013**, *4*, 1331.

61 Li, Z.; Zhang, J.; Guan, B.; Wang, D.; Liu, L.-M.; Lou, X. W. D., A sulfur host based on titanium monoxide@ carbon hollow spheres for advanced lithium–sulfur batteries, *Nature Communications,* **2016**, *7*, 13065.

62 Sun, Z.; Zhang, J.; Yin, L.; Hu, G.; Fang, R.; Cheng, H.-M.; Li, F., Conductive porous vanadium nitride/graphene composite as chemical anchor of polysulfides for lithium-sulfur batteries, *Nature Communications,* **2017**, *8*, 14627.

63 Cui, Z.; Zu, C.; Zhou, W.; Manthiram, A.; Goodenough, J. B., Mesoporous titanium nitride-enabled highly stable lithium-sulfur batteries, *Advanced Materials,* **2016**, *28*, 6926-6931.

64 Choi, N.-S.; Han, J.-G.; Ha, S.-Y.; Park, I.; Back, C.-K., Recent advances in the electrolytes for interfacial stability of high-voltage cathodes in lithium-ion batteries, *RSC Advances,* **2015**, *5*, 2732-2748.

65 Kalhoff, J.; Eshetu, G. G.; Bresser, D.; Passerini, S., Safer electrolytes for lithium-ion batteries: State of the art and perspectives, *ChemSusChem,* **2015**, *8*, 2154-2175.

66 Bhatt, M. D.; O'Dwyer, C., Recent progress in theoretical and computational investigations of Li-ion battery materials and electrolytes, *Physical Chemistry Chemical Physics,* **2015**, *17*, 4799-4844.

67 Cheng, L.; Assary, R. S.; Qu, X.; Jain, A.; Ong, S. P.; Rajput, N. N.; Persson, K.; Curtiss, L. A., Accelerating electrolyte discovery for energy storage with high-throughput screening, *Journal of Physical Chemistry Letters,* **2015**, *6*, 283-291.

68 Tutusaus, O.; Mohtadi, R., Paving the way towards highly stable and practical electrolytes for rechargeable magnesium batteries, *ChemElectroChem,* **2015**, *2*, 51-57.

69 Aurbach, D.; Lu, Z.; Schechter, A.; Gofer, Y.; Gizbar, H.; Turgeman, R.; Cohen, Y.; Moshkovich, M.; Levi, E., Prototype systems for rechargeable magnesium batteries, *Nature,* **2000**, *407*, 724-727

70 Ponrouch, A.; Monti, D.; Boschin, A.; Steen, B.; Johansson, P.; Palacin, M. R., Non-aqueous electrolytes for sodium-ion batteries, *Journal of Materials Chemistry A: Materials for Energy and Sustainability,* **2015**, *3*, 22-42.

71 Hassoun, J.; Scrosati, B., Review--Advances in anode and electrolyte materials for the progress of lithium-ion and beyond lithium-ion batteries, *Journal of the Electrochemical Society,* **2015**, *162*, A2582-A2588.

72 Zhang, S.; Ueno, K.; Dokko, K.; Watanabe, M., Recent advances in electrolytes for lithium-sulfur batteries, *Advanced Energy Materials,* **2015**, *5*, DOI: 10.1002/aenm.201500117.

73 Laoire, C. O.; Mukerjee, S.; Abraham, K. M.; Plichta, E. J.; Hendrickson, M. A., Influence of nonaqueous solvents on the electrochemistry of oxygen in the rechargeable lithium-air battery, *Journal of Physical Chemistry C,* **2010**, *114*, 9178-9186.

74 Noack, J.; Roznyatovskaya, N.; Herr, T.; Fischer, P., The chemistry of redox-flow batteries, *Angewandte Chemie-International Edition,* **2015**, *54*, 9775-9808.

75 Bachman, J. C.; Muy, S.; Grimaud, A.; Chang, H.-H.; Pour, N.; Lux, S. F.; Paschos, O.; Maglia, F.; Lupart, S.; Lamp, P.; Giordano, L.; Shao-Horn, Y., Inorganic solid-state electrolytes for lithium batteries: Mechanisms and properties governing ion conduction, *Chemical Reviews,* **2016,** *116,* 140-162.

76 Kim, J. G.; Son, B.; Mukherjee, S.; Schuppert, N.; Bates, A.; Kwon, O.; Choi, M. J.; Chung, H. Y.; Park, S., A review of lithium and non-lithium based solid state batteries, *Journal of Power Sources,* **2015,** *282,* 299-322.

77 Wang, Y.; Zhong, W.-H., Development of electrolytes towards achieving safe and high-performance energy-storage devices: A review, *ChemElectroChem,* **2015,** *2,* 22-36.

78 Le, M. L. P.; Alloin, F.; Strobel, P.; Leprêtre, J.-C.; Pérez del Valle, C.; Judeinstein, P., Structure−properties relationships of lithium electrolytes based on ionic liquid, *Journal of Physical Chemistry B,* **2010,** *114,* 894-903.

79 DiLeo, R. A.; Marschilok, A. C.; Takeuchi, K. J.; Takeuchi, E. S., Battery electrolytes based on unsaturated ring ionic liquids: Conductivity and electrochemical stability, *Journal of the Electrochemical Society,* **2013,** *160,* A1399-A1405.

80 Huie, M. M.; Cama, C. A.; Smith, P. F.; Yin, J.; Marschilok, A. C.; Takeuchi, K. J.; Takeuchi, E. S., Ionic liquid hybrids: Progress toward non-corrosive electrolytes with high-voltage oxidation stability for magnesium-ion based batteries, *Electrochimica Acta,* **2016,** *219,* 267-276.

81 Osada, I.; de Vries, H.; Scrosati, B.; Passerini, S., Ionic-liquid-based polymer electrolytes for battery applications, *Angewandte Chemie, International Edition,* **2016,** *55,* 500-513.

82 Shaplov, A. S.; Marcilla, R.; Mecerreyes, D., Recent advances in innovative polymer electrolytes based on poly(ionic liquid)s, *Electrochimica Acta,* **2015,** *175,* 18-34.

83 Xue, Z.; He, D.; Xie, X., Poly(ethylene oxide)-based electrolytes for lithium-ion batteries, *Journal of Materials Chemistry A: Materials for Energy and Sustainability,* **2015,** *3,* 19218-19253.

84 Tikekar, M. D.; Choudhury, S.; Tu, Z.; Archer, L. A., Design principles for electrolytes and interfaces for stable lithium-metal batteries, *Nature Energy,* **2016,** *1,* 16114.

85 Bates, J. B.; Dudney, N. J.; Gruzalski, G. R.; Zuhr, R. A.; Choudhury, A.; Luck, C. F.; Robertson, J. D., Fabrication and characterization of amorphous lithium electrolyte thin films and rechargeable thin-film batteries, *Journal of Power Sources,* **1993,** *43,* 103-110.

86 Kozen, A. C.; Lin, C.-F.; Pearse, A. J.; Schroeder, M. A.; Han, X.; Hu, L.; Lee, S.-B.; Rubloff, G. W.; Noked, M., Next-generation lithium metal anode engineering via atomic layer deposition, *ACS Nano,* **2015,** *9,* 5884-5892.

87 Tu, Z.; Kambe, Y.; Lu, Y.; Archer, L. A., Nanoporous polymer-ceramic composite electrolytes for lithium metal batteries, *Advanced Energy Materials,* **2014,** *4,* DOI: 10.1002/aenm.201300654.

4.3 Materials to System Level

Translating a maximum fraction of the theoretical energy content (energy density, specific energy) from the electroactive materials level to the cell and pack levels describes the primary challenge in developing a viable battery chemistry. Near theoretical or, at the very least, optimum performance is achieved at the materials level and transferred to functional electrodes as described in the preceding section. The goal at the cell level is to preserve as much of the material level energy content by minimizing added mass and volume of inactive materials and packaging.[1,2] Electrode capacity dictated by thickness and porosity is tailored to provide sufficient ion transport to meet desired power requirements. Electrolytes employed must provide both the ionic conductivity and full wetting of the electrodes so that target capacity can be accessed. For conversion electrochemical processes, such as the chalcogenides O_2 and S_8, sufficient volume must be designed into the cathode to allow for discharge product (i.e., lithium peroxide and lithium sulfide) formation within the cathode to ensure both electronic and ionic continuity within the electrode. Metal deposition and dissolution at a metal anode is a particularly challenging design problem as the local volume loss (dissolution) and gain (deposition) must be taken into account. That requires a cell stack kept in compression at an effective force constant that allows accommodation of these net volume changes. Compatibility of electrode materials, electrolyte, and inactive cell materials must also be considered. A number of high voltage oxide cathodes are sufficiently reactive with alkyl carbonates and supporting electrolyte salts like lithium hexafluorophosphate coupled with residual moisture. This instability limits the use of these oxides in nanostructured form and can necessitate protective coatings. Fluoride is beneficial in passivating the typical 15-μm-thick Al foils used as current collectors onto which composite electrode slurries are cast. Materials concepts designed to maximize stored energy content must be integrated, requiring a high degree of compatibility, to ensure that both energy and kinetics are maintained at the cell level.

4.3.1 DEGRADATION

The calendar and cycle life of a battery are largely dictated by a range of degradation processes that take place in a battery over time and with use.[3,4] The basic structure and properties of the electrode materials and their interfaces must be maintained to ensure that the desired electrochemical reaction remains the dominant redox pathway. Battery anodes, composed of reactive metals (Li, Na, Mg as metals, alloys, or intercalants), are subject to degradation under both equilibrium (storage) and active deposition/dissolution conditions. Formation of surface films, which ideally approach the properties of the SEI – blocking of electron and solvent/anion transport – plays a role in slowing or preventing self-discharge and facilitating more efficient (de)intercalation, (de)alloying, or deposition/stripping.[5] Significant effort has been made to design for anode stability through the properties of the electrolyte and through the use of additives demonstrated to enhance cycle life and cell performance. SEI formation on the prismatic surface of graphite is an established phenomenon in LIBs and the subject of many reviews. Controlled electroreduction of alklycarbonates, mixtures of cyclic and linear, and lithium salts results in surface films that allow Li^+ ion intercalation but prevent solvent co-intercalation, preventing the exfoliation of the graphite host. These films are forming and evolving on the surfaces of and at the contact points between host particles in composite anodes, resulting in increased interfacial impedance with time and use and decreased kinetics.

Stable film formation on alloying hosts such as the semi-metal Si has proven to be a more difficult challenge.[6] The chemistry of the lithiated Si surface is different from that of carbon and, when coupled with swelling-induced deformation, leads to continued parasitic loss of Li and the electrolyte. Pulverization of Si particles yields loss of electrical continuity, stranded host material, and capacity loss. Several novel nanoscale architectures show promise in accommodating large mechanical strain and directing deformation toward electrolyte-free interfaces; however, issues of volume efficiency need to be addressed for these structures to compete with graphite.

Metal anodes are the most efficient use of mass and volume, as the host penalty is eliminated, but provide no host scaffold onto which a SEI is physically supported. Without a mechanically stable SEI, continued consumption of both Li and electrolyte inventory occurs.[7] Despite this vulnerability, Li has been shown to cycle with coulombic efficiency up to 99.8% in select electrolytes, at modest deposition current density and cycled capacity, under conditions where dimensional control of the metal is maintained. Reports exist of the use of polymer membranes and barrier films at Li surfaces to reduce parasitic loss and facilitate compact Li deposition. Dendrite suppression and resulting cell failure and safety concerns have been topics of considerable research recently. Novel potential solutions to this problem include high surface area substrates, membranes with pores below critical dimensions to suppress asperity formation, and structured electrolytes to suppress anion depletion.

Cathode materials are also susceptible to interfacial and bulk degradation leading to reduction in cell performance.[8] Transition metal oxides used for LIBs tend to be reactive toward alkylcarbonate solvents resulting in decomposition byproduct formation, gas evolution, and surface film formation. Film formation can increase interfacial impedance, which impacts the kinetics of working cation (de)insertion and can compromise the electrical connectivity of the host particle to the percolation network. Oxide corrosion takes place in the presence of HF produced by the reaction of trace moisture with the $LiPF_6$ supporting electrolyte salt. Dissolution of soluble metal cations, such as Mn^{2+}, takes place with resulting transport to the anode where they comprise the protective nature of the anode SEI. Cathode particles can be coating with nanometric films of carbon, $AlPO_4$, and various ion transmissive oxides to stabilize the particle. From the bulk perspective, aging can take place through structural disordering, phase transition, and strain-induced fracture in the host particles. These changes also retard kinetics resulting in cell polarization and can render particles inactive resulting in capacity loss.

4.3.2 SAFETY

The cumulative degradation in materials eventually leads to cell failure.[9] Failure may take several forms, including excessive cell polarization, accelerated capacity fade, and thermal runaway for the more reactive systems resulting in cell venting.[10] Cell venting in LIBs can lead to combustion of the volatile solvents, possible propagation among cells, and battery fires. The release of moisture sensitive fluoride salts and hydrogen fluoride production with pack rupture or fire represents a significant chemical exposure hazard. The origin of loss of thermal control is inherently a materials problem where metal particles, poor alignment of separator and electrode, insufficient insulation between electrodes, and poor electrical contact between electrodes and tabs can result in eventual electrode shorting and overheating. Metal particles and other imperfections are viewed as defects and represent a unique problem as separator thickness is pushed to thinner dimensions to increase energy density. Defects are not detected during early stage cycling, but produce electrode shorting with extended cycling resulting in excess Joule heating and eventual loss of thermal control. Electrode shorting can also take place with metal (e.g., Li) dendrites that penetrate through the separator. Materials solutions to preventing thermal runaway include shutdown separators whose pores seal at elevated temperature reducing material transport between electrodes and cathode materials like metal phosphates that release oxygen at considerably higher temperatures. These protections address the early stage transition from initiation to the onset of thermal runaway, but yield minimal benefit beyond the threshold. Electrolyte flammability reduction has been explored through the use of fluorinated solvents and ionic liquids. Cell failure prevention devices including

positive temperature coefficient devices and fusible links are used to physically disconnect cells within packs, and a battery management system serves to regulate power drawn from and introduced to cells based on state of health signatures. Overall pack design and cell placement impact the probability of failure propagating between cells.

References

1 Gallagher, K.G.; Goebel, S.; Greszler, T.; Mathias, M.; Oelerich, W.; Eroglu, D.; Srinivasan, V., Quantifying the promise of lithium-air batteries for electric vehicles, *Energy Environ. Sci.,* **2014**, *7*, 1555, DOI:10.1039/c3ee43870.

2 Eroglu, D.; Zavadil, K.R.; Gallagher, K.G., Critical link between materials chemistry and cell-level design for high energy density and low cost lithium-sulfur transportation battery, *J. Electrochem. Soc.,* **2015**, *162*, A982, DOI:10.1149/2.0611506jes.

3 Vetter, J.; Novák, P.; Wagner, M.R.; Veit, C.; Möller, K.-C.; Besenhard, J.O.; Winter, M.; Wohlfahrt-Mehrens, M.; Vogler, C.; Hammouche, A., Ageing mechanisms in lithium-ion batteries, *J. Power Sources,* **2005**, *147*, 269 DOI:10.1016/j.jpowsour.2005.01.006.

4 Barré, A.; Deguilhem, B.; Grolleau, S.; Gérard, M.; Suard, F.; Riu, D., A review of lithium-ion battery ageing mechanisms and estimations for automotive applications, *J. Power Sources*, **2013**, *241*, 680, DOI:10.1016/j.jpowsour.2013.05.040.

5 X.-B.; Zhang, R.; Zhao, C.-Z.; Wei, F.; Zhang, J.-G.; Zhang, Q., A review of solid electrolyte interphases on lithium metal anode, *Adv. Sci*., **2016**, *3*, 1500213, DOI:10.1002/advs.201500213.

6 Casimir, A.; Zhang, H.; Ogoke, O.; Amine, J.C.; Lu, J.; Wu, G., Silicon-based anodes for lithium-ion batteries: Effectiveness of materials synthesis and electrode preparation, *Nano Energy*, **2016**, *27*, 359, DOI:10.1016/j.nanoen.2016.07.023.

7 Zhang, K. Lee, G.-H.; Park, M.; Li, W.; Kang, Y.M., Recent developments of the lithium metal anode for rechargeable non-aqueous batteries, *Adv. Energy Mater.,* **2016**, *6*, 1600811, DOI:10.1002/aenm.201600811.

8 Hasbrand, R.; Cherashinin, G.; Ehrenberg, H.; Gröting, M.; Albe, K., Fundamental degradation mechanisms of layered oxide Li-ion battery cathode materials: Methodology, insights, and novel approaches, *Mater. Sci. Eng. B*, **2015**, *192*, 3, DOI:10.1016/j.mseb.2014.11.014.

9 Palacín, M.R.; de Guibert, A., Why do batteries fail, *Science*, **2016**, *351*, 1253292, DOI:10.1126/science.1253292.

10 Abada, S.; Marlair, G.; Lecoq, A.; Petit, M.; Sauvant-Moynot, V.; Huet, F., Safety focused modeling of lithium-ion batteries: A review, *J. Power Sources,* **2016**, *306*, 178, DOI:10.1016/j.jpowsour.2015.11.100.

4.4 Testing and Characterization Tools - Uncertainty Quantification

Improving the performance and lifetime of energy storage systems (ESS) necessitates significantly better understanding of the electrochemical processes taking place within the storage device and of the failure and degradation mechanisms of the storage system. Characterization at atomic and mesoscale scales and especially at interfaces during charge and discharge is essential. Due to the inherent complexity of ESS, achieving this level of understanding requires multiple techniques (different length and time scales) and sensitivities (modalities). In addition, there is a need to couple *in situ/operando* with *ex-situ* studies, because these have different levels of data fidelity, as well as detailed investigations enabled by the use of model systems. The important outcome of this characterization is a rational design of improved ESS. Over the past decades, much progress has been made in using particle- and photon-based spectroscopy, as well as scattering and imaging techniques.[1,2,3]

Various spectroscopies are used to probe the chemical and electronic structures of ESS, with some emphasis on near surface regions (e.g., in metal oxide cathodes) and interfaces such as the SEI. Both hard and soft X-ray absorption spectroscopy (XAS) have been extensively reviewed, including ESS applications.[4] *Operando* hard X-ray XAS provides insight into oxidation state and is routinely used for ESS. The soft X-ray spectroscopies are more sensitive and quantitative probes of chemical and electronic structure, allowing tracking of the state of charge, and have several modalities, including standard XAS, X-ray emission spectroscopy (XES), resonant inelastic X-ray scattering (RIXS),[3] and photoemission spectroscopy (XPS). Depending on the spectroscopy and detection scheme (e.g., transmitted or emitted fluorescence X-rays, total or Auger electrons), these can be made surface or near-bulk sensitive by variation of the penetration or detection depth. Thus, these soft X-ray spectroscopies are sensitive to interfaces and surfaces. As an example, Figure 4-5 shows the Mn and Co L edge XAS for stoichiometric NMC after 20 cycles for different voltage windows, exhibiting more reduced transition metals for higher voltage cutoffs.[5] Most soft X-ray work to date has been *ex situ*, but recently *in situ* cells have been developed and more *in situ* investigations are being reported. RIXS has been used to characterize ESS less frequently, but potentially has exquisite chemical sensitivity. These X-ray spectroscopies can be complemented by optical spectroscopies, such as Fourier transform infrared (FT-IR),[6] which is more sensitive to organics. Differential electrochemical mass spectrometry has recently emerged as a valuable *in situ* mass-resolved monitor of gaseous and volatile reactants, reaction intermediates and products during charge/discharge: for example, the evolution of O_2 at high potentials in Li-excess metal oxides.[7]

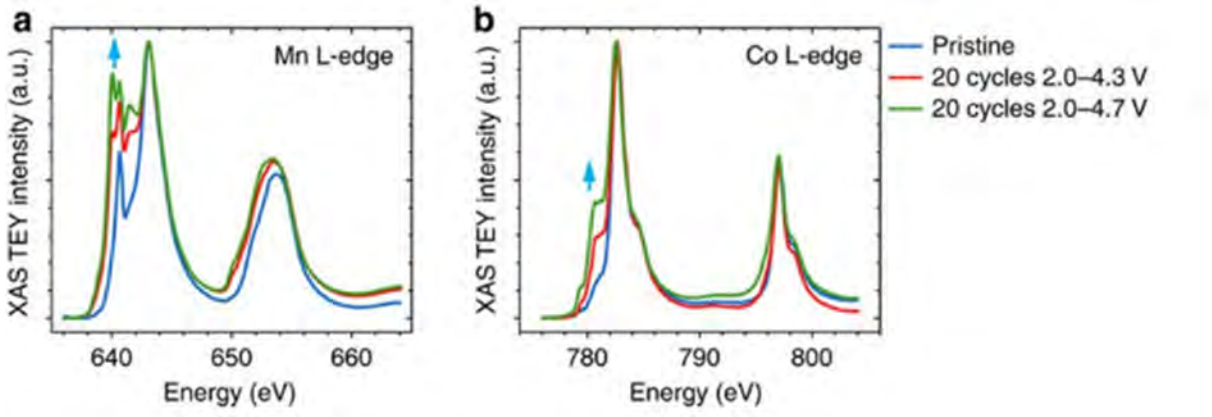

Figure 4-5. XAS of stoichiometric $LiNi_xMn_xCo_{1-2x}O_2$ (NMC) in pristine state and after 20 cycles for 2.0-4.3 V and 20 cycles for 2.0-4.7 V: (a) Mn L-edge and (b) Co L-edge. Arrows show reduction of transition metals.[5]

X-ray and neutron powder diffraction (XPD and NPD, respectively) and extended X-ray absorption fine structure (EXAFS) are well developed techniques to probe average atomic structure and are routinely applied in ESS,[8,9]although NPD is less often used (partly due to lack of sources). The more recent use of high energy X-rays (>20 keV) is advantageous in terms of penetrating power through cells. With high quality powder diffraction data, Rietveld refinement gives accurate average atomic structure for crystalline electrodes. Total scattering or pair distribution function (PDF) analysis has developed over about the past 15 years and uses Bragg scattering and diffuse scattering to provide insight beyond the average structure.[10] This complements EXAFS and is now more often used. *Operando* or *in situ* measurements are important, as shown for example by Liu et al.,[8] who used time-resolved XPD to demonstrate the formation of a predicted intermediate $LiFePO_4$ under high charge/discharge rates (10C). This illustrates the importance of *operando* methods to capture transients. However, *in situ* analyses can suffer from lack of data fidelity (e.g., angular ranges are obscured, or preferential orientation occurs) that limits the information content in diffraction. Thus, *ex-situ* XPD and NPD can complement *in situ* diffraction and give more detailed atomic structure results with less ambiguity. A challenge is to adopt these methods to solid-state electrolytes. Nuclear magnetic resonance (NMR) is a sensitive local probe of bulk atomic environments[11] that is used for *in situ* characterization of electrodes and, importantly, electrolytes: for example, the identification of soluble polysulfides in Li/S batteries.[12] However, NMR is not frequently used for ESS.

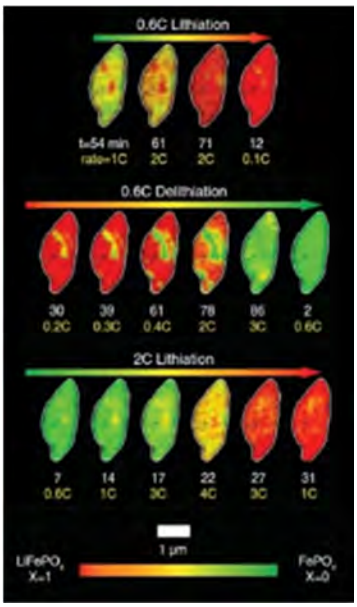

Figure 4-6. Representative *operando* *S*TXM frames of Li insertion and extraction for Li_xFePO_4. The *operando* Li composition frames show a single particle over multiple lithiation and delithiation cycles at varying charging or discharging rates. The color represents the Li composition where green is x=0, and red is x=1. Rearranged from Ref. 13.

ESS devices and their constituent electrodes are inherently complex and heterogeneous, consisting of electrochemically active materials, binders, electrolyte, and reaction products. Consequently, spatially resolved imaging over a range of length scales is essential, in particular, imaging modes that are sensitive to chemical species. As a result many imaging techniques have proven useful both *operando* and *ex situ*. These include X-ray based microscopies, such as transmission X-ray microscopy (TXM), micro-computed tomography (µCT), scanning transmission X-ray microscopy (STXM), electron microcopies, and scanning probe microscopies (SPMs). For X-rays, there are two imaging modalities: morphological or tomographical and chemical (e.g., spectro-microscopies). The latter is especially powerful as this allows mapping phase changes in both primary and secondary particles. The full field TXM and µCT are mostly used with hard X-rays, while STXM uses soft X-rays. Soft X-rays are more chemically sensitive and so allow greater fidelity. In contrast, *operando* and *in situ* investigations are much easier with TXM/µCT (hard X-rays), although there has been recent development of *in situ* STXM but at some sacrifice in resolution. A beautiful example of spectro-microscopy is shown in Figure 4-6, where STXM is used to track the reaction dynamics of $LiFePO_4$ by measuring the relative concentrations of Fe^{2+} and Fe^{3+}.[13] The conclusion is that nanoscale spatial variations in rate and composition control the lithiation pathway. These images are 2D, which is adequate because the particles are platelets, but in general 3D, which is inherent to tomography µCT and achievable in TXM, is much more informative. A nice example by Ebner et al.[14] demonstrated µCT imaging of SnO particles at high speed (15 minutes) and large field of view (2 mm) and observed volume expansion and insight into phase/chemical behavior. This study made advantageous use of higher energy X-rays for imaging realistic cells.

The technique of electron microscopy has seen tremendous advances in the last decade, and these advances have been used to understand the microstructure of a wide range of ESS materials. Some advances include aberration correction using both the scanning transmission (STEM) and transmission (TEM) imaging modes,[15]

electron sources, detectors and spectrometers,[16] electron energy loss spectroscopy (EELS), atom-by-atom energy dispersive X-ray spectroscopy (equivalent to X-ray fluorescence),[17] and chemically sensitive electron tomography for three-dimensional characterization.[18] Perhaps the most important advances have occurred in the areas of *in-situ* characterization.[19] There have been two primary approaches developed that allow real-time imaging of the lithiation of electrode materials. The first of these utilizes a mobile scanning transmission microscopy tip within the TEM to provide either a lithium electrolyte[20] or lithium[21] local to the electrode material: the application of bias drives the lithium into the material. This *in-situ* approach has the advantage of allowing the full range of atomic-resolution STEM/TEM approaches. A second approach exploits recent advances in liquid cell microscopy[22] and microfabrication technology, to build a quasi-battery system within the electron microscope.[23,24] This approach has the advantage of being *in-situ*, but at the cost of resolution loss and degradation of analytical signal due to the scattering that results from the presence of the confining silicon nitride windows, as well as the liquid itself.

The use of SPM in ESS research is still in its infancy. This technique holds the potential to bridge the gap of characterization techniques on length scales between atoms and devices, if the challenge of quantification of SPM signals can be solved. For example, SPM has been used to study ion intercalation in layered materials based on the change in mechanical properties. [25]

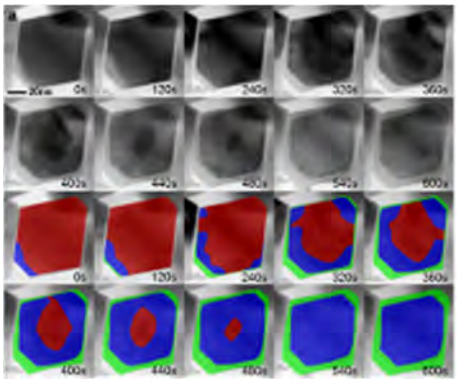

Figure 4-7. *In situ* observation of two-step phase transformation during the lithiation of Fe_3O_4.[30]

Over the past decade, researchers have adopted a reductionist approach by using model, but still relevant, systems to obtain a detailed understanding of ESS, especially related to interfaces such as the SEI. Typically, this involves *in situ* characterization of single crystals (e.g., Si), thin films, or open cell geometries for nanostructured electrodes as used for TEM (see above). This methodology uses techniques such as surface X-ray and neutron scattering and TEM to provide exquisite details on interface structure and chemistry at length scales less than 1 nm. Due to the simplicity of the experiment, direct comparison to theory is often more straightforward than for more complex half-cells. Often, highly idealized geometries and *in situ* cells are used, with the knowledge gained transferable to real cells. For example, X-ray and neutron reflectivity have provided insight into the formation and "breathing" of the SEI on Si,[26,27] as well as phase transformations (Figure 4-7). One challenge, which can potentially provide great insights, is to more accurately relate the electrochemistry (measured in the characterization cell) to the interface structure changes. This will allow quantitatively connecting the electrode state of charge to the spatial distribution of Li, directly addressing the question: "Where does the Li go?"

The dynamics in ESS span a tremendous range of time scales from femtoseconds for ion hopping to years for lifetimes. The characterizations described above have all been used for slower dynamics associated with charge/discharge processes (seconds to hours) and cycle life (hours to days). However, faster dynamics associated, for example, with ion motion or transport across interfaces and the SEI, have been investigated with electrochemical impedance spectroscopies (EIS), NMR, and advanced SPM techniques,[28] although often the information obtained is qualitative.

Over the past few years, there have been a few emerging techniques with a potential to greatly enhance our understanding of ESS. These are partly driven by the increased coherence of X-ray sources (e.g., the Advanced Photon Source-Upgrade) that enable combining real and reciprocal space methods into coherent diffractive imaging (CDI), including Bragg CDI and ptychography.[29] Thus far, only a few examples have been

reported. While these are promising, further development is needed to make CDI technique robust and more broadly useful. There is also an increase in combining complementary characterization techniques (i.e., multimodal) to provide a more holistic picture of ESS. The use of several techniques yields more reliable and valuable insight and enables cross correlation of the finding, for example, FT-IR and XAS or X-ray diffraction (XRD) and imaging. In addition, with the advance of upgraded light sources, qualitative improvements are expected in imaging, possibly approaching the sub-nm scale.

References

1 Lu, J.; Wu, T.; Amine, K., State-of-the-art characterization techniques for advanced lithium-ion batteries, *Nat. Energy*, **2017,** *2*, 17011.

2 Nelson Weker, J.; Toney, M. F., Emerging in situ and operando nanoscale X-ray imaging techniques for energy storage materials, *Adv. Funct. Mater.,* **2015,** *25*, 1622–1637. doi:10.1002/adfm.201403409

3 Liu, X.; Yang, W.; Liu, Z., Recent progress on synchrotron-based in-situ soft X-ray spectroscopy for energy materials, **2014,** *Adv. Mater., 26*, 7710.

4 Giorgetti, M., A review on the structural studies of batteries and host materials by X-ray absorption spectroscopy, *ISRN Materials Science*, **2013,** 938625, doi:10.1155/2013/938625.

5 Lin, F.; Markus, I. M.; Nordlund, D.; Weng, T.-C.; Asta, M. D.; Xin, H. L.; Doeff, M. M., Surface reconstruction and chemical evolution of stoichiometric layered cathode materials for lithium-ion batteries, *Nat. Commun.,* **2014,** *5***,** 3529 .

6 Verma, P.; Maire, P.; Novak, P., A review of the features and analyses of the solid electrolyte interphase in Li-ion batteries, *Electrochim. Acta,* **2010,** *55,* doi.org/10.1016/j.electacta.2010.05.072.

7 Grey, C.P.; Tarascon, J.M., Sustainability and in situ monitoring in battery development, *Nature Mater.,* **2017,** *16*, 45–56, doi:10.1038/nmat4777.

8 Liu, H.; Strobridge, F. C.; Borkiewicz, O. J.; Wiaderek, K. M.; Chapman, K. W.; Chupas, P. J.; Grey, C. P., Batteries capturing metastable structures during high-rate cycling of $LiFePO_4$ nanoparticle electrodes, *Science*, **2014**, *344*, 1252817.

9 Mohanty, D.; Li, J.; Abraham, D.P.; Huq, A.; Payzant, E.A.; Wood III, D.L.;, Daniel, C.., Unraveling the voltage-fade mechanism in high-energy-density lithium-ion batteries: Origin of the tetrahedral cations for spinel conversion, *Chem. Mater.,* **2014**, *26*, 6272–6280, DOI: 10.1021/cm5031415.

10 Jung, H.; Allan, P.K.; Hu, Y.-Y.; Borkiewicz, O.J.; Wang, X.-L.; Han, W.-Q.; Du, L.-S.; Pickard, C.J.; Chupas, P.J.; Chapman, K.W.; Morris, A.J.; Grey, C.P., Elucidation of the local and long-range structural changes that occur in germanium anodes in lithium-ion batteries, *Chem. Mater.,* **2015**, *27* (3), 1031–1041. DOI: 10.1021/cm504312x.

11 Pecher, O.; Carretero-González, J.; Griffith, K.J.; Grey, C.P.; Materials' methods: NMR in battery research, *Chem. Mater.,* **2017,** *29* (1), 213-242, DOI:10.1063/1.4961903.

12 See, K.A.; Leskes, M.; Griffin, J.M.; Britto, S.; Matthews, P.D.; Emly, A.; Van der Ven, A.; Wright, D.S.; Morris, A.J.; Grey, C.P.; Seshadri, R., "Ab initio structure search and in situ ^{7}Li NMR studies of discharge products in the Li–S battery system, *J. Amer. Chem. Soc.,* **2014,** *136*, 16368-16377, DOI: 10.1021/ja508982p.

13 Lim, J.; Li, Y. Y.; Alsem, D. H.; So, H.; Lee, S. C.; Bai, P.; Cogswell, D. A.; Liu, X. Z.; Jin, N.; Yu, Y. S.; Salmon, N. J.; Shapiro, D. A.; Bazant, M. Z.; Tyliszczak, T.; Chueh, W. C., Origin and hysteresis of lithium compositional spatiodynamics within battery primary particles, *Science*, **2016**, *353*, 566-571.

14 Ebner, M.; Marone, F.; Stampanoni, M.; Wood, V., Visualization and quantification of electrochemical and mechanical degradation in Li ion batteries, *Science*, **2013,** *342,* 716.

15 Smith, D.J., Progress and problems for atomic-resolution electron microscopy, *Micron*, **2012,** *43*, 504–508.

16 Krivanek, O.L.; Chisholm, M.F.; Nicolosi, V.; Pennycook, T.J.; Corbin, G.J.; Dellby, N.; Murfitt, M.F.; Own, C.S.; Szilagyi, Z.S.; Oxley, M.P.; Pantelides, S.T., Atom-by-atom structural and chemical analysis by annular dark-field electron microscopy, *Nature*, **2010,** *464* (7288), 571-574.

17 d'Alfonso, A.J.; Freitag, B.; Klenov, D.; Allen, L.J., Atomic-resolution chemical mapping using energy-dispersive X-ray spectroscopy, *Physical Review B*, **2010,** *81* (10), 100101.

18 Weyland, M.; Midgley, P., Electron tomography, in *Transmission Electron Microscopy*, Springer International Publishing, pp. 343-376 (2016).

19 Taheri, M.L.; Stach, E.A.; Arslan, I.; Crozier, P.A.; Kabius, B.C.; LaGrange, T.; Minor, A.M.; Takeda, S.; Tanase, M.; Wagner, J.B.; Sharma, R., Current status and future directions for in situ transmission electron microscopy, *Ultramicroscopy*, **2016,** *170*, 86-95.

20 Wang, C.M.; Xu, W.; Liu, J.; Choi, D.W.; Arey, B.; Saraf, L.V.; Zhang, J.G.; Yang, Z.G.; Thevuthasan, S.; Baer, D.R.; Salmon, N., In situ transmission electron microscopy and spectroscopy studies of interfaces in Li ion batteries: Challenges and opportunities, *J. Mater. Res.,* 2010, *25* (8), 1541-1547.

21 Wang, F.; Robert, R.; Chernova, N.A.; Pereira, N.; Omenya, F.; Badway, F.; Hua, X.; Ruotolo, M.; Zhang, R.; Wu, L.; Volkov, V., Conversion reaction mechanisms in lithium ion batteries: study of the binary metal fluoride electrodes, *J. Amer. Chem. Soc.*, **2011,** *133* (46), 18828-18836.

22 Ross, F.M., Opportunities and challenges in liquid cell electron microscopy, *Science*, **2015,** *350* (6267), aaa9886.

23 Gu, M.; Parent, L.R.; Mehdi, B.L.; Unocic, R.R.; McDowell, M.T.; Sacci, R.L.; Xu, W.; Connell, J.G.; Xu, P.; Abellan, P.; Chen, X., Demonstration of an electrochemical liquid cell for operando transmission electron microscopy observation of the lithiation/delithiation behavior of Si nanowire battery anodes, *Nano Letters*, **2013,** *13* (12), 6106-6112.

24 Holtz, M.E.; Yu, Y.; Gunceler, D.; Gao, J.; Sundararaman, R.; Schwarz, K.A.; Arias, T.A.; Abruña, H.D.;Muller, D.A., Nanoscale imaging of lithium ion distribution during in situ operation of battery electrode and electrolyte, *Nano Letters*, **2014,** *14* (3), 1453-1459.

25 Come, J.; Xie, Y.; Naguib, M.; Jesse, S.; Kalinin, S.; Gogotsi, Y.; Kent, P.R.C.; Balke, N., Nanoscale elastic changes in 2D $Ti_3C_2T_x$ (MXene) pseudocapacitive electrodes, *Advan. Ener. Mater.* **2016,** *6*, 1502290, DOI: 10.1002/aenm.201502290.

26 Cao, C.; Steinrück, H.G.; Shyam, B.; Stone, K.H.; Toney, M.F., In-situ study of silicon electrode lithiation with X-ray reflectivity. *Nano Lett.,* **2016,** *16,* 7394−7401, DOI: 10.1021/acs.nanolett.6b02926.

27 Veith, G. M.; Doucet, M.; Baldwin, J. K.; Sacci, R. L.; Fears, T. M.; Wang, Y.; Browning, J. F., *J. Phys. Chem. C,* **2015,** *119* (35), 20339-20349.

28 Balke, N.; Jesse, S.; Kim, Y.; Adamczyk, L.; Tselev, A.; Ivanov, I.N.; Dudney, N.J.; Kalinin, S.V., "Real space mapping of Li-ion transport in amorphous Si anodes with nanometer resolution, Nano *Lett., 10* (9), 3420-3425.

29 Hitchcock, A.P.; Toney, M.F.; Synch, J., Spectromicroscopy and coherent diffraction imaging: focus on energy materials applications, *Radiation*, **2014,** *21*, 1019-1030, DOI: 10.1107/S1600577514013046.

30 He, K.; Zhang, S.; Li, J.; Yu, X.; Meng, Q.; Zhu, Y.; Hu, E.; Sun, K.; Yun, H.; Yang, X.Q.; Zhu, Y., Visualizing non-equilibrium lithiation of spinel oxide via in situ transmission electron microscopy, *Nature Communications*, **2016,** *7*, 11441.

4.5 Modeling and Simulation

Materials modeling has undergone a revolution the last 10-20 years due to rapidly growing computing power and the development of more efficient and robust algorithms for describing the laws of physics. As a result, modeling is playing an increasingly important role in energy storage research, spanning length scales from first-principles methods to atomistic and continuum methods. The paragraphs below summarize the current state of the art, highlighting the growing areas and applications.

4.5.1 FIRST-PRINCIPLES MODELING

First-principles modeling rests on quantum mechanics to describe the state of a material, whether it be a liquid electrolyte, a molecule, a solid, and interface or a combination thereof. While the exact solution of the full many-bodied Schrodinger equation describing a material is not solvable today, the series of approximations used to turn it into a tractable problem defines the particular flavor of first-principles method used. The most widely used implementation, “standard” density-functional theory (DFT), is a ground-state method, implying that any property that is associated with the *equilibrium state* of the material is well described. It is worth noting that first-principles methods today are limited to systems with < 1000 atoms and molecular dynamics simulation times of 13–30 ps. Despite these limitations, standard DFT has proven extremely powerful in describing existing and even predicting novel functional materials.[1,2,3,4,5] See, for example, Figure 4-8. Relevant properties such as equilibrium voltages, phase stability and transformations, ionic mobility and diffusion, capacities, safety, etc., are now readily calculated and used as information about materials behavior and performance as well as metrics for novel materials design. While many processes in energy storage devices occur out-of-equilibrium, the measured properties often manifest as small perturbations of the equilibrium value. For example, in solids, the polarization of a material due to kinetics, interfacial resistance, etc., results in a voltage profile

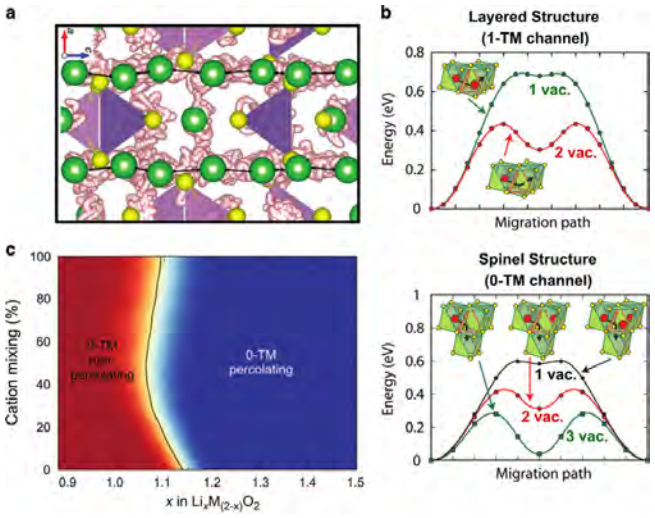

Figure 4-8. Examples of first-principles modeling in Li-ion materials spanning (a) *ab initio* molecular dynamics simulations of solid state electrolytes, (b) lithium diffusion through layered and spinel $LiTiS_2$ and (c) lithium percolation probability in cation-mixed $Li_xM_{2-x}O_2$. From Ref. 2 and references therein. Image c reproduced with permission of American Chemical Society.

away from the equilibrium curve; however, the calculated equilibrium voltage is based on rigorous thermodynamics and, hence, provides the “baseline" behavior of the material and its intrinsic capabilities. Similarly, severe discrepancies between measured and calculated ionic diffusion behavior are usually not due to inaccuracies in the applied equilibrium theory, but instead traced back to diffusion bottlenecks at different length scales.[3,4] Conversely, the ability of modeling to rapidly separate components and processes that are notoriously difficult to measure or de-convolute, such as liquid and interfacial reactions, is providing drivers for understanding and inspiration for further experimental investigations.[6,7]

The maturity and robustness of DFT implementations have also recently resulted in its combination with sophisticated automation software infrastructures and high-performance computing, enabling so-called ”high-throughput” calculations.[8,9,10] In these applications, the calculations span large chemical and structure spaces, and this has enabled unprecedented materials data and insights into the correlations between structure, chemistry, and properties. Capitalizing on these insights leads to design and accelerated materials prediction and discovery. Examples of predictions of novel energy storage materials which have been subsequently experimentally realized are Li-ion and multi-valent cathode materials and solid-state electrolytes.[4]

Outside of standard DFT, more sophisticated first-principles methods, such as GW and quantum Monte Carlo, are gaining traction as “gold-standard” benchmark methodologies,[11,12] which are highly valuable in providing excited state properties and/or more accurate equilibrium results. While still requiring manual intervention, and adding orders of magnitude to the computation time, their usage is likely to follow similar trajectories as DFT as the algorithms increase in robustness and easy-of-use.

4.5.2 INTER-ATOMIC POTENTIAL METHODS AND CLASSICAL MOLECULAR DYNAMICS

Interatomic potential or atomistic methods rest upon the specification of an effective potential model, which expresses the total energy of the system as a function of the nuclear coordinates. Hence, input data from experiments and/or first-principles calculations are used to fit the specific form of the potential such that the system in question is well-described. These approaches, while generally less transferable and reliable for describing charge transfer effects and absolute energetics as compared to first-principles methods, produce reasonable trends, and are indispensable in being able to handle much larger systems (thousands to millions of atoms) and time scales expanded by a hundred. Use of interatomic potentials and long time-scale molecular dynamics (>1 ns) is particularly useful for studying liquids, interfaces, long-range defects, kinetics, and nanostructures as functions of temperature and/or composition (Figure 4-9).[12,13,14,15] For example, the complex conformation due to dispersion forces of organic molecules in liquid electrolytes[16] is necessary to obtain a correct solvation structure and requires the longer simulation time scales that today are only accessible to classical molecular dynamics.

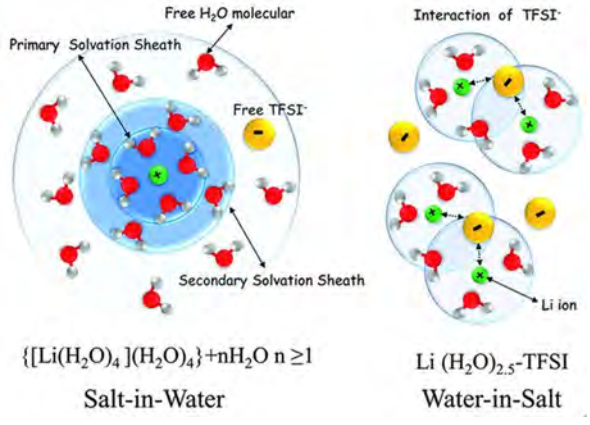

Figure 4-9. Molecular dynamics simulation of the solvation structure of LiTFSI in water as a function of concentration.[15]

Recently, two new potential types have been suggested that could improve the transferability and accuracy of inter-atomic potentials: Gaussian Approximation Potentials (GAP)[17] and potentials based on artificial Neural Networks (NN).[18,19] In these cases, the interpolation of the high-dimensional potential energy surface is obtained by using a flexible, non-linear functional form based on a set of reference structures. The amount of reference data needed is significantly higher than that for the fitting of more restrictive potential

forms; however, combined with the rapidly increasing first-principles data accessible through the Materials Genome, the popularity of these potentials is expected to grow.

4.5.3 CONTINUUM MODELING

Since the pioneering work of John Newman in establishing the macro-homogeneous approach in modeling battery electrodes, continuum-scale models have become an important tool in understanding how materials properties can translate into battery behavior.[20,21,22,23] While these models have provided deep insight into battery operation,[24,25,26] they average many of the microscopic details in the electrode, such as the actual particle shape and the tortuous nature of the pores. In addition, the active material is typically treated as a single-phase intercalative or phase change process with assumptions that the reaction is uniform across the particle.[27,28] These assumptions result in the models being more qualitative than quantitative.[29,30]

Over the last decade, many advances in the area of continuum modeling have pointed to a future where many of the properties of the battery can be calculated on a computer.[10,31,32] At the material level, there is increasing use of phase growth and phase-field models to accurately describe the nature of the reaction and to capture the complexity of the phase movement without simplifying assumptions.[33,34,35] In addition, models for systems that undergo dissolution/re-precipitation[36,37] and deposition (such as Li metal)[38,39] have seen resurgence. In addition, models now describe the mechanical effects in the material,[40,41] and couple the mechanical with the electrochemical process to understand effects such as voltage hysteresis and particle cracking.[42,43] Challenges remain in modeling anisotropic growth of phases, nucleation effects, effect of crystal facets and orientation, grain boundaries, etc.

Moving from the material scale to the electrode and device scale, there has been significant interest in building on the porous electrode model by performing 3D microstructure-based simulations,[44,45,46] with detailed representation of the porous nature of the battery electrodes obtained by various techniques, including focused ion beam-scanning electron microscopy and X-ray tomography.[47,48] The drastic improvements in computing power over the last decade have led to these models being used more often; however, the field is still in its infancy. These models are now limited by the inability to image binder regions,[49] especially in the solvent medium where swelling is known to occur.[50] There have also been attempts to model anisotropic reaction between particles (the so-called “particle-by-particle” model[51,52]) and move away from the core assumption of the macro-homogeneous approach that all particles in the porous electrode are equivalent.

Models that capture the assembly of electrodes into a cell, interaction of cells in a pack, with description of thermal characteristics have also become of great importance for industry to design systems at scale.[53,54] Pack level effects, such as temperature gradients, impact battery life, which in turn can lead to cell-to-cell cross-talk, requiring models to be strongly coupled from the materials to the pack in order to ensure better predictive capabilities for the future.[55] Better first principle models also allow development of better battery management systems, especially with the use of reduced order models that allow fast run times without scarifying accuracy.

4.5.4 TECHNO-ECONOMIC MODELING

Over the past decade, the use of techno-economic (TE) models have taken on greater importance in the field. TE models combine simplified cell models (as described above) and cell sizing models and include material and manufacturing cost in addition to the weight and volume penalties when combining electrolyte and electrolyte materials into cells, modules, and packs. TE models allow extrapolation of electrode-level properties (e.g., voltage, capacity, solubility, etc.) of new material to device level impacts in terms of energy density, specific energy, and cost. Also critical is the ability of TE models to work backwards: wherein device-level targets can be translated into material level metrics so that material scientists and electrochemists have a way to measure progress without the need to resort to expensive cell and pack fabrication.

TE models have been used very successfully in Li-ion batteries, based on BatPaC, where the value of this approach has been demonstrated.[56,57] The model is now routinely used to evaluate material innovations at the

pack level and has guided the research agenda in that field. In the last 5 years, this model has been extended to study newer chemistries such as Li-S, Li-air, and Mg-ion batteries.[58,59,60] In addition, the concept has been adapted to examine flow batteries, both aqueous and non-aqueous, for grid-storage applications.[61]

TE models are completed by approaches that seek to examine the availability of natural resources wherein the concept of availability of metals to scale into large scale production is also incorporated into the picture.[62]

TE models are most useful when they serve as a guide for the research, and are not meant to be the sole input in judging research progress. Rather, the models allow researchers to focus attention on the critical cost or energy bottleneck so that one can accelerate development of the technology.

References

1 Meng, Y.S.; Arroyo-de Dompablo, M.E., First principles computational materials design for energy storage materials in lithium ion batteries, *Energy Environ. Sci*., **2009,** *2* (6), 589.

2 Urban, A.; Seo, D.; Ceder, G., Computational understanding of Li-ion batteries, *npj Computational Materials,* **2016,** *2,* 16002, doi:10.1038/npjcompumats.2016.2.

3 Persson, K.; Sethuraman, V.A.; Hardwick, L.J.; Hinuma, Y.; Meng, Y.S.; van der Ven, A.; Srinivasan, V.; Kostecki, R.; Ceder, G., Lithium diffusion in graphitic carbon, J. *Phys. Chem. Lett.,* **2010,** *1* (8), 1176–1180.

4 Malik, R.; Burch, D.; Bazant, M.; Ceder, G., Particle size dependence of the ionic diffusivity, *Nanoletters*, **2010,** *10*, 4123–4127.

5 Jain, A.; Shin, Y.; Persson, K.A., Computational predictions of energy materials using density functional theory, *Nat. Rev. Mater.,* **2016,** *1*, 15004.

6 Soto, F.A., Balbuena, P.B., Effect of the electrolyte composition on SEI reactions at Si anodes of Li-ion batteries, *J. Phys. Chem. C,* **2015,** *119*, 7060−7068.

7 Leung, K.; Rempe, S.B.; Foster, M.E.; Ma, Y.; Martinez, J.M.; Sai, N.; Balbuena, P.B., Modeling electrochemical decomposition of fluoroethylene carbonate on silicon anode surfaces in lithium ion batteries, *J. Electrochem. Soc.,* **2014,** 161 (3), A213-A221.

8 Jain, A.; Ong, S.P.; Hautier, G.; Chen, W.; Richards, W.D.; Dacek, S.; Cholia, S.; Gunter, D.; Skinner, D.; Ceder, G.; Persson, K.A., Commentary: The Materials Project: A materials genome approach to accelerating materials innovation, *APL Mater*., **2013,** *1*, 11002.

9 Saal, J.E.; Kirklin, S.; Aykol, M.; Meredig, B.; Wolverton, C., Materials design and discovery with high-throughput density functional theory: The open quantum materials database (OQMD), *JOM*, **2013,** *65*, 1501–1509.

10 Cheng, L.; Assary, R.S.; Qu, X.; Jain, A.; Ong, S.P.; Rajput, N.N.; Persson, K.; Curtiss, L.A.,Accelerating Electrolyte discovery for energy storage with high-throughput screening, *J. Phys. Chem. Lett.*, **2015,** *6*, 283–291.

11 Govoni, M.; Galli, G., Large scale GW calculations, *J. Chem. Theory Comput*., **2015,** *11*, 2680−2696.

12 Ganesh, P.; Kim, J.; Park, C.; Yoon, M.; Reboredo, F.A.; Kent, P.R.C., Binding and diffusion of lithium in graphite : Quantum Monte Carlo benchmarks and validation of van der Waals density functional methods, *J. Chem. Theory Comput*., **2014,** *10*, 5318−5323.

13 Fisher, C.A.J.; Islam, S., Lithium and sodium battery cathode materials: computational insights into voltage, diffusion and nanostructural properties, *Chem. Soc. Rev*., **2014,** *43*, 185.

14 Ong, M.T.; Verners, O.; Draeger, E.W.; Van Duin, A.C.T.; Lordi, V.; Pask, J.E., Lithium ion solvation and diffusion in bulk organic electrolytes from first-principles and classical reactive molecular dynamics, *J. Phys. Chem. B,* **2015,** *119*, 1535–1545.

15 Suo, L.; Borodin, O.; Gao, T.; Olguin, M.; Ho, J.; Fan, X.; Luo, C.; Wang, C.; Xu, K., "Water-in-salt" electrolyte enables high-voltage aqueous lithium-ion chemistries, *Science*, **2015,** *350*, 938-943.

16 Rajput, N.N.; Qu, X.; Sa, N.; Burrell, A.K.; Persson, K.A., The coupling between stability and ion pair formation in magnesium electrolytes from first-principles quantum mechanics and classical molecular dynamics, *J. Am. Chem. Soc.*, **2015,** 137, 3411–3420.

17 Bartók, P.; Payne, M.C.; Kondor, R.; Csányi, G., Gaussian approximation potentials: The accuracy of quantum mechanics, without the electrons, *Phys. Rev. Lett*., **2010,** *104*, 136403-1–136403-4.

18 Blank, T.B.; Brown, S.D.; Calhoun, A.W.; Doren, D.J., Neural-network models of potential-energy surfaces, *J. Chem. Phys.,* **1995,** *103*, 4129-4137.

19 Lorenz, S.; Gross, A.; Scheffler, M., Representing high-dimensional potential-energy surfaces for reactions at surfaces by neural networks, *Chem. Phys. Lett*., **2004,** *395*, 210-215.

20 Newman, J.; Tiedemann, W., Porous-electrode theory with battery applications, *AIChE Journal*, **1975,** *21*, 25-41.

21 Ma, Y.; Doyle, M.; Fuller, T.F.; Doeff, M.M.; De Jonghe, L.C.; Newman, J., The measurement of a complete set of transport properties for a concentrated solid polymer electrolyte solution, *J. Electrochem. Soc.,* **1995,** *142*, 1859-1868.

22 Doyle, M.; Fuller, T.F.; Newman, J., Modeling of galvanostatic charge and discharge of the lithium/polymer/insertion cell, *J. Electrochem. Soc.*, **1993,** *140*, 1526-1533.

23 Doyle, M.; Newman, J., Analysis of transference number measurements based on the potentiostatic polarization of solid polymer electrolytes, *J. Electrochem. Soc.*, **1995,** *142*, 3465-3468.

24 Doyle, M.; Newman, J.; Gozdz, A.S.; Schmutz, C.N.; Tarascon, J.M., Comparison of modeling predictions with experimental data from plastic lithium ion cells, *J. Electrochem. Soc.*, **1996,** *143*, 1890-1903.

25 Arora, P.; Doyle, M.; Gozdz, A.S.; White, R.E.; Newman, J., Comparison between computer simulations and experimental data for high-rate discharge of plastic lithium-ion batteries, *J. Power Sources*, **2000,** *88*, 219-231.

26 Ramadass, P.; Haran, B.; White, R.; Popov, B.N., Mathematical modeling of the capacity fade of Li-ion cells, *J. Power Sources*, **2003,** *123*, 230-240.

27 Srinivasan, V.; Newman, J., Discharge model for the lithium iron-phosphate electrode, *J. Electrochem. Soc.*, **2004,** *151*, A1517-A1529.

28 Cai, L.; White, R.E., Mathematical modeling of a lithium ion battery with thermal effects in COMSOL Inc. Multiphysics (MP) software, *J. Power Sources*, **2011,** *196*, 5985-5989.

29 Ramadesigan, V.; Northrop, P.W.C.; De, S.; Santhanagopalan, S.; Braatz, R.D.; Subramanian, V.R., modeling and simulation of lithium-ion batteries from a systems engineering perspective, *J. Electrochem. Soc.*, **2012,** *159*, R31-R45.

30 Jokar, A.; Rajabloo, B.; Desilets, M.; Lacroix, M., Review of simplified pseudo-two-dimensional models of lithium-ion batteries, *J. Power Sources*, **2016,** *327*, 44-55.

31 Qi, Y.; Hector, L.G.; James, C.; Kim, K.J., Lithium concentration dependent elastic properties of battery electrode materials from first principles calculations, *J. Electrochem. Soc.*, **2014,** *161*, F3010-F3018.

32 Ozaki, H.; Kuratani, K.; Kiyobayashi, T., Monte-Carlo simulations of the ionic transport of electrolyte solutions at high concentrations based on the pseudo-lattice model, *J. Electrochem. Soc.*, **2016,** *163*, H576-H583.

33 Liang, L.; Qi, Y.; Xue, F.; Bhattacharya, S.; Harris, S.J.; Chen, L.Q., Nonlinear phase-filed model for electrode-electrolyte interface evolution, *Phys. Rev. E*, **2012,** *86*, 051609.

34 Gallagher, K.G.; Dees, D.W.; Jansen, A.N.; Abraham, D.P.; Kang, S.H., A volume averaged approach to the numerical modeling of phase-transition intercalation electrodes presented for Li_xC_6, *J. Electrochem. Soc.*, **2012,** *159*, A2029-A2037.

35 Bai, P.; Cogswell, D.A.; Bazant, M.Z., Suppression of phase separation in $LiFePO_4$ nanoparticles during battery discharge, *Nano Lett.*, **2011,** *11*, 4890-4896.

36 Cogswell, D.A., Quantitative phase-field modeling of dendritic electrodeposition, *Phys. Rev. E*, **2015,** *92*, 011301(R).

37 Ghaznavi, M.; Chen,P., Analysis of a mathematical model of lithium-sulfur cells. Part III: Electrochemical reaction kinetics, transport properties and charging, *Electrochim. Acta*, **2014,** *137*, 575-585.

38 Chen, L.; Zhang, H.W.; Liang, L.Y.; Liu, Z.; Qi, Y.; Lu, P.; Chen, J.; Chen, L.Q., Modulation of dendritic patterns during electrodeposition: A nonlinear phase-field model, *J. Power Sources*, **2015,** *300*, 376-385.

39 Ely, D.R.; Jana, A.; Garcia, R.E., Phase field kinetics of lithium electrodeposits, *J. Power Sources*, **2014,** *272*, 581-594.

40 Christensen, J.; Newman, J., Stress generation and fracture in lithium insertion materials, *J. Solid State Electrochem.*, **2006**, *10*, 293-319.

41 Verbrugge, M.W.; Cheng, Y.T., Stress and strain-energy distributions within diffusion-controlled insertion-electrode particles subjected to periodic potential excitations, *J. Electrochem. Soc.*, **2009,** *156*, A927-A937.

42 Bucci, G.; Nadimpalli, S.P.V.; Sethuraman, V.A.; Bower, A.F.; Guduru, P.R., Measurement and modeling of the mechanical and electrochemical response of amorphous Si thin film electrodes during cyclic lithiation, *J. Mech. Phys. Solids*, **2014,** *62*, 276-294.

43 Grantab, R.; Shenoy, V.B., Location and orientation-dependent progressive crack propagation in cylindrical graphite electrode particles, *J. Electrochem. Soc.*, **2011,** *158*, A948-A954.

44 Garcia, R.E.; Chiang, Y.M.; Carter, W.C.; Limthongkul, P.; Bishop, C.M., Microstructural modeling and design of rechargeable lithium-ion batteries, *J. Electrochem. Soc.*, **2005,** *152*, A255-A263.

45 Wiedemann, A.H.; Goldin, G.M.; Barnett, S.A.; Zhu, H.; Kee, R.J., Effects of three-dimensional cathode microstructure on the performance of lithium-ion battery cathodes, *Electrochemica Acta*, **2013,** *88*, 580-588.

46 Roberts, S.A.; Brunini, V.E.; Long, K.N.; Grillet, A.M.; A framework for three-dimensional mesoscale modeling of anisotropic swelling and mechanical deformation in lithium-ion electrodes, *J. Electrochem. Soc.*, **2014,** *161*, F3052-F3059.

47 Gilbert, J.A.; Bareno, J.; Spila, Trask, S.E.; Miller, D.J.; Polzin, B.J.; Jansen, A.N.; Abraham, D.P., Cycling behavior of NCM523/graphite lithium-ion cells in the 3-4.4V range: Diagnostic studies of full cells and harvested electrodes, *J. Electrochem. Soc.*, **2017,** *164,* A6054-A6065.

48 Ebner, M.; Geldmacher, F.; Marone, F.; Stampanoni, M.; Wood, V., X-ray tomography of porous, transition metal oxide based lithium ion battery electrodes, *Adv. Ener. Mater.*, **2013,** *3*, 845-850, 2013.

49 Shearing, P.; Wu, Y.; Harris, S.J.; Brandon, N., In situ X-ray spectroscopy and imaging of battery materials, *Electrochem. Soc. Interface*, **2001,** 43-47, Fall.

50 Takahashi, K. Higa, K.; Mair, S.; Chintapalli, M.; Balsara, N.; Srinivasan, V., Mechanical degradation of graphite/PVDF composite electrodes: A model-experimental study, *J. Electrochem. Soc.*, **2016,** *163*, A385-A395.

51 Li, Y.; Gabaly, F.E.; Ferguson, T.R.; Smith, R.B.; Bartelt, N.C.; Sugar, J.D.; Fenton, K.R.; Cogswell, D.A.; Kilcoyne, A.L.D.; Tyliszczak, T.; Bazant, M.Z.; Chueh, C.W., Current-induced transition from particle-by-particle to concurrent intercalation in phase-separating battery electrodes*, Nature Mater.,* **2014,** *13*, 1149-1156.

52 Orvananos, B.; Ferguson, T.R.; Yu, H.C.; Bazant, M.Z.; Thornton, K., “Particle-level modeling of the charge-discharge behavior of nanoparticulate phase-separating Li-ion battery electrodes, *J. Electrochem. Soc.*, **2014,** *161*, A535-A546.

53 Wang, C.Y.; Srinivasan, V., Computational battery dynamics (CBD) – electrochemical/thermal coupled modeling and multi-scale modeling, *J. Power Sources*, **2002,** *110*, 364-376.

54 Pannala, S.; Turner, J.A.; Allu, S.; Elwasif, W.R.; Kalnaus, S.;Simunovic, S.; Kumar, A.; Billings, J.J.; Wang, H.; Nanda, J., Multiscale modeling and characterization for performance and safety of lithium-ion batteries, *J. Appl. Phys.*, **2015,** *118*, 072017.

55 Wang, C.Y.; Zhang, G.; Ge, S.; Xu, T.; Ji, Y.; Yang, X.G.; Leng, Y., Lithium-ion battery structure that self-heats at low temperatures, *Nature*, **2016,** *529*, 515-518.

56 Gallagher, K. G.; Nelson, P.A., Manufacturing costs of batteries for electric vehicles, in Lithium-Ion Batteries: advances and Applications, Elsevier, pp. 97-126, **2013**.

57 Ciez, R. E.; Whitacre, J.F., Comparison between cylindrical and prismatic lithium-ion cell costs using a process based cost model, *J. Power Sources,* **2017,** *340*, 273-281.

58 Eroglu, D.; Zavadil, K.R.; Gallagher, K.G., Critical link between materials chemistry and cell-level design for high energy density and low cost lithium-sulfur transportation battery, *J. Electrochem. Soc.*, **2015,** *162,* A982-A990.

59 Gallagher, K.G.; Goebel, S.; Greszler, T.; Mathias, M.; Oelerich, W,; Eroglu, D.; Srinivasan, V., Quantifying the promise of lithium–air batteries for electric vehicles, *Ener. Environ. Sci*., **2014,** 7, 1555-1563.

60 Canepa, P., Gautam, G.S.; Hannah, D.C.; Malik, R.; Liu, M.; Gallagher, K.G.; Persson, K.A.; Ceder, G., Odyssey of multivalent cathode materials: Open questions and future challenges, *Chem. Rev*., **2017,** *117*, 4287-4341.

61 Darling, R. M.; Gallagher, K.G.; Kowalski,J.A.; Ha, S.; Brushett, F.R., Pathways to low-cost electrochemical energy storage: A comparison of aqueous and nonaqueous flow batteries, *Ener. Environ. Sci*., **2014,** *7*, 3459-3477.

62 Wadia, C.; Albertus, P.; Srinivasan. V., Resource constraints on the battery energy storage potential for grid and transportation applications, *J. Power Sources,* **2011,** *196*, 1593-1598.

4.6 Synthesis of Materials

Today, the design principles for creating better materials for electrochemical energy storage are often well understood. For example, structural frameworks for high Li-ion conductivity have been identified.[1] Rules to create intercalation cathodes with good Mg^{2+} mobility[2] or high Li capacity[3] exist. Such design ideas can be supported with *ab-initio* calculations to evaluate the properties of potentially interesting new compounds. As a result, materials innovation is moving from an intuitive and trial-and-error approach, to a more directed approach where specific new chemistries and crystal structures are targeted. Such advances in computational materials modeling, as well as in the understanding of electrochemical storage materials, are leading to a future where many properties of real and virtual compounds can be available on demand, enabling rapid screening in material design efforts.

These successes in accelerated materials design have moved the bottleneck in materials development towards the *synthesis* of novel compounds, and much of the momentum and efficiency gained in the design process becomes gated by trial-and-error synthesis techniques. Today, there are multiple cases known of compounds predicted to be transformative for the energy storage field, but which have not yet been successfully synthesized. Hence, what is needed is a more predictive and quantitative approach towards synthesis so that novel compound ideas can be tested in a matter of days, rather than months or years. In addition, a more quantitative understanding of synthesizability can place better bounds on the compositional and structural space to which design optimization should be confined, so that its relevance for technology can be enhanced.

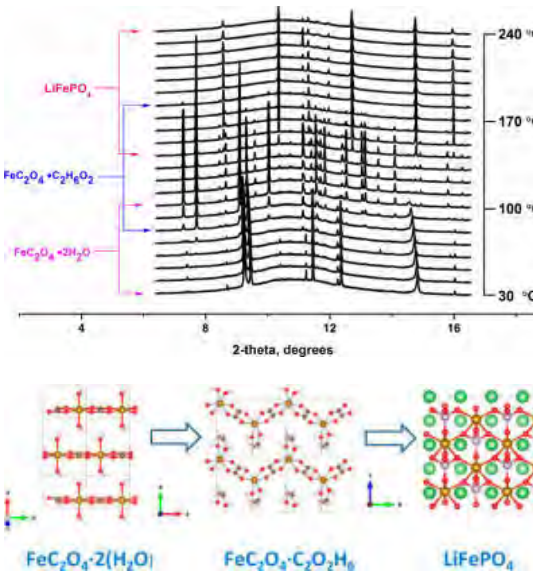

Figure 4-10. *In-situ* XRD of intermediate phases observed during the solvothermal synthesis of $LiFePO_4$ cathode materials.[5]

While there is no predictive theory of synthesis today, several complementary steps are being taken to develop more insight and predictability of synthesis. For example, *in-situ* characterization of synthesis[4] is helping to understand the reaction path of precursors, as well as intermediates that form in a reaction. This knowledge is crucial as intermediate phases often set the morphology and homogeneity of the end product, or they can be used

to restrict a system to metastable crystal structures and compositions. In the example shown in Figure 4-10, *in-situ* XRD is used to identify an intermediate phase formed during the solvothermal synthesis of $LiFePO_4$.[5]

Atomic-scale modeling of synthesis is in its early stage, but some successes exist in predicting the process conditions under which stable or metastable phases can be nucleated. For example, Figure 4-11 shows a nucleation map of different crystal structures of $CaCO_3$ as function of supersaturation and Mg/Ca ratio in water.[6] In this case, the Mg content in water modifies the relative surface energy of both polymorphs in such a way that at high enough Mg content in solution, the metastable phase (aragonite) has the lowest nucleation barrier, and as a result, precipitates out of solution. A similar approach has been followed to understand when FeS_2 forms pyrite (the stable phase) vs. marcasite (the metastable phase).[7] These new approaches to predict synthetic pathways have not been applied to materials for energy storage, but are likely to become an exciting new direction to create novel electrode or electrolyte compounds.

A distinctly novel approach that has been proposed[8] would be to use the massive amounts of data in the published literature on synthesis methods to create structured synthesis databases on which machine learning methods can be applied, similar to machine learning methods of crystal structure prediction derived from the Inorganic Crystal Structure Database. Such a scheme could lead directly to a better understanding and predictability of synthesis recipes for novel battery materials.

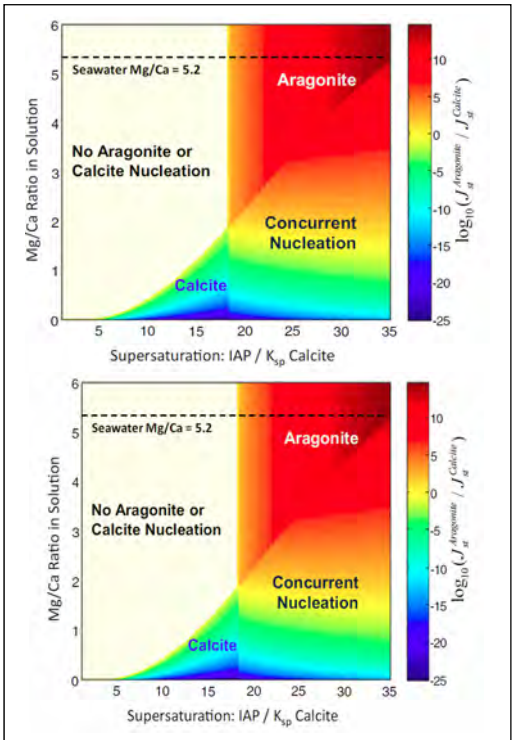

Figure 4-11. Competitive nucleation between polymorphs of $CaCO_3$ (top) and FeS_2 (bottom) as a function of solution chemistry during hydrothermal synthesis.[6]

References

1 Wang, Y.; Richards, W.D.; Ong, S.P.; Miara, L.; Kim, J.C.; Mo, Y.; Ceder, G., Design principles for solid-state lithium superionic conductors, *Nature Mater.*, **2015,** *14* (10), 1026-1031.

2 Rong, Z.; Malik, R.; Canepa, P.; Gopalakrishnan, S.G.; Liu, M.; Jain, A.; Persson, K.; Ceder, G., Materials design rules for multivalent ion mobility in intercalation structures, *Chem. Mater.,* **2015,** *27* (17), 6016–6021.

3 Lee, J.; Urban, A.; Li, X.; Su, D.; Hautier, G.; Ceder, G., Unlocking the potential of cation-disordered oxides for rechargeable lithium batteries*, Science*, **2014,** *343* (6170), 519-522.

4 Wang, L.; Bai, J.; Gao, P.; Wang, X.; Looney, J.P.; Wang, F., Structure tracking aided design and synthesis of $Li_3V_2(PO_4)_3$ nanocrystals as high-power cathodes for lithium ion batteries, *Chem. Mater.*, **2015,** *27* (16), 5712-5718.

5 Bai, J., Hong, J.; Chen, H.; Graetz, J.; Wang, F., Solvothermal synthesis of $LiMn_{1-x}Fe_xPO_4$ cathode materials: A study of reaction mechanisms by time-resolved in situ synchrotron X-ray diffraction, *J. Phys. Chem. C,* **2015,** *119*, 2266-2276.

6 Sun, W.; Jayaraman, S.; Chen, W.; Persson, K.A.; Ceder, G., Nucleation of metastable aragonite $CaCO_3$ in seawater, *Proc. Nat. Acad. Sci.,* **2015,** *112*, 3199-3204.

7 Kitchaev, D. A., Ceder, G., Evaluating structure selection in the hydrothermal growth of FeS_2 pyrite and marcasite, *Nature Commun.* **2016,** *7*, 3799, doi:10.1038/ncomms13799.

8 Kim, E.; Huang, K.; Saunders, A.; McCallum, A.; Ceder, G.; Olivetti, E., A data-driven framework for materials synthesis discovery, in preparation (2017).

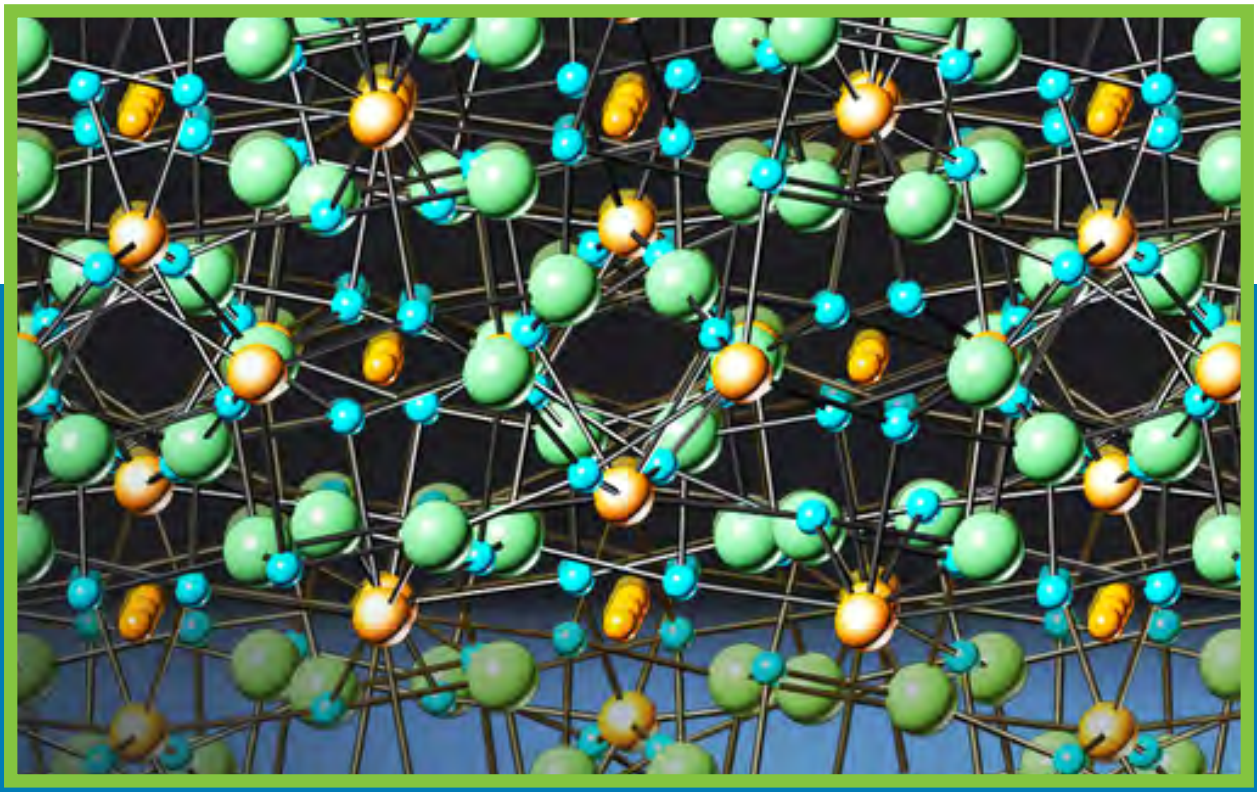

U.S. DEPARTMENT OF ENERGY | Office of Science